UNIVERSIDADE DE BRASÍLIA
Faculdade UnB Planaltina
Programa de Pós-Graduação em Ciências Ambientais

Rodrigo Ribeiro Mayrink

TRAÇADORES ISOTÓPICOS PARA QUELÔNIOS AMAZÔNICOS NO CONTEXTO DO TRÁFICO DE ANIMAIS SILVESTRES

Brasília
2026

UNIVERSIDADE DE BRASÍLIA
Faculdade UnB Planaltina
Programa de Pós-Graduação em Ciências Ambientais

Rodrigo Ribeiro Mayrink

TRAÇADORES ISOTÓPICOS PARA QUELÔNIOS AMAZÔNICOS NO CONTEXTO DO TRÁFICO DE ANIMAIS SILVESTRES

Tese apresentada ao Programa de Pós-Graduação em Ciências Ambientais da Universidade de Brasília, como requisito para obtenção do título de Doutor em Ciências Ambientais.

Orientadora: Prof. Dra. Gabriela Bielefeld Nardoto

Brasília
2026

Ficha catalográfica elaborada automaticamente,
com os dados fornecidos pelo(a) autor(a)

M474t

Mayrink, Rodrigo Ribeiro
TRAÇADORES ISOTÓPICOS PARA QUELÔNIOS AMAZÔNICOS NO CONTEXTO DO TRÁFICO DE ANIMAIS SILVESTRES / Rodrigo Ribeiro Mayrink; orientador Gabriela Bielefeld Nardoto. Brasília, 2026.
146 p.

Tese(Doutorado em Ciências Ambientais) Universidade de Brasília, 2026.

1. isótopos estáveis e radiogênicos. 2. incorporação isotópica. 3. tráfico de animais silvestres. 4. lavagem de vida silvestre. 5. quelônios amazônicos. I. Nardoto, Gabriela Bielefeld, orient. II. Título.

UNIVERSIDADE DE BRASÍLIA
Faculdade UnB Planaltina
Programa de Pós-Graduação em Ciências Ambientais

Rodrigo Ribeiro Mayrink

TRAÇADORES ISOTÓPICOS PARA QUELÔNIOS AMAZÔNICOS NO CONTEXTO DO TRÁFICO DE ANIMAIS SILVESTRES

Banca examinadora:

- **Prof. Dra. Gabriela Bielefeld Nardoto** – Universidade de Brasília (presidente)
- **Prof. Dr. Renato Caparroz** – Universidade de Brasília (membro titular interno)
- **Prof. Dr. Plínio Barbosa de Camargo** – Centro de Energia Nuclear na Agricultura da Universidade de São Paulo (CENA/USP) (membro titular externo)
- **Prof. Dra. Willandia de Aquino Chaves** – Virginia Polytechnic Institute and State University (membro titular externo)
- **Prof. Dr. Rodrigo Diana Navarro** – Universidade de Brasília (membro suplente interno)

"O correr da vida embrulha tudo, a vida é assim: esquenta e esfria, aperta e daí afrouxa, sossega e depois desinquieta. O que ela quer da gente é coragem. (...) Ser capaz de ficar alegre a mais, no meio da alegria, e inda mais alegre ainda no meio da tristeza! Só assim de repente, na horinha em que se quer, de propósito — por coragem. Será? Era o que eu às vezes achava. Ao clarear do dia."

(Guimarães Rosa, Grande Sertão Veredas)

Agradecimentos:

A conclusão deste projeto só foi possível graças a muita ajuda, vinda de um grande número de pessoas. Por isso, agradeço enormemente a cada uma delas:

À minha orientadora, Prof. Dra. Gabriela Bielefeld Nardoto, pela parceria, por ter aberto as portas para este projeto, por todos os ensinamentos, confiança e paciência ao longo desses anos de pesquisa.

À minha família: meus pais, pelo exemplo de uma vida inteira; minhas irmãs, pela disposição em assumir os encargos compartilhados da nossa rotina, para que eu pudesse me dedicar aos estudos; meus sobrinhos, pelo afeto sempre reconfortante.

À Carla, pelo apoio, pelo incentivo e pela compreensão nos momentos de ausência.

À Polícia Federal, pela liberação para eu me dedicar aos estudos.

À Rufford Foundation, pelo valioso auxílio financeiro (financiamento n. 37985-1).

Ao Prof. Dr. Roberto Ventura Santos, pelo inestimável apoio para a execução e custeio das análises isotópicas de estrôncio, além da participação na banca de qualificação.

Aos colegas e amigos Fábio Salvador, então Diretor Técnico-Científico da Polícia Federal, e Luiz Spricigo Jr., então Diretor do Instituto Nacional de Criminalística, por todo apoio que deram à fase inicial deste projeto de pesquisa, no âmbito do Projeto LANIF – Laboratório Nacional de Isótopos Forenses – da Polícia Federal.

Ao colega e amigo Alexandre Saraiva, então Superintendente da Polícia Federal no Amazonas, por ter garantido apoio institucional e logístico daquela unidade para etapas essenciais desta pesquisa.

Ao PPGCA/FUP/UnB, professores e colegas de classe, pelo aprendizado e convívio.

Ao Decanato de Pós-Graduação da UnB, pelo auxílio financeiro (Edital DPG 002/2021).

Ao EIS (Environmental Isotopes Studies) e aos colegas de pós-graduação e iniciação científica que o integram, pelo profícuo aprendizado ao longo desses últimos anos e também pelo convívio, ainda que quase sempre virtual. Dentre eles, especialmente à Luiza Brasileiro e ao André Pereira, pela parceria no capítulo do livro Isótopos Forenses e pelas enriquecedoras conversas sobre isótopos aplicados à fauna. E à Luiza, também, pela ajuda com análises estatísticas.

Ao INPA (Instituto Nacional de Pesquisa da Amazônia), por ter possibilitado a execução de parte dos experimentos desta tese em seu Centro de Estudos dos Quelônios da Amazônia (Cequa).

À Sabrina Menezes e a todos da equipe do Cequa/INPA que contribuíram com a manutenção dos animais e com a coleta de amostras do experimento de turnover isotópico.

À Marilene Brazil, por viabilizar contatos que se mostraram indispensáveis para a coleta de amostras em animais de vida livre.

Ao Prof. Dr. Paulo Andrade, pelas contribuições nas discussões dos dados e pelo apoio logístico para a coleta de amostras de animais de cativeiro; razão pela qual eu também agradeço à sua

equipe de dedicados pós-graduandos que auxiliaram enormemente nas coletas: João Alfredo da Mota Duarte, Eleyson Barboza, Ramon Duque Melo, Gilberto Batista Viana Filho e Thayanne Lopes.

Aos criatórios Fazenda Bicho do Rio e Balneário 3 Irmãos, pela cessão de amostras de animais de cativeiro.

Ao Prof. Dr. Luiz Martinelli, pelos sábios conselhos em relação à condução deste trabalho, e pela ajuda com a calibração dos resultados das análises isotópicas de carbono e nitrogênio.

Ao Prof. Dr. Vladimir Eliodoro Costa e a toda a equipe do Centro de Isótopos Estáveis da UNESP/Botucatu, pela oportunidade de aprendizado e por todo o apoio na preparação das amostras e análises.

Ao Laboratório de Ecologia Isotópica do Centro de Energia Nuclear na Agricultura da USP, pela realização das análises laboratoriais de carbono e nitrogênio.

À Prof. Dra. Willandia Chaves e à Lísley Gomes, por me apresentarem as dimensões humanas da conservação da biodiversidade; e, à Prof. Willandia, também pela participação na banca de defesa da tese.

Ao Prof. Dr. Plínio Camargo, pela participação nas bancas de qualificação e de defesa da tese.

Ao Prof. Dr. Renato Caparroz, pela participação na banca de defesa da tese.

Ao Prof. Dr. Rodrigo Navarro, pela participação nas bancas de qualificação e de defesa da tese.

Aos colegas e amigos do SETEC/PF/MG Marcus Vinícius Andrade, João Luiz de Oliveira, Luigi Martini e Gustavo Parma, por viabilizarem a conciliação da fase final do doutorado com o trabalho pericial no setor.

À Izabela Raso e à Saleth Horta, por terem acreditado neste projeto, pelo profissionalismo e por todo o apoio prestado durante fase de escrita da tese.

Ao colega e amigo Fábio Costa, por ter desbravado a trilha dos isótopos forenses na Polícia Federal, propiciando as condições para que este doutorado acontecesse; e também pelas contribuições nas discussões do trabalho.

À Camila Ferrara, por ter me apresentado o instigante mundo da conservação dos quelônios, pelo fornecimento de amostras de animais de vida livre e pelas contribuições em uma das publicações derivadas desta tese.

Ao Alexandre Gontijo e à Camilla Kafino, pela colaboração nos exames de MEV-EDS.

À Fernanda Costa de Aquino, pelo auxílio na preparação de amostras para exames laboratoriais e pelo fornecimento de amostras.

Aos demais colegas e amigos que colaboraram com o fornecimento de amostras: Daniel Vieira Crepaldi, Aline Andriolo, Márcia Gomes da Silva Oliveira, Ronaldo Formiga do Nascimento Filho, Roberto Cabral Borges, Caroline Vieira Cooke, Alberto Klefasz, Fábio Andrew Gomes Cunha e Maria Augusta Paes Agostini.

Resumo

O tráfico de animais silvestres é um dos principais vetores de perda de biodiversidade em escala global. Na Amazônia brasileira, a caça e o comércio ilegais de tartarugas de água doce para consumo humano são provavelmente o principal problema de tráfico de animais, envolvendo enormes volumes de animais traficados e redes organizadas de comércio ilegal. Esse cenário persiste apesar de décadas de esforços de conservação e da presença de um setor formal de criação em cativeiro voltado a abastecer o mercado com produtos legalizados. Mesmo com criadouros licenciados, permanecem preocupações quanto à lavagem de vida silvestre, na qual animais capturados na natureza são comercializados como se fossem oriundos de cativeiro. A técnica isotópica, particularmente baseada em $\delta^{13}C$ e $\delta^{15}N$, destaca-se como ferramenta forense para a detecção da lavagem de vida silvestre. Isso porque os tecidos animais incorporam a composição isotópica da dieta, e as rações de cativeiro frequentemente diferem isotopicamente das dietas naturais, permitindo discriminar origens de vida livre *versus* cativeiro. De modo complementar, razões isotópicas de estrôncio ($^{87}Sr/^{86}Sr$) podem registrar assinaturas associadas à hidrogeoquímica regional, embasando inferências de procedência geográfica de animais traficados. Esta tese estabelece um arcabouço científico forense para subsidiar investigações de tráfico de quelônios amazônicos, com especial foco na tartaruga-da-amazônia (*Podocnemis expansa*). O estudo integra uma análise de criminologia ambiental e de regulação dos mecanismos de lavagem, com ênfase na legislação brasileira, além de métodos laboratoriais para discriminar origem de vida livre *versus* cativeiro e para inferir a procedência geográfica de animais apreendidos. O Capítulo 1 sintetiza a literatura sobre lavagem de vida silvestre e lavagem de dinheiro associadas ao tráfico de vida silvestre, esclarecendo conceitos-chave sobre o tema. Também avalia o contexto normativo e de aplicação da lei no Brasil, propondo aprimoramentos para fortalecer respostas antilavagem e antitráfico. O Capítulo 2 quantifica a dinâmica de incorporação isotópica em *P. expansa*, determinando fatores de discriminação trófica (TDFs; $\Delta^{13}C$ e $\Delta^{15}N$) e parâmetros de turnover isotópico ($\delta^{13}C$) em quatro tecidos (sangue total, queratina do escudo, unha e pele), por meio de um experimento controlado de troca de dieta. Meias-vidas isotópicas e TDFs diferiram entre tecidos, fornecendo parâmetros calibrados que refinam inferências temporais sobre mudanças alimentares, úteis tanto em estudos de ecologia trófica quanto em interpretações forenses. O Capítulo 3 contém um estudo forense aplicado conduzido na Amazônia brasileira, que utilizou $\delta^{13}C$, $\delta^{15}N$ e $^{87}Sr/^{86}Sr$. O $\delta^{13}C$ distinguiu tartarugas de vida livre das mantidas em cativeiro, mostrando-se útil para a detecção de lavagem de vida silvestre. O $\delta^{15}N$, por sua vez, apresentou potencial para ajudar a diferenciar assinaturas isotópicas específicas de cada criadouro. Tartarugas de vida livre refletiram as assinaturas de $^{87}Sr/^{86}Sr$ dos corpos d'água que habitavam, o que fornece base para inferências sobre origem geográfica de espécimes apreendidos. Em conjunto, os resultados desta tese demonstram que o enfrentamento do tráfico de tartarugas amazônicas requer instrumentos institucionais – incluindo um adequado ordenamento jurídico e estratégias antilavagem de dinheiro adaptadas ao crime de tráfico de fauna – e evidências científicas robustas. Ao aplicar a rastreabilidade isotópica à realidade do tráfico de quelônios amazônicos no Brasil, a abordagem aqui proposta pode fortalecer inspeções na cadeia de comércio formal e o rastreamento de apreensões, além de aprimorar a base probatória para decisões investigativas e judiciais. Pode também orientar ações de manejo, como a reintrodução apropriada de animais confiscados com base em regiões de origem inferidas.

Palavras-chave: isótopos estáveis; isótopos radiogênicos; incorporação isotópica; tráfico de animais silvestres; lavagem de vida silvestre; *Podocnemis expansa*.

Abstract

Wildlife trafficking is a major driver of biodiversity loss worldwide. In the Brazilian Amazon, poaching and illegal trade of freshwater turtles for human consumption are likely the most important form of wildlife trafficking, involving large volumes of trafficked animals and organized illegal commerce networks. This pressure has persisted despite decades of conservation efforts and the existence of a formal captive-breeding sector intended to supply legal products to consumer markets. Even with licensed breeding operations, concerns persist over wildlife laundering, whereby illegally captured wild individuals are falsely marketed as captive-bred. Isotopic methods – particularly using $\delta^{13}C$ and $\delta^{15}N$ – have emerged as valuable forensic tools for detecting wildlife laundering because animal tissues reflect dietary isotope composition, and captive feeds are often isotopically distinct from natural diets, allowing discrimination between wild and captive origins. In addition, strontium isotope ratios ($^{87}Sr/^{86}Sr$) can record signatures associated with regional hydrogeochemistry, providing a basis for inferences about the geographic provenance of trafficked animals. This thesis establishes a forensic scientific framework to support investigations into the trafficking of Amazonian chelonians, with a particular focus on the giant South American river turtle (*Podocnemis expansa*). The study integrates an analysis of environmental criminology and the regulation of laundering mechanisms, with emphasis on Brazilian legislation, together with laboratory methods to discriminate wild *versus* captive origin and to infer the geographic provenance of seized animals. Chapter 1 synthesizes the literature on wildlife laundering and money laundering associated with illegal wildlife trade, clarifying key concepts on the subject. It also examines the Brazilian regulatory and law-enforcement context and proposes improvements to strengthen anti-laundering and anti-trafficking responses. Chapter 2 quantifies isotopic incorporation dynamics in *P. expansa* by determining trophic discrimination factors (TDFs; $\Delta^{13}C$ and $\Delta^{15}N$) and isotopic turnover parameters ($\delta^{13}C$) in four tissues (whole blood, scute keratin, claw, and skin), through a controlled diet-switch experiment. Isotopic half-lives and TDFs differed among tissues, providing calibrated parameters that refine temporal inferences about dietary shifts, with applications in both trophic ecology and forensic interpretation. Chapter 3 presents an applied forensic study conducted in the Brazilian Amazon using $\delta^{13}C$, $\delta^{15}N$ and $^{87}Sr/^{86}Sr$. $\delta^{13}C$ distinguished wild turtles from those maintained in captivity, demonstrating its usefulness for detecting wildlife laundering. In turn, $\delta^{15}N$ showed potential to help differentiate farm-specific isotopic signatures. Wild turtles reflected the $^{87}Sr/^{86}Sr$ signatures of the water bodies they inhabited, thereby providing a basis for inferences about the geographic origin of seized specimens. Taken together, the results of this thesis demonstrate that tackling Amazonian turtle trafficking requires both institutional instruments – including an adequate legal framework and anti-money-laundering strategies tailored to wildlife crime – and robust scientific evidence. By applying isotopic traceability to Amazonian chelonian trafficking in Brazil, the framework proposed here can strengthen inspections in the formal trade sector, support the tracing of seized animals, and improve the evidentiary basis for investigative and judicial decision-making. It can also inform management actions, such as the appropriate reintroduction of confiscated animals based on inferred regions of origin.

Keywords: stable isotopes; radiogenic isotopes; isotopic turnover; illegal wildlife trade; wildlife laundering; *Podocnemis expansa*.

Sumário

INTRODUÇÃO

HISTÓRICO DA EXPLORAÇÃO E CONSERVAÇÃO DOS QUELÔNIOS AMAZÔNICOS NO BRASIL E O PAPEL DA CIÊNCIA ISOTÓPICA COMO FERRAMENTA FORENSE NO COMBATE AO TRÁFICO DE ANIMAIS SILVESTRES

"Nos primeiros tempos, tantas eram as tartarugas na água quanto mosquitos no ar". Com essa frase, o naturalista inglês Henry Bates resumiu, ainda no final do séc. XIX, a marcante abundância dos quelônios de água doce na Amazônia (Bates, 1873). Com a ocorrência de 17 espécies de quelônios continentais (terrestres e de água doce), a Amazônia é uma das regiões de maior riqueza desses animais em todo o mundo (Rhodin *et al*., 2017).

Dentre os quelônios amazônicos, *Podocnemis expansa* (tartaruga-da-amazônia) destaca-se por constituir importante fonte de proteína animal para as comunidades tradicionais, sendo elemento marcante da cultura alimentar local (Chaves, Monroe & Sieving, 2019). Gilmore (1986) detalha a relevância da interação entre humanos e essa espécie no contexto socioambiental amazônico:

> "É de se presumir que nenhuma outra atividade etnozoológica nas bacias do Amazonas e Orinoco seja mais importante que a colheita da tartaruga fluvial de desova coletiva (*Podocnemis expansa*), conhecida como "gado do Amazonas" (...). A ampla área de distribuição, as incríveis quantidades reunidas para a desova em determinadas praias de areia, e a consequente disponibilidade de ovos, filhotes e fêmeas adultas tornaram esta espécie, literalmente, um esteio da vida e um organismo-chave nos aspectos fluviais da biota da floresta tropical. Não apenas o homem dependia desta tartaruga como alimento, mas também outros predadores, como os numerosos pássaros aquáticos e rapaces, peixes predadores, mamíferos carnívoros e jacarés. Nenhum outro animal dos trópicos da América do Sul produziu esta espécie."

O consumo de quelônios de água doce sempre fez parte do costume alimentar indígena na Amazônia. Contudo, foi no período colonial que a caça começou a se intensificar até alcançar níveis ameaçadores à conservação das espécies. Os colonizadores europeus estabeleceram-se definitivamente na Amazônia no início do século XVII, e desde então as tartarugas desempenharam um papel fundamental na dieta e nas necessidades domésticas dos colonos que exploraram a região. A profusão de tartarugas encontradas nas praias, notadamente a tartaruga-da-amazônia (*Podocnemis expansa)*, fez com que essa espécie se tornasse o principal alvo dos colonizadores. Ao longo de todo o período colonial, que se

estendeu até o início do século XIX, a tartaruga-da-amazônia foi uma fonte essencial de carne e óleo para os portugueses (Santos & Fiori, 2020).

Como consequência, as populações de *Podocnemis expansa* sofreram drástico declínio. Além do consumo da carne, a superexploração da espécie foi motivada pela utilização maciça dos ovos para alimentação humana e animal, para fabricação de manteiga para fins culinários e para uso como combustível de iluminação pública. Relatos estimam que até 48 milhões de ovos foram coletados anualmente para tais finalidades, nessa época (Salera Jr., Balestra & Luz, 2016). Em tempos mais recentes, além da caça, os quelônios de água doce amazônicos sofrem impactos antropogênicos das mais variadas naturezas, tais como desmatamento e alteração no uso da terra, urbanização, poluição hídrica e construção de barragens (de Paula Silva *et al*., 2025).

Várias espécies do gênero *Podocnemis* que ocorrem no Brasil (*P. unifilis, P. sextuberculata e P. erythrocephala*) são listadas como vulneráveis na lista vermelha da IUCN[1], assim como *Peltocephalus dumerilianus*, outro quelônio de água doce relevante no contexto da caça e consumo de carne na Amazônia brasileira. Adicionalmente, a espécie *Podocnemis lewyana*, que ocorre em território colombiano, é categorizada como criticamente ameaçada. Todo o gênero *Podocnemis* e a espécie *Peltocephalus dumerilianus* constam no Apêndice II da CITES[2].

A ameaça aos quelônios continentais (terrestres e de água doce) estende-se para muito além da Amazônia: das 356 espécies catalogadas no mundo, mais de 60% encontram-se ameaçadas ou já foram extintas (Lovich *et al*., 2018). Trata-se, portanto, de um grupo dentre os mais ameaçados do planeta. As causas desse quadro relacionam-se à destruição de habitats, à superexploração pela caça e às mudanças climáticas (uma vez que várias espécies têm determinação sexual dependente da temperatura de incubação). Possuindo geralmente alta densidade populacional e alcançando os valores mais elevados de biomassa/área dentre todas as espécies animais, os quelônios continentais desempenham funções ecológicas importantes como bioturbadores de solo, consumidores primários, dispersores de sementes

[1] IUCN – International Union for Conservation of Nature. Organização internacional dedicada à conservação dos recursos naturais, reunindo mais de 200 agências governamentais e 800 ONGs, oriundas de 140 países, e com quase 11.000 especialistas e pesquisadores associados. Mesmo sem força de lei, sua lista de espécies ameaçadas é utilizada como parâmetro técnico de alta confiabilidade em todo o mundo, sendo sua metodologia tida como referência para muitas das listas oficiais, incluindo a brasileira.

[2] CITES – Convention on International Trade in Endangered Species of Wild Fauna and Flora. Trata-se de um acordo internacional que regulamenta a exportação, importação e reexportação de animais e plantas, suas partes e derivados. Foi aprovado no Brasil pelo Decreto Legislativo nº 54, de 24 de junho de 1975 e promulgado pelo Decreto nº 76.623, de 17 de novembro de 1975. Sua implementação em território nacional se deu pelo Decreto nº 3.607, de 21 de setembro de 2000.

e ciclagem de nutrientes. Por tais razões, a depleção das populações de quelônios em escala global tem o potencial de acarretar relevantes prejuízos à biodiversidade, ecossistemas e serviços ecossistêmicos a eles associados (Lovich *et al*., 2018).

As primeiras ações de proteção dos quelônios amazônicos pelo governo brasileiro iniciaram-se na década de 1960. Em 1979, foi criado o primeiro projeto específico para esse fim no âmbito do órgão ambiental federal (então IBDF[3]): Projeto de Proteção e Manejo dos Quelônios da Amazônia, também conhecido como "Projeto Quelônios da Amazônia" (PQA). Em 1990, o Ibama[4] instituiu uma unidade especializada denominada Centro Nacional de Quelônios da Amazônia (Cenaqua), posteriormente renomeada, em 2001, para Centro de Conservação e Manejo de Répteis e Anfíbios (RAN)[5]. A legislação brasileira passou a autorizar a criação comercial de *Podocnemis expansa* (tartaruga-da-amazônia) e *Podocnemis unifilis* (tracajá) em 1992, com a publicação da Portaria Ibama n. 142/92. Quatro anos mais tarde, a Portaria Ibama n. 070/96 foi publicada para normatizar a comercialização de produtos e subprodutos das espécies provenientes dos criadouros comerciais regulamentados (Salera Jr. *et al*., 2016). Esses autores enfatizam que ambas as normas infralegais tinham como premissa o papel dos criadores comerciais em reduzir a pressão pela exploração ilegal dos animais de vida livre. Por fim, no plano federal, a criação comercial de quelônios de água doce permanece atualmente disciplinada pela Instrução Normativa Ibama n. 07/2015, especialmente por seu Anexo III. Após a descentralização da gestão da fauna silvestre promovida pela Lei Complementar n. 140/2011, a atividade também passou a estar sujeita às normas estaduais aplicáveis, especialmente aquelas relativas à aquicultura, ao licenciamento ambiental e ao manejo de fauna silvestre em cativeiro. Entre os estados amazônicos, há normas que enquadram, expressa ou potencialmente, os quelônios aquáticos nos regimes de aquicultura, licenciamento ambiental ou criação comercial, como ocorre no Amazonas, Pará, Tocantins, Rondônia e Roraima[6].

Mesmo com o intuito de a criação legalizada reduzir os impactos sobre as populações selvagens, estudos alertam para o fato de que os criadouros não substituíram significativamente o comércio clandestino; não aliviando, portanto, a pressão sobre os estoques naturais das espécies (Brazil *et al.*, 2025; Rebêlo & Pezzuti, 2000). A literatura

[3] Instituto Brasileiro de Desenvolvimento Florestal.
[4] Instituto Brasileiro de Meio Ambiente e dos Recursos Naturais Renováveis
[5] Atualmente denominado Centro Nacional de Pesquisa e Conservação de Répteis e Anfíbios e vinculado ao Instituto Chico Mendes de Conservação da Biodiversidade (ICMBio).
[6] Exemplos incluem a Lei AM n. 5.338/2020; Lei PA n. 6.713/2005; Resolução COEMA/PA n. 198/2026; Lei TO n. 2.034/2009; Resolução COEMA/TO n. 88/2018; Lei RO n. 3.437/2014; e Lei RR n. 2.073/2024.

registra a persistência do comércio ilegal de tartarugas de água doce, inclusive com a atuação de redes organizadas de contrabandistas (Pantoja-Lima *et al*., 2014; Kemenes & Pezzuti, 2007). A caça não regulamentada em grande escala é apontada por Antunes *et al*. (2016) como fator de potencial colapso das populações de espécies aquáticas da Amazônia – incluindo *Podocnemis expansa* –, acarretando a possibilidade do fenômeno por eles denominado de "rios vazios" (em alusão comparativa ao termo "florestas vazias").

Podocnemis expansa também se destaca nos índices de apreensões realizadas pelos órgãos de fiscalização ambiental. Na maior compilação sobre esse tema já feita no país a partir de dados oficiais, Destro *et al*. (2012) listaram a espécie como a sexta mais confiscada pelo Ibama e outros órgãos de fiscalização ambiental entre 2005 e 2009. Além de *P. expansa*, *Podocnemis sextuberculata* apareceu em 10º lugar e *Podocnemis unifilis* na 25ª posição, o que alçou a família Podocnemididae ao terceiro lugar entre as famílias mais frequentes, respondendo por 10% dos espécimes apreendidos; atrás apenas de Emberizidae (30%) e Thraupidae (13,3%). Como exemplo da dimensão numérica absoluta de tais índices, Kemenes & Pezzuti (2007) relataram que, entre os anos de 2000 e 2001, 3.992 exemplares do gênero *Podocnemis* e 122 redes de arrasto de quelônios foram confiscados apenas na região do Médio Rio Purus, no estado do Amazonas.

No que se refere à relação entre a criação de animais silvestres e a conservação da biodiversidade, é amplamente reconhecida a relevância da conservação *ex situ*, particularmente por meio da criação conservacionista de espécies silvestres ameaçadas de extinção. Por outro lado, a literatura científica tem consolidado o entendimento de que, de modo geral, a criação comercial de animais silvestres não reduz significativamente o tráfico e pode inclusive produzir efeitos contrários aos desejados em termos de conservação (Tensen, 2016). A promiscuidade entre a criação legalizada e o tráfico de animais silvestres, que pode dar origem ao fenômeno conhecido em inglês como *wildlife laundering* (lavagem ou esquentamento de vida silvestre, ou de animais silvestres), é fartamente relatada em várias partes do mundo (van Uhm, 2018)[7].

Em uma ampla revisão sobre o assunto, Tensen (2016) concluiu que a criação comercial atenderia aos objetivos de conservação somente quando a demanda de consumo não for impulsionada pela existência do comércio legal, e quando a criação legalizada conseguir oferecer animais a custos mais competitivos que os oriundos do tráfico. Em uma

[7] Ver a revisão bibliográfica sobre o tema contida no capítulo 1 desta tese.

síntese dos trabalhos revisados, a autora cita cinco condições que, se não forem respeitadas simultaneamente, podem levar a criação legalizada de animais silvestres a ter impacto negativo nas populações selvagens das espécies: (1) os produtos legais devem substituir efetivamente os ilegais, e os consumidores não podem mostrar preferência por animais capturados na natureza; (2) uma parte substancial da demanda de consumo deve ser atendida pela criação comercial, e a demanda geral não pode aumentar devido ao mercado legalizado; (3) os produtos legais precisam ter custo competitivo, a fim de combater os preços do mercado negro; (4) a criação de animais selvagens não pode depender de populações selvagens para repovoamento; e (5) o "esquentamento" ou "lavagem" de produtos ilegais no comércio legalizado não pode ocorrer.

No Brasil, várias publicações apontam a ocorrência de esquentamento ou lavagem de animais silvestres, na maioria dos casos relacionada à criação legalizada de aves (certamente por ser este o grupo mais comumente criado em cativeiro no país) (Stassart & Cardoso Jr., 2024; Charity & Ferreira, 2020; Mayrink, 2016; Alves *et al*., 2013; Kuhnen *et al*., 2012; Alves *et al*., 2010). Com relação aos quelônios, investigações policiais já apuraram o envolvimento da cadeia produtiva legalizada (criadouros, entrepostos e restaurantes) com o tráfico. Tais ações, inclusive, envolveram gravosas medidas judiciais restritivas de direito, tais como mandados de busca e apreensão, condução coercitiva e prisão (Polícia Federal, 2014). Além disso, apreensões de grande vulto, muitas vezes totalizando centenas de animais e ocorrendo de forma recorrente, denotam o suprimento ilegal em larga escala de quelônios para os mercados consumidores dos médios e grandes centros urbanos (Pantoja-Lima *et al*., 2014; ICMBio, 2016). Nessas situações, é natural que se levantem suspeitas de que tais animais ou produtos possam em algum momento ser internalizados na cadeia de comércio formal. Além da caça para consumo, quelônios silvestres são também alvo de tráfico para fins de animais de estimação (*pets*) ou coleção. Em uma operação realizada em 2018, o Serviço de Proteção da Natureza da Guarda Civil Espanhola interditou o maior criadouro ilegal de tartarugas da Europa, localizado na ilha de Maiorca. Foram apreendidos mais de 1.100 animais de 62 espécies (a maioria de origem asiática), sendo 14 ameaçadas de extinção. A rede de tráfico envolvia um pet shop na cidade de Barcelona. Dois cidadãos alemães e um espanhol foram presos acusados de crime ambiental e lavagem de dinheiro (Bohórquez, 2018).

Ao longo das últimas décadas, as populações silvestres de quelônios amazônicos de água doce têm se beneficiado de ações de manejo, monitoramento, fiscalização e pesquisa

realizadas por órgãos ambientais das diversas esferas de governo, instituições científicas e organizações não governamentais. Luz *et al*. (2022) contabilizam que, nos últimos 40 anos, foram manejados mais de 70 milhões de filhotes e monitoradas em torno de 800 mil matrizes de *Podocnemis* spp. (especialmente *P. expansa*, *P. unifilis* e *P. sextuberculata*) em 212 sítios de reprodução e desova nos estados das regiões Norte e Centro-Oeste. Iniciativas de conservação baseadas no engajamento de comunidades locais, tais como o Projeto Pé-de-Pincha (Andrade *et al*., 2015) e Projeto Médio Juruá (Campos-Silva *et al*., 2018) compõem a base do sucesso desses resultados. Devido à imensa extensão territorial da Bacia Amazônica e às limitações logísticas e estruturais inerentes àquele espaço geográfico, é virtualmente impossível que o poder público tenha plena capilaridade e constância de ações para exercer, sozinho, todas as medidas de conservação. Em função disso, o engajamento permanente das comunidades espalhadas ao longo da bacia é crucial para a preservação das espécies, no longo prazo.

Não obstante, é indispensável também que o Estado possua instrumentos eficazes para a repressão e dissuasão do tráfico e comércio ilegal da biodiversidade, inclusive para garantir a aplicação dos princípios e normas de proteção ambiental previstos na Constituição Federal de 1988, na Lei de Crimes Ambientais (Lei 9.605/98), nos acordos internacionais de que o país é signatário e nos demais dispositivos legais atinentes ao tema. Nesse sentido, cabe destacar que as ações de investigação policial e de persecução penal devem ser conduzidas com base nas técnicas mais modernas da ciência forense, de modo a assegurar que a perícia criminal tenha plena capacidade de demonstrar a autoria e a materialidade, bem como de evitar condenações equivocadas (Velho *et al*., 2021; Nucci, 2016). No contexto específico da caça na Amazônia, as ciências forenses adquirem papel relevante para a própria caracterização do tráfico em larga escala. A perícia criminal pode fornecer à justiça conclusões baseadas em critérios técnicos e objetivos, com sólido embasamento científico, que possam diferenciar a atividade ilegal de grande vulto (e, portanto, merecedora de maior atenção por parte dos órgãos de repressão) do consumo de subsistência dos recursos faunísticos por comunidades tradicionais.

Em casos de crimes contra a fauna silvestre, as análises forenses realizadas pela perícia criminal geralmente englobam a identificação das espécies traficadas (animais ou suas partes, produtos e subprodutos), a constatação de maus-tratos, a determinação de *causa mortis*, a atribuição de origem geográfica dos espécimes apreendidos e a diferenciação entre animais oriundos de vida livre ou cativeiro. Para realizar tais exames, os peritos criminais

lançam mão de conhecimentos de várias disciplinas das ciências naturais, tais como taxonomia, anatomia e patologia veterinárias, genética molecular e ciência do bem-estar animal, além de matérias da criminalística clássica (exames de local de crime e balística forense, por exemplo) (Costa *et al*., 2017; Mayrink *et al*., 2021).

Dentre as várias ferramentas tecnológicas utilizadas pela perícia criminal, a ciência isotópica forense tem ganhado crescente destaque em função de seu potencial para atribuição de origem e/ou autenticidade de vestígios (Nardoto *et al*., 2017; Chesson *et al*., 2018). A técnica isotópica começou a ser utilizada com mais intensidade para fins forenses a partir do final do século XX, e hoje sua aplicação em perícias criminais já é realizada nos mais modernos institutos de ciências forenses e órgãos policiais do mundo, a exemplo do Federal Bureau of Investigation (FBI, EUA), Bundeskriminalamt (BKA, Alemanha), Forensic Explosive Laboratory (FEL, Reino Unido), Netherlands Forensic Institute (NFI, Holanda), Australian Federal Police (AFP, Austrália), National Police Agency (NPA, Japão), e também na Polícia Federal brasileira (Andrade & Lasmar, 2020).

No âmbito dos crimes ambientais, destaca-se o emprego da ciência isotópica para o rastreamento de origem de fauna silvestre traficada e seus subprodutos, bem como para a diferenciação entre animais de vida livre e cativeiro (Brasileiro *et al*., 2023). Como alguns exemplos, Ziegler *et al*. (2016) realizaram análises multi-isotópicas ($\delta^{13}C$, $\delta^{15}N$, $\delta^{18}O$, $\delta^{2}H$ e $\delta^{34}S$) de 507 amostras de marfim de elefantes africanos e asiáticos (*Loxodonta africana* e *Elephas maximus*), com o objetivo de gerar um modelo de atribuição de proveniência de amostras de origem desconhecida para uso em ações de combate ao tráfico. Natusch *et al*. (2017) compararam as composições isotópicas e elementares da pele de pítons (*Python reticulatus* e *Python bivittatus*) de vida livre e criadas em cativeiro na Indonésia e no Vietnã. Diferenças em marcadores isotópicos e elementares entre cobras selvagens e cativas, bem como entre distintas origens geográficas, atestaram a eficácia da técnica como meio de determinar a origem das peles destinadas ao comércio internacional. Cerling *et al*. (2018), examinando $\delta^{13}C$, $\delta^{15}N$ e $^{87}Sr/^{86}Sr$ de pelos de rinocerontes negros (*Diceros bicornis*) no Quênia e confrontando os resultados com dados de geologia local e déficit hídrico, encontraram diferenças de razões isotópicas entre amostras de distintas origens geográficas. Alexander *et al*. (2019) utilizaram a conjugação de $\delta^{13}C$ e $\delta^{2}H$ para diferenciar grupos selvagens e cativos de papagaios-do-congo (*Psittacus erithacus*) e conseguiram, com isso, atestar que um lote de animais de origem desconhecida adveio de vida livre, e não de cativeiro. Jiguet *et al*. (2019) demonstraram que o $\delta^{2}H$ de penas de passeriformes capturados

ilegalmente na França funcionou como marcador para a diferenciação entre origens legal e ilegal. Gopi *et al*. (2019) estudaram a composição isotópica e elementar de amostras de robalo asiático (*Lates calcarifer*) oriundas de cultivo comercial e vida livre, conseguindo determinar a origem geográfica e os métodos de produção do pescado coletado em fontes australianas e asiáticas. Pereira *et al*. (2019) apontaram o potencial de uso das razões isotópicas $\delta^{13}C$ e $^{87}Sr/^{86}Sr$ de otólitos de pirarucu (*Arapaima* spp.) na Amazônia brasileira para o rastreamento de origem geográfica e diferenciação entre criação comercial e extrativismo (pesca). Hutchinson & Roberts (2020), estudando razões isotópicas de $\delta^{13}C$ e $\delta^{15}N$ de pelos de leão africano (*Panthera leo*), concluíram que um banco de dados isotópicos robusto de populações cativas e selvagens é uma solução potencial para diferenciar o comércio legítimo de leões em cativeiro do comércio ilegal de origem selvagem. Especificamente sobre quelônios, Hill *et al*. (2020), Hopkins *et al*. (2022, 2023), Sung *et al*. (2025) e Chatfield *et al*. (2026) demonstraram a aplicabilidade da análise isotópica de $\delta^{13}C$ e $\delta^{15}N$ de tecidos queratinizados de tartarugas de água doce para diferenciação entre origem cativa e silvestre.

Objetivos e estrutura da tese

Esta tese teve como objetivo central o desenvolvimento de uma abordagem multi-isotópica baseada em $\delta^{13}C$, $\delta^{15}N$ e $^{87}Sr/^{86}Sr$ para o estudo da dieta e distribuição geográfica de quelônios amazônicos, com foco na espécie *Podocnemis expansa* (tartaruga-da-amazônia).

O Capítulo 1 revisa a literatura sobre lavagem de animais silvestres (*wildlife laundering*) e lavagem de dinheiro associada ao tráfico de vida silvestre, traçando um panorama global sobre o tema. A partir dessa análise, o capítulo propõe uma definição abrangente para a lavagem de vida silvestre e discute a necessidade de integrar instrumentos de investigação financeira e abordagens antilavagem às estratégias de combate ao tráfico de animais. Por fim, aplica esse enquadramento ao contexto brasileiro, com avaliação crítica do arcabouço normativo atual e com uma proposta de aprimoramento legislativo e das políticas públicas de combate ao tráfico de fauna e flora no país.

O Capítulo 2 versa sobre um experimento de turnover isotópico com exemplares de tartaruga-da-amazônia (*Podocnemis expansa*), realizado com o propósito de estimar fatores de discriminação trófica e parâmetros da cinética de incorporação isotópica, como a constante de *turnover*, o tempo de residência isotópica e a meia-vida isotópica, para

diferentes tecidos (sangue, queratina do escudo, unha e pele). Dessa forma, pretendeu-se quantificar as velocidades com que as composições isotópicas desses tecidos respondem a mudanças na dieta, viabilizando inferências sobre momentos de transição alimentar dos animais. Tal análise é útil tanto para estudos de ecologia trófica, por exemplo ao permitir inferir a taxa de incorporação de novos recursos alimentares e eventuais mudanças no uso de habitats, quanto para aplicações forenses, como na definição da janela de detecção isotópica em cativeiro após captura ilegal na natureza e introdução em criatório para fins de esquentamento ou lavagem.

No Capítulo 3, a tese demonstra, por meio de um estudo aplicado conduzido na Amazônia brasileira, como isótopos estáveis de carbono e nitrogênio ($\delta^{13}C$ e $\delta^{15}N$) podem distinguir tartarugas de vida livre e de cativeiro, e como a razão isotópica de estrôncio ($^{87}Sr/^{86}Sr$) pode rastrear a origem geográfica de quelônios de água doce amazônicos. Os resultados evidenciam que animais de vida livre e de cativeiro se diferenciaram quanto aos valores de $\delta^{13}C$, o que fortalece seu uso como ferramenta aplicada à investigação de *wildlife laundering*, permitindo identificar animais selvagens potencialmente "esquentados" como cativos. O $\delta^{15}N$, por outro lado, demonstrou potencial para identificar padrões isotópicos particulares de cada criadouro. Além disso, os resultados de $^{87}Sr/^{86}Sr$ indicaram que as tartarugas refletem, em seus tecidos ósseos, a composição isotópica dos rios onde vivem, possibilitando assim inferir a origem geográfica de animais apreendidos e apoiar decisões periciais, de fiscalização e de reintrodução. No Capítulo 3 há também, em sua introdução, uma explicação sucinta sobre os conceitos básicos de isótopos estáveis (carbono e nitrogênio) e radiogênicos (estrôncio).

Em conjunto, os três capítulos articulam conservação, ciência forense e criminologia ambiental, mostrando que o combate ao tráfico de quelônios amazônicos exige tanto instrumentos institucionais e legais quanto ferramentas técnico-científicas capazes de sustentar decisões investigativas e judiciais. Ao conectar o problema do mercado ilegal com evidências laboratoriais baseadas na ciência isotópica, a tese propõe uma abordagem aplicada que pode contribuir tanto para qualificar a repressão ao crime ambiental quanto para aperfeiçoar estratégias de conservação baseadas em rastreabilidade e verificação de origem. Para além das aplicações forenses, os resultados do experimento de turnover isotópico fornecem um primeiro passo científico para futuros estudos de ecologia trófica de *Podocnemis expansa* e de outras espécies de quelônios dulcícolas da bacia amazônica.

Referências

Alexander J, Downs CT, Butler M, Woodborne S, Symes CT. 2019. Stable isotope analyses as a forensic tool to monitor illegally traded African grey parrots. *Animal Conservation* 22:134–143. DOI: 10.1111/acv.12445.

Alves RRN, Lima JR de F, Araújo HFP. 2013. The live bird trade in Brazil and its conservation implications: an overview. *Bird Conservation International* 23:53–65. DOI: 10.1017/S095927091200010X.

Alves RR da N, Nogueira EEG, Araujo HFP, Brooks SE. 2010. Bird-keeping in the Caatinga, NE Brazil. *Human Ecology* 38:147–156. DOI: 10.1007/s10745-009-9295-5.

Andrade PCM, Azevedo SH, Duarte JAM, Garcez JR, Oliveira PHG, Pinto JRS, Almeida Jr. CD. 2015. *Projeto Pé-de-pincha: Conservação e manejo de quelônios - Manual para Gestores Ambientais*. Manaus: Unisol/UFAM.

Andrade MVO, Lasmar MC. 2020. Uso de Isótopos Forenses - Panorama Internacional. *Revista Perícia Federal*:38–41.

Antunes AP, Fewster RM, Venticinque EM, Peres CA, Levi T, Rohe F, Shepard GH. 2016. Empty forest or empty rivers? A century of commercial hunting in Amazonia. *Science Advances* 2:e1600936. DOI: 10.1126/sciadv.1600936.

Bates HW. 1873. *The Naturalist on the River Amazon*. London: John Murray.

Bohórquez L. 2018. Desmantelado en Mallorca uno de los mayores criaderos ilegales de tortugas de Europa. *Available at https://elpais.com/politica/2018/08/22/actualidad/1534924731_345036.html* (accessed January 13, 2026).

Brasileiro L, Mayrink RR, Pereira AC, Costa FJV, Nardoto GB. 2023. Differentiating wild from captive animals: an isotopic approach. *PeerJ* 11. DOI: 10.7717/peerj.16460.

Brazil MVS, Chaves WA, Vidal MD, Tavares AS, Wilcove DS. 2025. The potential and limitations of turtle farming to contribute to conservation in the Brazilian Amazon. *Biological Conservation* 304:111055. DOI: 10.1016/j.biocon.2025.111055.

Campos-Silva J V., Hawes JE, Andrade PCM, Peres CA. 2018. Unintended multispecies co-benefits of an Amazonian community-based conservation programme. *Nature Sustainability* 1:650–656. DOI: 10.1038/s41893-018-0170-5.

Cerling TE, Andanje SA, Gakuya F, Kariuki JM, Kariuki L, Kingoo JW, Khayale C, Lekolool I, Macharia AN, Anderson CR, Fernandez DP, Hu L, Thomas SJ. 2018. Stable isotope ecology of black rhinos (Diceros bicornis) in Kenya. *Oecologia* 187:1095–1105. DOI: 10.1007/s00442-018-4185-4.

Charity S, Ferreira JM. 2020. *Wildlife Trafficking in Brazil*. Cambridge: TRAFFIC International.

Chatfield MWH, Frederick CA, Yorks D, Pollock E, Hopkins JB. 2026. Combating the illegal turtle trade using chemical markers. *The Journal of Wildlife Management* 90. DOI: 10.1002/jwmg.70141.

Chaves WA, Monroe MC, Sieving KE. 2019. Wild Meat Trade and Consumption in the Central Amazon, Brazil. *Human Ecology* 47:733–746. DOI: 10.1007/s10745-019-00107-6.

Chesson LA, Barnette JE, Bowen GJ, Brooks JR, Casale JF, Cerling TE, Cook CS, Douthitt CB, Howa JD, Hurley JM, Kreuzer HW, Lott MJ, Martinelli LA, O'Grady SP, Podlesak DW, Tipple BJ, Valenzuela LO, West JB. 2018. Applying the principles of isotope analysis in plant and animal ecology to forensic science in the Americas. *Oecologia* 187:1077–1094. DOI: 10.1007/s00442-018-4188-1.

Costa FJV, Ferreira JM, Monteiro KRG, Mayrink RR. 2017. *Ciência contra o Tráfico - Avanços no Combate ao Comércio Ilegal de Animais Silvestres*. João Pessoa: Imprell.

Costa FJV, Sena-Souza JP, Nardoto GB. 2019. Determinação da origem geográfica de vestígios utilizando isótopos estáveis: base científica e potencial de uso no Brasil. *Revista Brasileira de Ciências Policiais* 10:15–54.

Destro GFG, Lucena T, Monti R, Cabral R, Barreto R. 2012. Efforts to Combat Wild Animals Trafficking in Brazil. In: *Biodiversity Enrichment in a Diverse World*. InTech. DOI: 10.5772/48351.

Gilmore RM. 1986. Fauna e etnozoologia da América do Sul tropical. In: Ribeiro D ed. *Suma Etnológica Brasileira*. Petrópolis: Vozes, Finep, 187–234.

Gopi K, Mazumder D, Sammut J, Saintilan N, Crawford J, Gadd P. 2019. Isotopic and elemental profiling to trace the geographic origins of farmed and wild-caught Asian seabass (*Lates calcarifer*). *Aquaculture* 502:56–62. DOI: 10.1016/j.aquaculture.2018.12.012.

Hill KGW, Nielson KE, Tyler JJ, Mcinerney FA, Doubleday ZA, Frankham GJ, Johnson RN, Gillanders BM, Delean S, Cassey P. 2020. Pet or pest? Stable isotope methods for determining the provenance of an invasive alien species. *NeoBiota* 59:21–37. DOI: 10.3897/NEOBIOTA.59.53671.

Hopkins JB, Frederick CA, Yorks D, Pollock E, Chatfield MWH. 2022. Forensic Application of Stable Isotopes to Distinguish between Wild and Captive Turtles. *Biology* 11. DOI: 10.3390/biology11121728.

Hopkins JB, Frederick CA, Yorks D, Pollock E, Chatfield MWH. 2023. Advancing Forensic Chemical Analysis to Classify Wild and Captive Turtles. *Diversity* 15. DOI: 10.3390/d15101056.

Hutchinson A, Roberts DL. 2020. Differentiating captive and wild African lion (Panthera leo) populations in South Africa, using stable carbon and nitrogen isotope analysis. *Biodiversity and Conservation* 29:2255–2273. DOI: 10.1007/s10531-020-01972-0.

ICMBio. 2016. Operação devolve à natureza 800 tartarugas-da-Amazônia. *Available at https://www.gov.br/icmbio/pt-br/assuntos/noticias/ultimas-noticias/operacao-devolve-a-natureza-800-tartarugas-da-amazonia* (accessed October 16, 2024).

Jiguet F, Kardynal KJ, Hobson KA. 2019. Stable isotopes reveal captive vs wild origin of illegally captured songbirds in France. *Forensic Science International* 302. DOI: 10.1016/j.forsciint.2019.109884.

Kemenes A, Pezzuti JCB. 2007. Estimate of Trade Traffic of Podocnemis (Testudines, Pedocnemididae) from the Middle Purus River, Amazonas, Brazil. *Chelonian Conservation and Biology* 6(2):259–262. DOI: 10.2744/1071-8443(2007)6[259:EOTTOP]2.0.CO;2.

Kuhnen VV, Remor JO, Lima R. 2012. Breeding and trade of wildlife in Santa Catarina state, Brazil. *Brazilian Journal of Biology* 72, 59-64.

Lovich JE, Ennen JR, Agha M, Whitfield Gibbons J. 2018. Where have all the turtles gone, and why does it matter? *BioScience* 68:771–781. DOI: 10.1093/biosci/biy095.

Luz VL, Malvasio A, Balestra RAM, Salera Jr. G, Souza VL, Portelinha TCG, Uhlig VM, Portal RR. 2022. Conservation of Amazon Freshwater Turtles in Brazil. In: Lacava R V., Balestra RAM eds. *Brazilian Action Plan for the Conservation of Amazon Freshwater Turtles*. Brasília: IBAMA, 11–18.

Mayrink RR. 2016. Exame pericial para detecção de fraudes em anilhas oficiais de passeriformes: uma ferramenta para o combate ao tráfico de animais silvestres. Florianópolis: Universidade Federal de Santa Catarina.

Mayrink RR, Costa FJV, Queiroz ALL, Santos Filho AMP. 2021. Medicina veterinária forense. In: *Ciências Forenses - Uma Introdução às Principais Áreas da Criminalística*. Campinas: Millennium.

Nardoto GB, Ribeiro JF, Sena-Souza JP, Guaraldo AC, Saquetti CH. 2017. Rastreamento Forense: Uso dos Isótopos Estáveis no Combate ao Crime. In: Costa FJV, Ferreira JM, Monteiro KRG, Mayrink RR eds. *Ciência contra o Tráfico: Avanços no Combate ao Comércio Ilegal de Animais Silvestres*. João Pessoa: Imprell, 51–78.

Natusch DJD, Carter JF, Aust PW, Van Tri N, Tinggi U, Mumpuni, Riyanto A, Lyons JA. 2017. Serpent's source: Determining the source and geographic origin of traded python skins using isotopic and elemental markers. *Biological Conservation* 209:406–414. DOI: 10.1016/j.biocon.2017.02.042.

Nucci GDS. 2016. *Código de Processo Penal Comentado*. Rio de Janeiro: Forense.
Pantoja-Lima J, Aride PHR, de Oliveira AT, Félix-Silva D, Pezzuti JCB, Rebêlo GH. 2014. Chain of commercialization of Podocnemis spp. turtles (Testudines: Podocnemididae) in the Purus River, Amazon Basin, Brazil: Current status and perspectives. *Journal of Ethnobiology and Ethnomedicine* 10. DOI: 10.1186/1746-4269-10-8.
de Paula Silva LA, Michalski F, Norris D. 2025. Anthropogenic threats increase vulnerability of Podocnemis unifilis nesting areas in the most protected Brazilian Amazon State. *Frontiers in Ecology and Evolution* 13. DOI: 10.3389/fevo.2025.1622535.
Pereira LA, Santos R V., Hauser M, Duponchelle F, Carvajal F, Pecheyran C, Bérail S, Pouilly M. 2019. Commercial traceability of Arapaima spp. fisheries in the Amazon Basin: Can biogeochemical tags be useful. *Biogeosciences* 16:1781–1797. DOI: 10.5194/bg-16-1781-2019.
Polícia Federal. 2014. Operação Podocnemis combate a prática de crime ambiental em dois estados. *Available at https://www.pf.gov.br/agencia/noticias/2014/08/operacao-podocnemis-combate-a-pratica-de-crime-ambiental-em-dois-estados* (accessed July 29, 2020).
Rebêlo G, Pezzuti J. 2000. Percepções sobre o consumo de quelônios na Amazônia: sustentabilidade e alternativas ao manejo atual. *Ambiente & Sociedade*: 85–104. DOI: 10.1590/S1414-753X2000000100005.
Rhodin AGJ, Iverson JB, Bour R, Fritz U, Georges A, Shaffer HB, van Dijk PP. 2017. Turtles of the world: Annotated Checklist and Atlas of Taxonomy, Synonymy, Distribution and Conservation Status. In: Rhodin AGJ, Iverson JB, van Dijk PP, Saumure RA, Buhlmann KA, Pritchard PCH, Mittermeier RA eds. *Conservation Biology of Freshwater Turtles and Tortoises: A Compilation Project of the IUCN/SSC Tortoise and Freshwater Turtle Specialist Group. Chelonian Research Monographs*. 1–292. DOI: 10.3854/cmr.7.checklist.atlas.v8.2017.
Salera Jr. G, Balestra RAM, Luz VLF. 2016. Breve histórico da conservação dos quelônios amazônicos no Brasil. In: Balestra RAM ed. *Manejo Conservacionista e Monitoramento Populacional de Quelônios Amazônicos*. Brasília, 11–14.
Santos CFM, Fiori MM. 2020. Turtles, Indians and settlers: Podocnemis expansa exploitation and the Portuguese settlement in eighteenth-century Amazonia. *Topoi (Brazil)* 21:350–373. DOI: 10.1590/2237-101X02104404.
Stassart JS, Cardoso Jr. D. 2024. *A lavanderia de fauna silvestre: como riscos de fraude, corrupção e lavagem viabilizam o tráfico de vida silvestre*. São Paulo: Transparência Internacional Brasil. 137 p.
Sung Y-H, Liew JH, Chan WS, Fok AWL, Leung J, Wong HF, Baker DM, Bonebrake TC, Dingle C, Dudgeon D, Karraker NE, Lau A, Colon VA, Magouras I, Ades G, Crow P, Rose-Jeffreys L, Spencer R, Fong JJ. 2025. Stable isotope analysis successfully identifies wild-caught individuals of threatened Asian freshwater turtles in illegal trade. *Global Ecology and Conservation* 64:e03947. DOI: 10.1016/j.gecco.2025.e03947.
Velho JA, Geiser GC, Espindula A. 2021. Introdução às ciências forenses. In: Velho JA, Geiser GC, Espindula A eds. *Ciências forenses: uma introdução às principais áreas da criminalística moderna*. Campinas: Millennium, 1–18.
Tensen L. 2016. Under what circumstances can wildlife farming benefit species conservation? *Global Ecology and Conservation* 6:286–298. DOI: 10.1016/j.gecco.2016.03.007.
van Uhm DP. 2018. Wildlife and laundering: interaction between the under and upper world. In: Spapens T, White R, van Uhm D, Huisman W eds. *Green Crimes and Dirty Money*. Routledge, 197–214.
Ziegler S, Merker S, Streit B, Boner M, Jacob DE. 2016. Towards understanding isotope variability in elephant ivory to establish isotopic profiling and source-area determination. *Biological Conservation* 197:154–163. DOI: 10.1016/j.biocon.2016.03.008.

CAPÍTULO 1

WILDLIFE LAUNDERING AND MONEY LAUNDERING ASSOCIATED WITH THE ILLEGAL WILDLIFE TRADE: A GLOBAL OVERVIEW AND INSIGHTS FOR THE BRAZILIAN CONTEXT

Abstract

Wildlife trade (whether legal or illegal) is a large-scale worldwide phenomenon, with major biodiversity impacts and substantial financial flows. Increasing attention to the interface between legal and illegal markets has intensified research on wildlife laundering and money laundering associated with illegal wildlife trade (IWT). This chapter synthesizes the most recent scientific literature on wildlife laundering and money laundering linked to IWT, clarifies key concepts, examines relevant dimensions of these issues, and discusses implications for Brazil's legal and enforcement framework. Using the search terms "wildlife" and "launder*," we surveyed publications from the 1970s to 2024 in Web of Science and Google Scholar, identifying 354 sources: 196 peer-reviewed articles, 49 books or book chapters, and 109 grey literature documents. We categorized all publications by year and assessed peer-reviewed papers using 16 qualitative criteria. Most studies originated from the United States and the United Kingdom and focused primarily on Asia, Africa, and North America. More than 60 species were examined, mainly mammals, reptiles, and birds. From this synthesis, we propose a comprehensive, detailed definition of wildlife laundering. Overall, the evidence indicates that wildlife laundering is a sophisticated mechanism within IWT, particularly because it is intertwined with the formal wildlife production and trade sector. Due to its close relationship with money laundering, wildlife laundering requires coordinated and targeted action by both environmental enforcement agencies and financial authorities. Although global efforts to address IWT-related money laundering are emerging, substantial gaps persist both in Brazil and internationally. In Brazil – the world's most biodiverse country – wildlife laundering is a prevalent mechanism that enables illegal exploitation of native fauna and flora. Therefore, tackling wildlife laundering should be a core component of public policies aimed at curbing wildlife crime. This chapter strengthens understanding of wildlife laundering and IWT-linked money laundering and provides an evidence base for decision-makers and stakeholders, particularly those working to improve Brazil's regulatory framework on this issue.

Keywords: wildlife laundering, money laundering, wildlife trafficking, illegal wildlife trade, IWT, wildlife crime

HIGHLIGHTS

- Publications on wildlife laundering and money laundering linked to illegal wildlife trade (IWT) have grown since the 1970s, especially in the past decade.
- Wildlife laundering is a sophisticated mechanism in IWT and is closely intertwined with money laundering.
- Money laundering linked to IWT has distinctive features, deserving focused attention from both environmental and financial authorities.
- Efforts to address money laundering linked to IWT are starting to take shape on a global scale.
- In Brazil, tackling wildlife laundering and associated money laundering must be a core focus of public policies against IWT.

1.1 – Introduction

Wildlife trade is a major global driver of biodiversity loss (Mozer & Prost, 2023). Both authorized formal commerce and illegal wildlife trade (IWT) generate substantial financial revenues on a global scale (Fukushima, Mammola & Cardoso, 2020). The CITES (Convention on International Trade in Endangered Species of Wild Fauna and Flora) database indicates that over 100 million wild plants and animals are legally traded internationally each year (Harfoot *et al*., 2018). Given that CITES only regulates a small portion of the world's species (Mora *et al*., 2011; CITES, 2025), the total number of specimens traded is certainly much higher. This significant volume exerts a considerable impact on biodiversity: of the more than 31,000 species of terrestrial vertebrates, nearly one in five (approximately 24%) are affected by any form of trade; and predictions indicate that, in the future, more than 11,000 species will be at risk of extinction due to trade (Scheffers *et al*., 2019). The CITES database further indicates that the financial revenue generated by this economic activity is substantial. Over a 20-year period (from 1997 to 2016), the global legal trade in wildlife – including timber and fisheries – generated annual proceeds ranging from USD 2.9 trillion to USD 4.4 trillion (Andersson *et al*., 2021b). As an additional example, in China alone the wild-animal breeding sector is valued at approximately USD 8 billion annually (Roe & Lee, 2021). Regarding IWT, estimates from international organizations such as Interpol, the United Nations, and the World Bank suggest that it generates between USD 7 billion and USD 23 billion annually. This figure may escalate to between USD 48

billion and USD 216 billion when also accounting for illegal deforestation and illegal, unreported and unregulated fishing (Nellemann *et al*., 2016, 2018; World Bank, 2019).

In addition to the financial volume, IWT is often interconnected with other criminal activities such as corruption, document forgery, tax fraud, money laundering, trafficking in other illicit goods (drugs, weapons, precious minerals) and terrorism (Anagnostou & Doberstein, 2022). Another significant consequence of this illegal activity is the emergence of public-health risks. The majority of emerging infectious diseases that affect humans are zoonotic in origin, with a substantial proportion associated with wildlife (Cardoso *et al*., 2021). In addition to syndromes such as HIV, H1N1, H5N1, MERS, Ebola, SARS and Mpox, the recent COVID-19 pandemic has been hypothesized to be associated with wildlife markets (Mallapaty, 2025). This scenario highlights that, alongside substantial economic costs, the trade in wild animals can lead to serious loss of human lives (Aguiar *et al*., 2025).

Global demand for wild animals, fisheries, timber, and other wildlife products is steadily increasing, accompanied by a rising production and trade of fauna and flora products, including commerce through online platforms (Hinsley & Roberts, 2018; Boyd, McNevin & Davis, 2022; FAO, 2022; Meeks, Morton & Edwards, 2024). Concurrently, societies, governments, and international organizations are becoming increasingly vigilant in their efforts to protect biodiversity and combat IWT (ECOFEL, 2021; Cardoso *et al*., 2021). For instance, since 2015 the United Nations General Assembly has classified IWT as a serious crime and has repeatedly issued recommendations to Member States to enhance efforts to tackle this illicit activity (United Nations, 2015, 2025).

Given this context, it is increasingly important to understand the interface between legal and illegal wildlife trade, within which the phenomenon of wildlife laundering emerges. Wildlife laundering is a sophisticated mechanism associated with IWT, in which legal businesses are typically used to commingle licit and illicit transactions. Furthermore, from both conceptual and legal perspectives, it is closely related to money laundering. Therefore, the development of approaches to detect wildlife laundering and the use of financial investigations into wildlife crime are key strategies for dismantling IWT networks (FATF, 2020a; ECOFEL, 2021; Lupton, 2023).

Brazil is the most biodiverse country in the world and historically faces IWT and wildlife laundering. As an example, one of the earliest references in the scientific literature concerning wildlife laundering reported blue macaws being trafficked from Brazil to Bolivia

and then "legally" exported to the US, circumventing the prohibition of Brazilian legislation (Holden, 1979). Despite many legislative advances and enforcement efforts, the country still faces gaps in effectively addressing IWT and wildlife laundering (Charity & Ferreira, 2020).

The aim of this paper is (i) to review publications addressing wildlife laundering and money laundering associated with IWT; (ii) to analyze the conceptual, technical and legal aspects of wildlife laundering and money laundering associated with IWT; and (iii) to situate the analysis in Brazil, the most biodiverse country in the world. We compiled peer-reviewed articles, books, book chapters, and grey literature published from the 1970s to 2024. Based on the information gathered in the review, we propose a comprehensive and detailed definition of wildlife laundering, a gap that remains insufficiently addressed in the literature. We further assess the distinctive features of IWT-related money laundering and the emerging global efforts to counter it. Considering the Brazilian context, we analyze the country's current legal framework on the subject and propose incorporating the considerations discussed here into legislative reforms and public policies aimed at curbing IWT.

1.2 – Methods

We conducted a comprehensive compilation of the scientific literature by searching the Web of Science database (core collection), using the terms "wildlife" and "launder*" (a root applicable to both "laundering" and "laundered"). We did not specify a start date and set the end date to December 31, 2024. This search returned 57 peer-reviewed papers, from which five were excluded due to thematic divergence ("launder*" used in unrelated contexts). A similar search on the Google Scholar platform identified an additional 144 peer-reviewed papers, 49 books or book chapters, and 109 grey literature documents (reports from international organizations or NGOs, magazine articles, and other sources). This process culminated in a total of 354 publications, which were then categorized by their year of publication, ranging from 1977 to 2024.

The 196 peer-reviewed articles were then subjected to individual analysis to collect information categorized according to 16 qualitative parameters (Table 1). This content analysis was not conducted on books, book chapters, and grey literature to avoid overlapping information, as these publications typically rely on data or citations from original peer-reviewed papers. It is essential to note that many other articles address or touch on the subject, albeit without explicitly referencing the terms used in this review, such as Brancalion *et al*. (2018), Brasileiro *et al*. (2023), and Varrà *et al*. (2021). Due to the

impracticality of searching for these papers using specific terms, these publications were not included in the compilation; however, their existence demonstrates the extensive breadth of the subject within the scientific literature.

To characterize the Brazilian context, we also examined national legislation, case law, academic theses, and NGO reports. Drawing on these sources, we conducted a critical assessment of the Brazilian legal framework on the subject and proposed incorporating the considerations discussed here into legislative reforms and public policies to strengthen the response to wildlife laundering and IWT-linked money laundering in the country.

Table 1
Qualitative parameters examined in the 196 peer-reviewed articles.

Parameter	Description
Year	Year of publication (parameter collected for all 354 publications)
Journal area	The thematic area of the journal where the article was published
Country of publication	Country of institutional affiliation of the first author of the article
Continent of publication	Continent to which the country of the main author's institution belongs
Single or multiple countries	If the focus of the article is one or more countries
Country(ies) studied	Country mentioned as the focus of the article
Continent(s) studied	Continent to which the country under study belongs
Intensity of mention	Simple mention: This describes instances where the article only references the terms “wildlife” and “launder*” without further elaboration or analysis of the subject. Consistent approach: This refers to studies that actively engage with the topic, aiming to analyze, discuss, or explore it within the context of the research. Central theme: This applies to cases where “wildlife” and “launder*” serve as the primary focus of the article’s thematic investigation.
Wildlife laundering or money laundering	Whether the terms “wildlife” and “launder*” mentioned in the article refer to “wildlife launder*”, “wildlife” + “money launder*”, or both.
Involvement of breeders, growers or managers	Whether the article addresses wildlife laundering linked to fraud within production systems—such as breeding wild animals, cultivating plants, or managing wild species—or to fraud involving geographic origin or species substitution.
Taxonomic group	Mammals, reptiles, birds, amphibians, fish, invertebrates or plants
Taxon	Species or taxon as detailed as possible
Mention of CITES	Whether the article mentions CITES in the context of its research
Mention of Brazil	Whether the article mentions Brazil (even if not as the primary focus) or references Brazilian species.
Criminal convergence	Criminal offences mentioned in the article, in parallel with IWT
Forensic techniques	Forensic techniques cited in the article as tools for detecting wildlife laundering

1.3 – Results

1.3.1 – Literature synthesis

According to the publications compiled in this analysis, the term "wildlife laundering" was first introduced in the scientific literature in 1977 by Richard D. Smith in his article "The Monkey Business", which addressed the global trade in primates for scientific research (Smith, 1977). As a historical record, it is important to highlight the US Lacey Act, a law with worldwide significance as it prohibits the importation of fauna (including fisheries) and flora into the US if they were taken, possessed, transported, or sold in violation of any foreign law. Enacted in 1900 and still in force today, the law's original objective was to curb the possession and trade of supposedly legalized wild animals sourced from illegal hunting across US states with varying hunting prohibition statuses (Anderson, 1995). Although it does not explicitly mention the term "wildlife laundering", the Lacey Act was, therefore, a pioneering milestone in fighting this crime already at the turn of the 20th century.

Since the 1970s, the number of publications has shown an upward trend, with a particularly significant increase over the past decade (Fig. 1). The years 2016 and 2020 stand out due to the high number of publications. In 2016, Elliott and Schaedla published the Handbook of Transnational Environmental Crime, a book featuring 27 chapters of which 16 cite the search terms (Elliott & Schaedla, 2016).

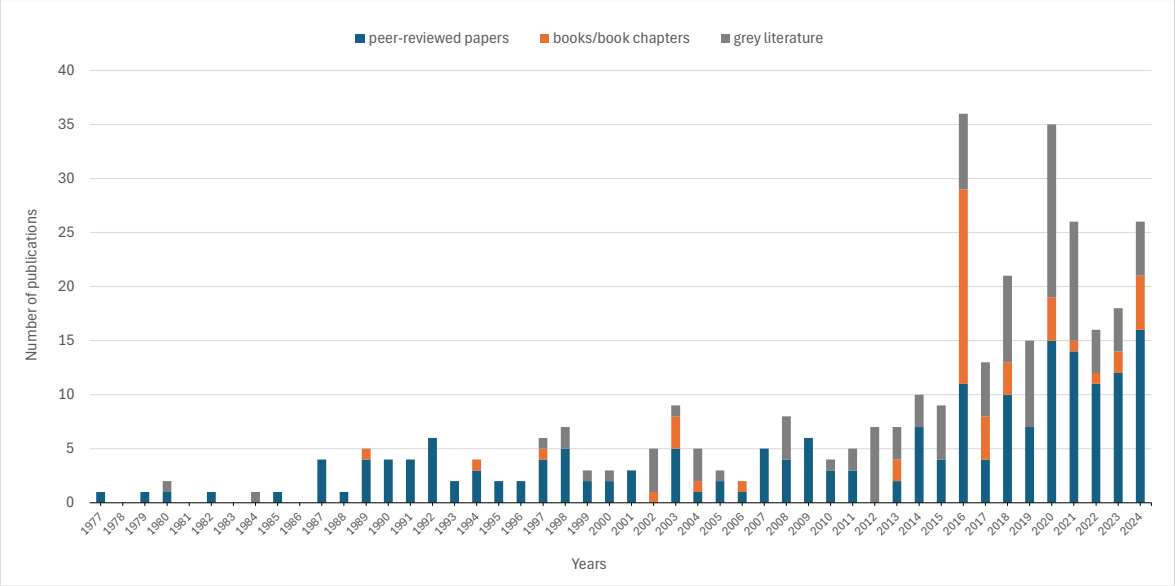

Figure 1 – Time series of the 354 publications in the scientific literature resulting from the search using the terms "wildlife" and "launder*" including peer-reviewed papers, books or book chapters, and grey literature documents.

The 196 peer-reviewed articles compiled in this review span diverse approaches, ranging from theoretical and legal analyses of international wildlife-trade treaties and conventions (e.g. Vice, 1997) to the development of forensic techniques (Andersson *et al*., 2021a) as well as case studies of wildlife laundering (Lyons & Natusch, 2011) and analyses of port vulnerability to landings of illegal, unreported, and unregulated (IUU) fish (Petrossian *et al*., 2015), among others. As a result, there was a great diversity in the thematic areas of the journals in which the articles were published (Fig. 2). Although relatively limited in number, publications in the field of financial crime also merit attention (Johnson, 2001; FATF, 2020a; ECOFEL, 2021; Lupton, 2023; Sullivan, 2023; Haris, 2024). Their presence in the literature reflects the growing recognition of wildlife laundering and IWT-related money laundering within economic and financial disciplines in recent years, extending the discussion beyond the field of biodiversity conservation.

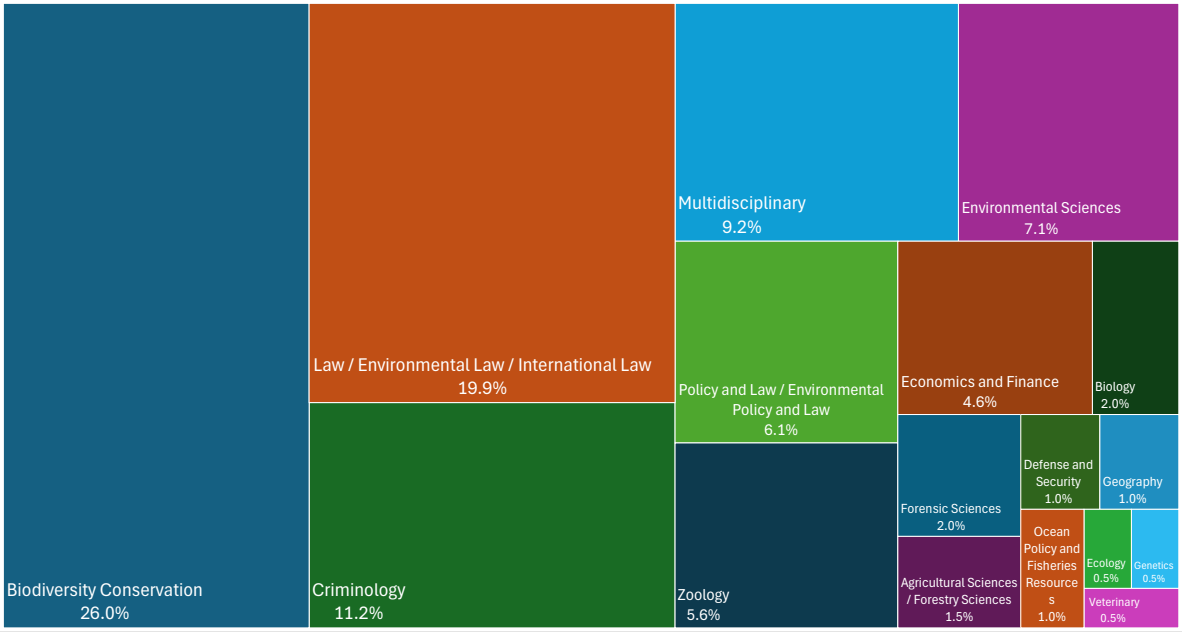

Figure 2 – Frequency panel displaying the knowledge areas of the journals in which the 196 peer-reviewed papers were published.

A total of 91 countries were identified as the focus of study in the articles (Fig. 3-A). The focal countries were located mainly in Asia (43.4%, n = 85), North America (22.4%, n = 44), and Africa (21.4%, n = 42). The remaining countries are from Europe (14.3%, n = 28), South America (8.7%, n = 17), Central America (3.1%, n = 6), Oceania (3.1%, n = 6), and Antarctica (0.5%, n = 1) (one paper may have focused on more than one continent). There were also 8.7% of the articles (n = 17) with a global perspective and 16.8% (n = 33) with a non-geographical approach. Among the most frequent countries, US and China tied for first place (21.4%, n = 42 each), followed by Vietnam (10.7%, n = 21), South Africa (9.7%, n = 19), United Kingdom (9.2%, n = 18), Hong Kong and Japan (8.2%, n = 16 each), Indonesia (7.7%, n = 15), Russia (6.1%, n = 12), Thailand (5.6%, n = 11), Singapore (5.1%, n = 10), Taiwan and Kenya (4.1%, n = 8 each), Cambodia, India, Zimbabwe, Australia and France (3.6%, n = 7 each) and Brazil, South Korea, Namibia and Spain (3.1%, n = 6 each).

With the aim of researching the origin of the scientific knowledge production on the subject, we also classified the papers according to the country of the first author's institutional affiliation (Fig. 3-B). Publications were concentrated in North America (37.2% of the articles, n = 73) and Europe (31.1%, n = 61), followed by Asia (12.2%, n = 24), Oceania (7.7%, n = 15), Africa (5.1%, n = 10), South America (1.5%, n = 3), and Central America (0.5%, n = 1); with 4.6% of the articles (n = 9) whose origin could not be determined. Fig. 3-B represents the distribution by country of origin, showing a strong concentration of publications by authors from the US (31.6%, n = 62) and the UK (18.9%, n = 37).

More than 60 species of animals and plants were studied or mentioned in the articles, belonging to various taxonomic groups (Fig. 3-C). Mammals emerged as the most frequent group, with notable focus on large African mammals such as elephants, referenced in 20.9% of the articles (n = 41), and rhinos (10.2%, n = 20). There was also a considerable proportion of articles (24.0%, n = 47) that had a general approach concerning taxa, without direct mention of any species or groups.

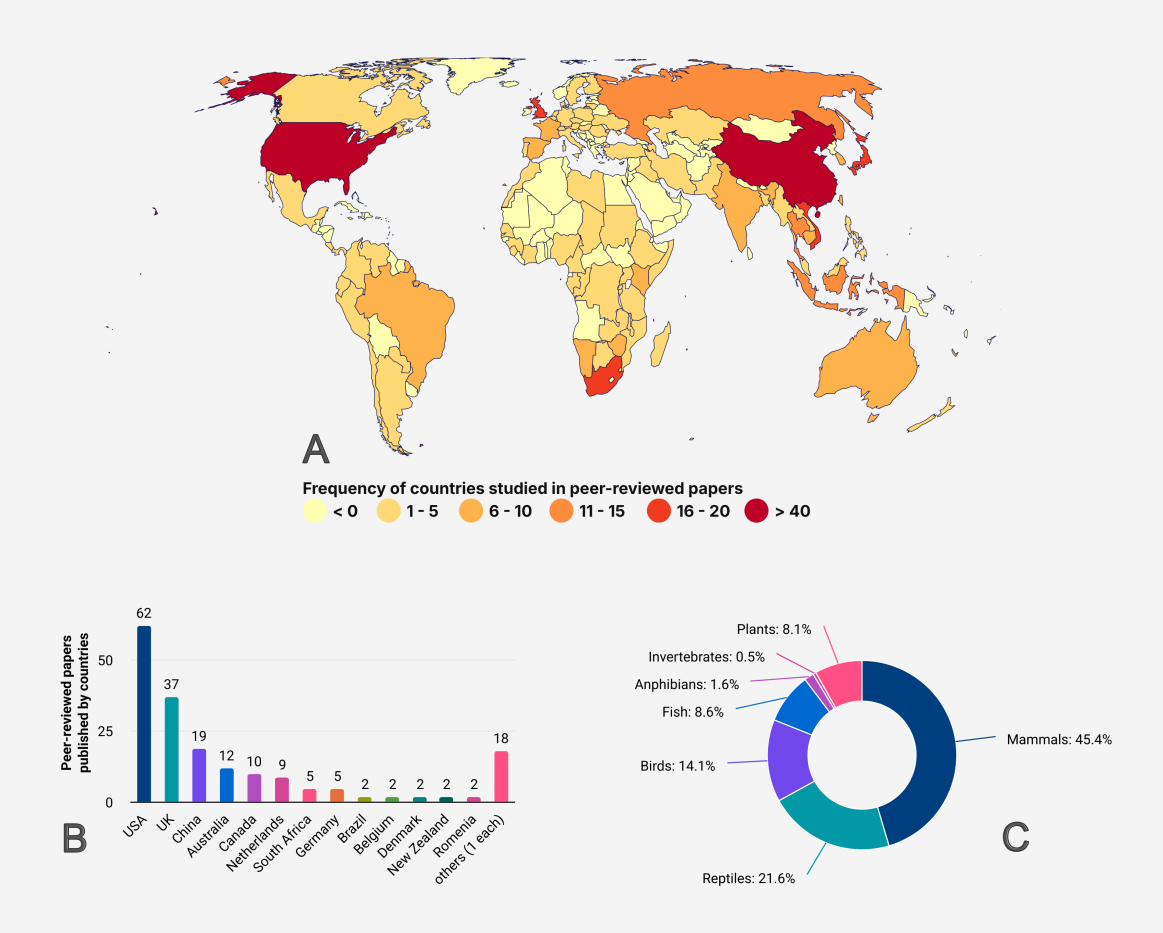

Figure 3 – Global overview of the 196 peer-reviewed articles searched for the terms "wildlife" and "launder*". Figure 3-A presents how frequently each country was the focal point of study in the papers. Figure 3-B displays the number of articles published by country, based on the institutional affiliation of the first author. Figure 3-C illustrates the frequency of taxonomic groups covered in the papers.

The searched terms "wildlife" and "launder*" referred to "wildlife laundering" in 79.1% of the papers (n = 155), to "wildlife" and "money laundering" in 13.8% of the publications (n = 27), and to both in 7.1% (n = 14). Wildlife laundering or money laundering associated with IWT was the central theme of 5.6% of the articles (n = 11), while 44.9% of the papers (n = 88) addressed the subjects consistently, and 49.5% (n = 97) merely cited them. Regarding the types of wildlife laundering (as conceptualized in section 1.3.2.3), from a subset of 169 papers, laundering involving the participation of breeders, growers or managers of wild species was reported in 52.1% of cases (n = 88). In contrast, laundering involving fraud in geographic origin or taxonomic identification (species substitution) occurred in 36.7% of cases (n = 62), whereas 11.2% of articles (n = 19) did not specify the type. CITES was mentioned in 83.7% of the articles (n = 164), while Brazil or Brazilian species were mentioned in 15.3% (n = 30).

The phenomenon of criminal convergence (Anagnostou & Doberstein, 2022) was prevalent in the articles. We detected 21 types of crime associated with IWT, the most frequent being corruption (61.2% of the papers, n = 52), document fraud (51.8%, n = 44), money laundering (43.5%, n = 37) and drug trafficking (16.5%, n = 14). Fig. 4 presents a word cloud illustrating the criminal convergence identified in the reviewed papers, whereas Fig. 5 shows all identified crime categories and their respective percentages. Finally, forensic techniques for detecting wildlife laundering were cited in 20.9% of the articles (n = 41). Among the 51 citations present in these papers (one paper may have cited more than one method), genetics was the most commonly employed technique, accounting for 52.9% of the citations (n = 27). Isotopic analysis ranked second (23.5%, n = 12), followed by elementary chemical analysis (9.8%, n = 5), and morphological assessment (7.8%, n = 4). Other techniques collectively contributed to 5.9% of the instances (n = 3).

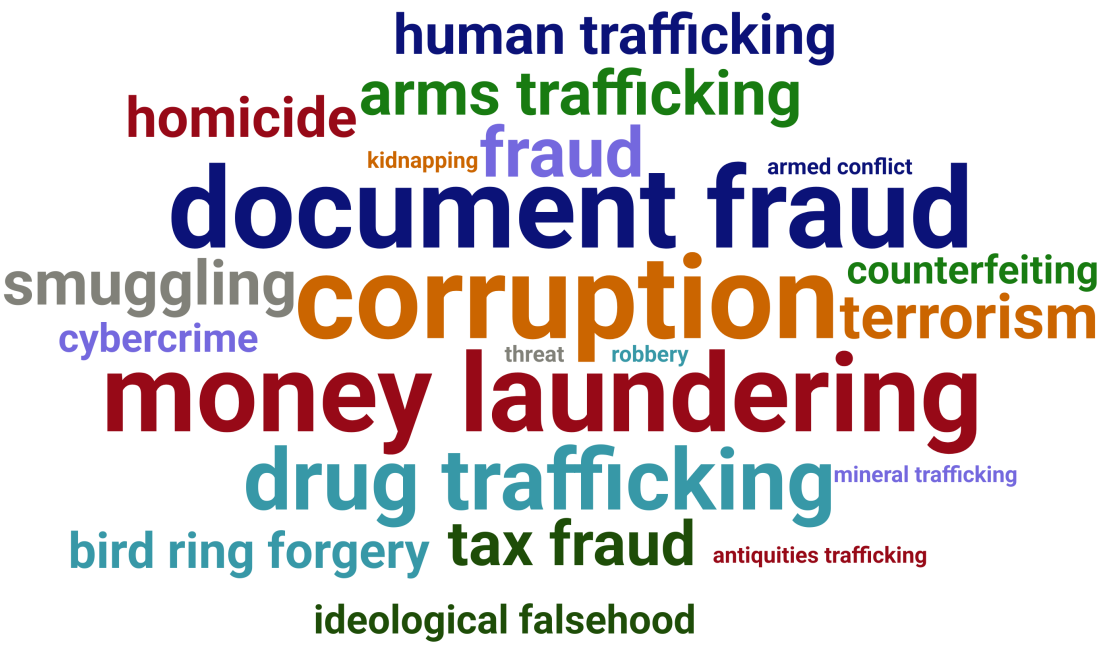

Figure 4 – Word cloud of the criminal convergence related to IWT identified in the 196 peer-reviewed papers.

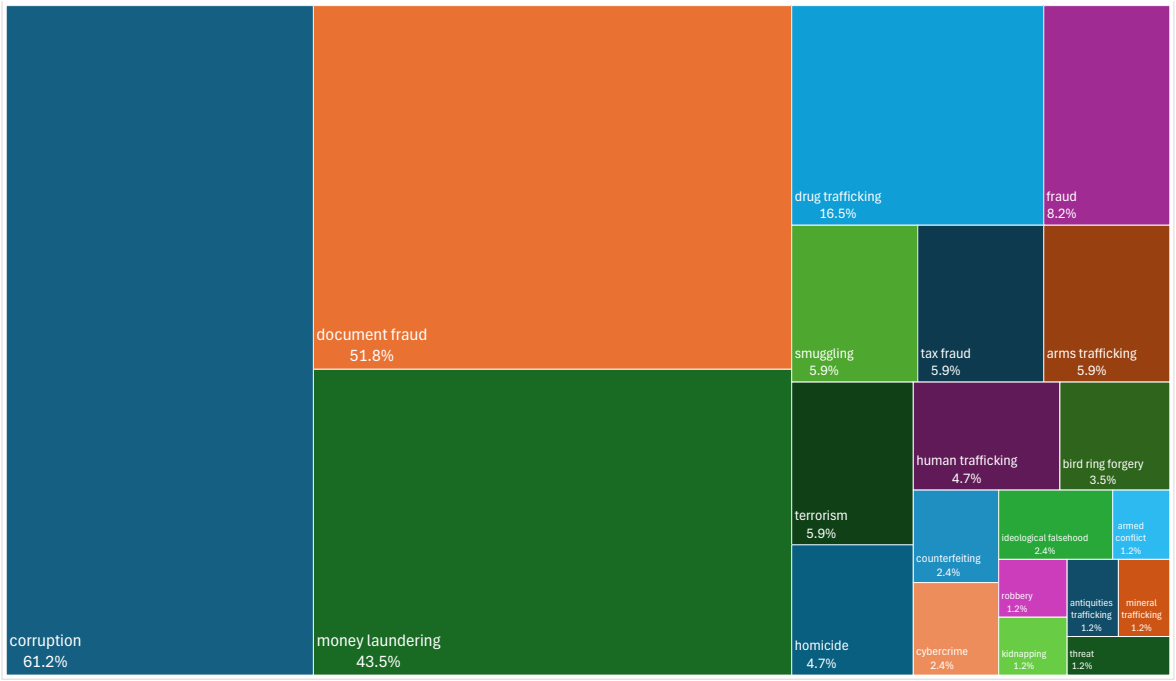

Figure 5 – Frequency panel of the criminal convergence related to IWT identified in the 196 peer-reviewed papers.

1.3.2 – Conceptual analysis

1.3.2.1 – Concept of wildlife

The scientific literature diverges on how broadly the term wildlife should be conceptualized. Cardoso *et al*. (2021) note that the term is often used in a limited sense, referring only to wild animals, especially terrestrial vertebrates. In this sense, the term does not encompass plants/timber or even fish (fishery resources). For example, a joint report by Interpol and UNEP (United Nations Environment Programme) divides environmental crimes into five categories: illegal wildlife trade, forest crime, fisheries crimes, illegal mining, and illegal disposal of polluting waste (Nellemann *et al*., 2016). In turn, Kazmar (2000) distinguishes between animals and plants, reserving the term wildlife only for the former. In contrast to this narrow scope, many other publications adopt a broader interpretation of the term wildlife, encompassing wild animals (including invertebrates and fishery resources), plants (including timber), and even fungi (Margulies *et al*., 2019; Dickinson, 2022; Hinsley, Hughes & Margulies, 2024; Oyanedel, Levi & Furci, 2024). Our approach aligns with this broader interpretation by adopting the widest possible understanding of the term wildlife.

1.3.2.2 – Concept of laundering

In relation to IWT, Viollaz *et al*. (2018) describe laundering as "the legitimization of resources from an illegal act through fraud and false indication of their origin". In general terms, this concept aligns with the specialized literature on financial crimes, which often associates "laundering" with "money", creating the term "money laundering" (Sullivan, 2023; Goodell *et al*., 2025). More detailed definitions emphasize, however, that laundering can occur not only with money but also with any goods or property derived directly or indirectly from a criminal offence. Therefore, laundering of all kinds of assets derived from crimes is conceptually equivalent to money laundering (Riccardi & Reuter, 2024).

The concept of money laundering was set out in the United Nations (UN) Vienna 1988 Convention against Illicit Traffic in Narcotic Drugs and Psychotropic Substances as "the conversion or transfer of property, knowing that such property is derived from any offence(s), [...] for the purpose of concealing or disguising the illicit origin of the property or of assisting any person who is involved in such offence(s) to evade the legal consequences of his actions" (United Nations, 1988; UNODC, 2025). Nowadays, there are many variations of this definition, whose core idea is to characterize laundering as the procedures carried out to disguise the illegal origin of assets derived from criminal offences, integrating them into the legitimate economy (Korejo *et al*., 2021; Gilmour & Hicks, 2023). While the term "laundering" suggests a process of cleansing, the reality is that funds or assets derived from criminal activity cannot be truly "cleaned". The fundamental objective of laundering is to render illicit funds (or any asset derived from criminal activities) usable and indistinguishable from legitimately obtained money or assets (Gilmour & Hicks, 2023). The process of money laundering is didactically divided into three phases, which in practice may overlap or intermingle (Longa, 2025):

- Placement: the process of distancing illicit funds from their direct association with criminal activity. This can be done, for example, through deposits into bank accounts (usually in small amounts to avoid detection) or the purchase of goods;
- Layering: the process of concealing the origin of the funds through complex transactions designed to obscure the audit trail and hinder investigative efforts. Common methods include wire transfers, buying and selling stocks, or using shell companies;

- Integration: the stage at which illicit funds are reintroduced into the economy as if they were legitimate, thus allowing the perpetrator to access and use the proceeds without raising suspicion. This can occur through investments in legal businesses, the purchase of real estate or other assets, making it difficult to link the money to the original crime.

A key aspect of laundering is that it is not an isolated crime; it depends on underlying criminal activities that generate illicit proceeds and form the basis of the laundering process. These underlying criminal activities are referred to as predicate offences. Therefore, demonstrating the occurrence of a predicate offence is essential for the successful prosecution of laundering cases (Shaffer, 2024; Erken & Türkşen, 2024). In some jurisdictions, the list of predicate offences underlying laundering is limited; for example, China's money laundering regulation encompasses seven categories of predicate crimes (Huang, 2025). Conversely, other countries have much more extensive sets, like the European Union, with 22 broad categorizations of predicate crimes (European Union, 2018); or the US, with over 200 recognized predicate offences detailed in its Money Laundering Control Act (US, 1986). There is also the "all crimes approach", under which legislation states that any crime can be a predicate offence for laundering. Studying 110 countries, Wingard & Pascual (2018) found that 57 (52%) adopted an "all crimes approach", while 53 (48%) had limited lists of crimes as predicate offences. A similar result (49% of jurisdictions adopting the "all crimes approach") was found in a 2021 survey conducted with 45 countries (FATF, 2021).

Anti-money laundering (AML) legal and enforcement frameworks are widespread worldwide. In addition to national legislation and agencies, regional multilateral bodies exist across all continents, alongside two independent global bodies: the Financial Action Task Force (FATF, or GAFI in some Latin languages) and the Egmont Group. Both bodies bring together Financial Intelligence Units (FIUs) from around the world, promoting international cooperation and helping strengthen the global framework for investigating and prosecuting illicit financial flows linked to serious crimes (Egmont Group, 2025; FATF, 2025a,b).

1.3.2.3 – Defining wildlife laundering

Richard Smith, in his 1977 article "The Monkey Business", which appears to have introduced the term "wildlife laundering" in scientific literature, defined it as follows: "'laundering' of wildlife occurs when animals taken illegally in their country of origin are smuggled to another country which has no laws or permit requirements to show legal export" (Smith, 1977). This concept, however, encompasses only one of the three modalities of wildlife laundering described in the scientific literature: (i) laundering through fraud related to the geographic origin of the animal, plant, or by-products. There is also (ii) laundering by fraud in the animal or plant species, when a prohibited species or one with a lower market value is sold as another, of permitted trade or higher value (Giagkazoglou *et al*., 2024); and (iii) laundering through fraud in the production system, when animals or plants are illegally collected from the wild and traded as products from legalized systems, i.e. captive breeding of wild animals or fish, plants cultivation or wild species management (e.g. sustainable management programs for timber tree species or fishery resources) (Brandis *et al*., 2025; Auliya *et al*., 2025; Morton *et al*., 2024; Brancalion *et al*., 2018; Hinsley & Roberts, 2018; Lyons & Natusch, 2011). Finally, in addition to these three types of wildlife laundering, the literature also mentions the concept of "reverse laundering", when a legally produced animal or plant is introduced into the illegal market to enhance its commercial value due to the buyer's preference for wild products, even if they are illegal (Alonso & van Uhm, 2023).

Summarizing insights from the scientific literature, we propose the following definition of wildlife laundering: the concealment of fraud related to geographic origin, taxonomic identification, or production, breeding, cultivation, or management of wild animals, fisheries, plants, fungi or their by-products, with the aim of imparting a false appearance of legality and facilitating their entry into formal supply chains or other forms of exploitation for private purposes. We consider that this definition is consistent with the traditional notion of laundering in accounting and financial disciplines, specifically tailoring it to the context of IWT.

1.3.3 – Money laundering associated with the illegal wildlife trade

In 2015, the UN General Assembly adopted a resolution urging its Member States "to review and amend national legislation as necessary and appropriate so that offences connected to illegal wildlife trade are treated as predicate offences […] for the purposes of domestic money laundering offences" (United Nations, 2015), a

recommendation that has been reiterated multiple times in subsequent years. In 2018, a study reported that approximately 60% of countries (65 out of 110 studied) complied with the UN recommendation, the vast majority (57 jurisdictions) through the "all crimes approach" (Wingard & Pascual, 2018).

International AML organizations have also been increasingly concerned about money laundering associated with IWT. The United for Wildlife – an initiative founded by Prince William and The Royal Foundation to protect endangered species from illegal trade – launched its Financial Task Force in 2018. Headed by the banking sector, this coalition includes 30 financial institutions committed to a series of goals focused on detecting and addressing financial flows linked to IWT (UfW, 2025). At the instigation of United for Wildlife, in 2019 the FATF held its first meeting on tackling IWT as a financial crime (FATF, 2020b). In 2020, the FATF published a comprehensive report on money laundering and IWT, providing an overview of the global landscape based on inputs from around 50 countries. The report recommended strategies for integrating financial analysis into wildlife crime investigations and outlined key indicators for detecting laundering activities derived from IWT (FATF, 2020a). A similar report was published in 2021 by the Egmont Group, which compiled information from questionnaires answered by 59 FIUs and 29 environmental enforcement agencies worldwide, as well as inputs from a series of workshops held on all continents (ECOFEL, 2021).

Money laundering associated with IWT has distinctive features. For example, it often relies on wildlife-sector front companies or institutions that maintain legitimate operations in parallel with illicit activities. This overlap facilitates the movement of trafficked specimens and products and conceals the origin of funds by mixing illegal proceeds with lawful financial flows (FATF, 2020a; Lupton, 2023). Understanding which sectors are most exposed to IWT can guide FIUs and enforcement agencies in designing targeted indicators and alert mechanisms related to wildlife crime money laundering. Furthermore, the participation of commercial entities indicates the potential existence of more organized and sophisticated trafficking networks handling larger volumes of illegal wildlife (ECOFEL, 2021). The main industries potentially linked to wildlife laundering and related money laundering include the logging and timber sector, wildlife farms and breeders, pet shops, zoos and wildlife parks, ecotourism, hunting, trinkets and jewelry, traditional medicine, pharmaceutical companies producing medicines with wildlife-derived ingredients, food and restaurants, fashion, art and décor, transportation and shipping (FATF,

2020a; ECOFEL, 2021; Lupton, 2023). In addition to companies, certain categories of individuals also warrant attention from financial intelligence authorities monitoring money laundering related to IWT. Besides owners and employees of the aforementioned companies, this group includes government officials working in wildlife protection and management bodies, wildlife rehabilitation centers, research institutes, forestry services, CITES authorities, customs and border control agencies. Large cash deposits, frequent wire transfers, multiple cash deposits or withdrawals, and wealth inconsistent with declared income can serve as important red flags for detecting wildlife laundering and IWT-related money laundering (FATF, 2020a; ECOFEL, 2021).

Another peculiarity of money laundering associated with IWT is the intense use of cash (FATF, 2020a; Traffic, 2021). In many situations, cash is the primary method of payment used in IWT (ECOFEL, 2021). Cash can be used throughout the trafficking chain but is especially prevalent in the initial stages – poaching and local sale – which occur in source countries or regions (Traffic, 2021). Transactions typically involve small amounts between poachers and intermediaries, but even larger deals may rely on cash to obscure money trails (ECOFEL, 2021). Consequently, the heavy use of cash makes it difficult for authorities to detect and reconstruct the financial flows in wildlife crime cases (FATF, 2020a; Traffic, 2021). Equally difficult to trace is barter trade, when parties exchange wildlife for other goods, whether legal or illegal. This can occur both in small exchanges between poachers and intermediaries and in large transactions involving luxury goods or illegal commodities such as precious minerals, vehicles, electronics, contraband, drugs, or other wildlife (Anagnostou, 2021; Lavorgna & Sajeva, 2021; van Uhm *et al*., 2021; UNODC, 2024). Along with cash and barter, the literature reports the increasingly common use of mobile and online payment platforms (such as Alipay, PayPal or WeChat Pay), financial transfer services (such as Western Union or prepaid cards), marketplace websites, social media, and even cryptocurrencies (Dick, 2019; FATF, 2020a; Traffic, 2021). Finally, the banking sector can also be used for illicit transactions and money laundering linked to IWT (Chatain *et al*., 2022; Lupton, 2023).

Using an AML framework to combat wildlife crime offers several advantages, as AML laws often impose higher penalties than those for wildlife offences, serving as a more effective deterrent. In a survey conducted among 48 Member States, the UN found that although in 90% of countries IWT was classified as a criminal offence, in just under half of them (48% of cases) it was considered a serious crime according to criteria established by

the UN Convention against Transnational Organized Crime ("offence punishable by a maximum deprivation of liberty of at least four years or a more serious penalty") (United Nations, 2023). Consequently, as a worldwide trend, a small minority of IWT cases result in convictions with prison sentences, and an even smaller proportion lead to severe penalties of four or more years of imprisonment (Batt *et al*., 2017; Saraiva, 2021). To address this shortcoming, authorities can expand wildlife crime prosecutions to encompass financial offences, thereby enabling the enforcement of laws that impose harsher sanctions than those typically outlined in most IWT regulations (Dick, 2019). Moreover, supplementing traditional wildlife law enforcement efforts with financial investigations can uncover additional evidence, as the serious nature of money laundering offences often grants greater investigative powers that usually remain underutilized in wildlife crime cases. Besides leading to seizures of significant assets, a money laundering conviction can be especially disruptive for an IWT network. Financial investigations can shift focus beyond poaching to target broader illegal activities like wildlife laundering, money laundering, and ancillary offences. This enables authorities to fully identify organized crime groups and facilitators, including high-level actors like businesses (Dick, 2019; ECOFEL, 2021).

Despite all the advantages, legal gaps and implementation challenges persist in applying financial investigation and AML strategies to the prosecution of IWT (UNODC, 2018; FATF, 2020a; Haris, 2024). In many countries, both the public and private sectors have under-prioritized the investigation and disruption of financial flows linked to IWT. Systematic collection, analysis, and sharing of financial data in wildlife crime investigations remain rare – a gap often compounded by the low priority accorded to this type of crime within AML agencies (FATF, 2020a; Haris, 2024). In practice, enforcement actions targeting IWT typically initiate and conclude with the confiscation of illicit wildlife specimens and products (Reid & Keatinge, 2020). In doing so, authorities end up focusing only on wildlife assets – such as live animals, animal products or timber – while neglecting to pursue the proceeds of environmental crime (ECOFEL, 2021). This situation tends to be more severe in developing countries, many of which are highly biodiverse and source areas for IWT (Osorio, 2024; Haris, 2024; Sultan *et al*., 2025). As a result, even with the legal provision for IWT to be a predicate offence for money laundering, the use of financial approaches to address wildlife crime is often scarce (FATF, 2020a; Haris, 2024). This not only impairs the detection of money laundering but also hinders the complete identification and sanctioning of IWT syndicates, since limited use of financial data and delayed or absent

financial investigations can facilitate the relocation or concealment of wildlife crime networks and assets (Dick, 2019; FATF, 2020a).

Addressing financial crimes related to IWT requires coordinated efforts among diverse bodies, such as environmental enforcement agencies, criminal investigation bodies, FIUs, anti-corruption entities, and CITES authorities (FATF, 2020c). Among them, the role of FIUs is particularly important. They can significantly strengthen wildlife crime investigations by offering crucial insights into financial transactions, identifying the originators and beneficiaries, and analyzing payment patterns to uncover illicit activities (FATF, 2020a; ECOFEL, 2021). The involvement of FIUs in wildlife crime investigations is often scarce or even absent, representing a significant obstacle to governmental efforts to counter IWT (Batt, Feltham & Becker, 2017). Similarly, the banking sector may play a critical role in detecting money laundering associated with IWT. By implementing targeted protocols and compliance measures, financial institutions can identify suspicious patterns and transactions indicative of IWT and monitor potential money launderers across various sectors linked to the wildlife trade. Furthermore, the sector can develop systems and protocols for exchanging and reporting suspicious financial information at both national and international levels (Golban, 2021; Lupton, 2023). It is especially relevant considering that very few countries have engaged in regular international cooperation on financial flows linked to IWT (FATF, 2020a). Beyond banks, other private sector institutions – both financial and non-financial – should also be encouraged to cooperate in efforts to address money laundering related to IWT. Examples include payment service providers and high-value goods dealers, such as real estate agencies, vehicle dealerships, art galleries, antique shops, auction houses, and other luxury collectibles, which can be used to launder proceeds from IWT (FATF, 2020c).

Forensic science is another crucial area in investigations of wildlife laundering and money laundering linked to IWT, both in terms of adapting evidence collection and examination procedures and in developing specific techniques for detecting laundering. For example, in crime scene investigations, targeted approaches should focus not only on evidence related to animals, plants, or their by-products, but also on clues potentially associated with financial crimes and money laundering, such as receipts, accounting logbooks/ledgers, inventories of breeding stock and merchandise, invoices, card readers, and QR codes (Reid & Keatinge, 2020). Forensic experts specialized in financial crime and cybercrime also need to be trained to identify relevant information about wildlife in

commercial and fiscal documents, mobile phone data, computers, cloud storage, cryptocurrency records, marketplaces and social media, among others (FATF, 2020c,d). It is also essential to highlight the importance of the forensic techniques specifically developed to detect wildlife laundering, including forensic genetics, stable and radiogenic isotope analyses, and elementary chemical analyses (Brandis *et al*., 2018; Kafino *et al*., 2024; Kanthaswamy, 2024). By confirming the clandestine origins of wild animals, fisheries, plants, or their by-products, these methods play a vital role in establishing IWT as a predicate offence for the crime of laundering.

1.3.4 – Considerations regarding the Brazilian context

Brazil's Environmental Crimes Act (Federal Law no. 9605/1998) designates IWT as a criminal offence. Concerning financial crimes, the country's AML legislation (Federal Law no. 9613/1998) was amended in 2012, establishing the "all crimes approach" to predicate offences. Since then, the Brazilian legal framework has been sufficient to support investigations into laundering activities related to wildlife crime. Furthermore, in 2019 the Public Prosecutor's Office of São Paulo (the most populous and economically developed state in the country) published a statement reaffirming to all prosecutors that "the crime of trafficking of eggs, larvae and wildlife specimens (art. 29, §1º, III, of Law no. 9605/98) can be considered as a predicate offence to money laundering, under the terms of the Law no. 9613/98, amended by Law no. 12683/12" (Notice no. 175/2019-PGJ/MPSP, statement no. 8).

Several public bodies are involved in addressing IWT, wildlife laundering, and money laundering in Brazil. IBAMA, the federal environmental agency, is responsible for environmental inspection, control, and monitoring, exercising nationwide environmental police power. Criminal investigations related to IWT at federal level are conducted by the Brazilian Federal Police, which established a dedicated environmental division in 2003 to combat these crimes. The National Institute of Criminalistics and its regional offices and laboratories in every state of the country – the forensic branch of the Brazilian Federal Police – are responsible for forensic examinations in criminal investigations and court proceedings related to wildlife crime at the federal level. Among the techniques for detecting wildlife laundering, forensic genetics has been employed since 2006 and forensic isotope analysis since 2019. This forensic authority also has extensive expertise in other areas such as accounting and financial forensics, cyber forensics and digital evidence examinations, forensic document analysis, and examinations of animal identification devices, which are likewise routinely applied to wildlife crime cases. In addition to the federal institutions, each

state has its own environmental agency, police force, and forensic institute in charge of countering IWT locally.

Regarding financial authorities, COAF (Council for Financial Activities Control) is the Brazilian FIU, responsible for detecting and preventing money laundering and terrorist financing (COAF, 2024). The Central Bank of Brazil also plays a role in preventing money laundering by regulating and supervising financial institutions, aiming to avoid the financial system from being used for illicit activities (BCB, 2025). Finally, Brazil has the ENCCLA – the National Strategy for Combating Corruption and Money Laundering – a broad national coordination network of public agencies across different branches and levels of government, working together to develop policies and implement solutions to counter corruption and money laundering. Since 2021, ENCCLA has been proposing measures to strengthen the fight against corruption and money laundering related to environmental crimes, including IWT (ENCCLA, 2021; Stassart & Cardoso Jr., 2024). In 2025, ENCCLA approved its Action 10/2025, focused on preventing and combatting IWT through anti-corruption and AML approaches (ENCCLA, 2025a). The initiative culminated in a report that synthesized key concepts and relevant legislation and presented case studies from IWT investigations that documented both wildlife laundering and the laundering of related assets. It also described Brazil's wildlife breeding control systems, detailing the strategies offenders use to launder wildlife and IWT-linked proceeds by capitalizing on regulatory and procedural loopholes in these systems. Finally, the report set out targeted recommendations to address these gaps (ENCCLA, 2025b).

The first investigations by the Brazilian Federal Police concerning wildlife laundering began in the 1990s. Costa *et al.* (2007) collected primary data from 16 police investigations conducted between 1998 and 2007 that scrutinized the involvement of commercial, conservationist, scientific, and hobbyist breeders in IWT. In all cases, illegally sourced animals had been laundered through procedures carried out by the breeders in order to fraudulently legitimize their possession and trade. In a later study, Mayrink (2016) analyzed more than 1,000 Federal Police forensic reports on the authenticity of songbird identification leg rings from Brazil's Control and Monitoring System for Hobbyist Songbird Breeding Activities (SisPass), covering 2006–2015. In 2020, this system recorded more than 3.5 million native birds registered to hobbyist breeders (IBAMA, 2020). The study found a high rate of fraud involving these identification devices: over 60% of bands were counterfeit or tampered with, underscoring the prevalence of wildlife laundering in Brazil. One notable

example of this kind of fraud is Operation Fibra, launched in 2014 by the Federal Police and IBAMA. The operation uncovered a wildlife laundering scheme involving over 600 breeders who, through the corruption of an environmental agency's outsourced staff member with access to SISPASS, illegally inserted more than 20,000 illegal rings in the system, laundering approximately 15,000 illegally sourced birds (Stassart & Cardoso Jr., 2024, p. 52). Another significant IBAMA operation related to SisPass, known as Operation Delivery, involved the on-site distribution, by IBAMA staff, of identification rings requested by breeders; these were delivered only after officers verified in person that the chicks had hatched on the breeder's premises. This approach replaced the traditional method of mailing the rings. Focusing on the five most popular SISPASS species, Operation Delivery resulted in a 76% reduction in ring requests, with some gauges experiencing decreases of up to 97%. Estimates indicate that, during each iteration of the operation (i.e., each breeding season), around 140,000 rings were not distributed, thereby hindering the laundering of a comparable number of illegally sourced birds (Charity & Ferreira, 2020; IBAMA, 2020).

In 2024, a report by the NGOs Transparency International and Freeland Brasil compiled around two dozen cases of trafficking in wild animals in Brazil associated with wildlife laundering and money laundering (Stassart & Cardoso Jr., 2024). Among these cases, the Federal Police's Operation Oxóssi stands out for having uncovered a large IWT network in Rio de Janeiro state, resulting in more than 100 arrests. Active for at least five years, the syndicate trafficked more than 500,000 animals, including birds, reptiles, big cats, deer and monkeys from conservation areas in Rio de Janeiro and other states. The network used a pet shop as a front to launder wildlife and illicit proceeds and maintained links to members of local law enforcement, as well as international connections in Europe (Stassart & Cardoso Jr., 2024, p. 84).

COAF has also handled IWT cases – for example, detecting the trafficking of endangered Amazonian fish eggs by analyzing patterns of multiple cash deposits and withdrawals by traffickers in cities along the Amazon River and in border regions (ECOFEL, 2021). Although its role in wildlife crime investigations is still developing (Stassart & Cardoso Jr., 2024), significant progress has been made in recent years. A notable example was the ENCCLA's action 10/2022, which addressed the link between environmental crimes and corruption, fraud, and money laundering. This action recommended sharing data from various IBAMA systems with COAF (ENCCLA, 2022). For instance, providing COAF with

automated access to IBAMA's database on wildlife breeders' stock inventories would facilitate the detection of illegal trade and its associated financial flows.

In addition to enforcement operations by the Federal Police, IBAMA, and other federal and state agencies, the scientific literature also corroborates evidence of wildlife laundering in Brazil. Alves *et al*. (2013) argue that commercial breeding of common (non-rare) bird species is not a viable alternative to illegal trade in Brazil, since many birds are laundered through falsification of identification rings, driven by price disparities – legally bred birds can cost up to ten times more than trafficked ones. Regueira & Bernard (2012) found that buyers in clandestine wild bird markets in northeastern Brazil include professional breeders seeking breeding stock to renew their collections. Practices or cases related to laundering of wild animals are also mentioned by Alves *et al*. (2010), Kuhnen *et al*. (2012), Charity & Ferreira (2020) and Stassart & Cardoso Jr. (2024). Regarding forest products, Brancalion *et al*. (2018) identified inconsistencies between timber volumes estimated in Brazil's forest inventory and those recorded in logging licenses in the Eastern Amazon, indicating potential fraud. Their assessments revealed a pattern of overestimating the value of timber species in official permits, and field evaluations confirmed that illegally harvested timber was being laundered as legitimate through the licensing system.

Although IWT is criminalized in Brazil, it is still not considered a serious crime according to UN criteria ("offence punishable by a maximum deprivation of liberty of at least four years or a more serious penalty"). Under the Environmental Crimes Act (Federal Law no. 9605/1998), provisions related to trafficking in wild animals as well as timber and other plant-based products carry penalties of up to one year of detention. As a result, offenders are generally eligible for alternative sanctions rather than imprisonment. Consequently, wildlife crime investigations often need to link traffickers to other crimes – for example, receiving goods obtained by crime, falsification of public documents, or criminal association – to secure more severe sentences. In this context, the FATF emphasizes the significance of ancillary offences, particularly in ensuring the prosecution of controllers of IWT syndicates, even when they do not have direct contact with the trafficked products. However, the FATF also notes that the absence of a comprehensive legal framework categorizing IWT as a serious crime hampers the effective implementation of measures to combat money laundering connected to wildlife crime (FATF, 2020a).

Despite the cases mentioned earlier, wildlife traffickers are seldom prosecuted for laundering in Brazil, as authorities generally overlook this aspect of environmental crime

(Saraiva, 2021). For example, a search on a widely used case law database (Jusbrasil) reveals only 136 cases containing both "wild animal trafficking" and "laundering" in Brazilian courts. By contrast, a search for "drugs trafficking" and "laundering" yields over 10,000 results. It is important to note that Brazilian criminal law recognizes that a single criminal act may harm multiple legally protected interests. In wildlife laundering cases related to IWT, for example, the conduct may simultaneously constitute a wildlife offence, a financial crime, and other associated offences. In such situations, criminal liability arises under two or more applicable statutes, such as the Environmental Crimes Act and the Money Laundering Act, resulting in increased penalties under Articles 69 and 70 of the Brazilian Penal Code (Decree-Law no. 2848/1940, as amended by Law no. 7209/1984). The Brazilian Supreme Court has endorsed this approach in environmental cases, rejecting the exclusive application of the Environmental Crimes Act based on the understanding that the more specific statute does not automatically displace other applicable criminal laws (STF, 2012). Nevertheless, wildlife offences in Brazil are still often classified exclusively under the Environmental Crimes Act by police officers and prosecutors on the ground that it is the more specific statute. We attribute this practice to the limited awareness among Brazilian law enforcement authorities of the true importance and urgency of safeguarding the country's biodiversity. If laundering is not identified at an early stage of criminal prosecution, it is unlikely that wildlife traffickers involved in money laundering will face trial in higher courts. Moreover, given the lenient penalties for IWT in Brazil, offenders often cannot be arrested in *flagrante delicto* unless laundering or another serious associated offence is identified, thereby increasing the risk of impunity (Saraiva, 2021).

At present, over 30 legislative bills are under discussion in the Brazilian Parliament to strengthen the crackdown on IWT, most of which focus on enhancing penalties for wild animal trafficking. Among the most innovative are those drafted with input from a diverse range of professionals involved in wildlife law enforcement and conservation, including judges, prosecutors, police officers, environmental agency staff, and NGO representatives (Ataíde Jr., 2024). These bills aim to amend the Environmental Crimes Act to classify the trafficking of wild animals and their parts as a serious crime, proposing prison terms of one to five or six years for the basic offence (depending on the specific bill) and three to eight years for the aggravated offence.

Drawing on the information presented in this paper and the current Brazilian legal framework, we advocate including wildlife laundering – as defined in section 1.3.2.3

– as an aggravating circumstance of the aggravated offence of wildlife trafficking in a future amendment of the Environmental Crimes Act. We consider this a crucial strategy to ensure appropriate sanctions for this highly sophisticated mechanism within IWT. The proposed amendment should cover trafficking in wild animals and their parts, as well as native timber and other forest products. This broader approach would establish a comprehensive legal framework that fully captures the scope of "wildlife," thereby strengthening overall legal protection for biodiversity.

It is important to recall that, as mentioned at the beginning of this section, the Brazilian Laundering Act has adopted the "all crimes approach" since 2012. This law defines laundering as the act of "concealing or disguising the nature, origin, location, disposition, movement, or ownership of goods, rights, or values that directly or indirectly derive from a criminal offence". Accordingly, once trafficked wild animals, plants, and their parts or by-products are considered illegal goods resulting from a crime, they can be classified as assets for the purposes of the Laundering Act (Stassart & Cardoso Jr., 2024). This already provides Brazil with a sufficient legal framework to investigate and punish wildlife laundering and IWT-related money laundering. Nevertheless, even with this legal provision in place, we believe it is important to explicitly include wildlife laundering in the Environmental Crimes Act, to further clarify and strengthen Brazil's legislation to combat IWT. In this regard, Reid & Keatinge (2020) emphasize that changes to the legal framework create a supportive environment that encourages authorities to implement AML measures and conduct financial investigations related to IWT. In addition to including laundering as an aggravating factor, penalty provisions should be harmonized. While some legislative bills propose imprisonment of three to eight years for aggravated IWT offences, the Laundering Act stipulates terms of three to ten years for the crime of laundering. To ensure uniformity and legal certainty, the aggravating circumstance for wildlife laundering in the Environmental Crimes Act should mirror the Laundering Act's imprisonment range.

Beyond reforming the legal framework, we argue that it is essential for the Brazilian government to establish a unified, comprehensive national policy to tackle IWT, encompassing wild animals, fishery resources, timber, and other forest products. As the most biodiverse country on Earth, with biomes such as the Amazon facing serious threats, Brazil must intensify conservation initiatives for both fauna and flora. Although current efforts by various Brazilian agencies are valuable and commendable, implementing a unified and coordinated national policy would be significantly more effective in combating wildlife

crime. Such a strategy would streamline workflows and foster synergies between the bodies involved in the issue, at different levels of government. It should engage a broad range of entities, including different ministries; federal and state environmental enforcement agencies; investigative police and forensic institutes at both levels; highway patrols; municipal guards; wildlife rehabilitation centers; national and state park authorities; forestry services; customs; financial intelligence unit; public prosecutor's offices; and the judiciary, among others.

In our view, a central strategy of this policy should be to curb wildlife laundering and money laundering associated with IWT, given that the legal breeding, production, and use of wildlife in the country are currently plagued by high levels of fraud. Examples include logging, particularly in the Amazon, and the captive breeding of wild animals, such as under the songbird breeding control system (Mayrink, 2016; Brancalion *et al*., 2018; IBAMA, 2020). This strategy should focus on strengthening the capacity of forensic institutes, criminal investigative bodies, and environmental enforcement agencies to detect wildlife laundering. It should also promote information sharing across enforcement bodies and enhance financial investigative methods to effectively trace proceeds laundered by wildlife traffickers. Ultimately, it is essential that Brazilian public authorities prioritize the detection and dismantling of wildlife laundering and IWT-linked money laundering as a core component of the country's national strategy to combat wildlife crime.

1.4 – Conclusion

To our knowledge, this is the first study to synthesize the scientific literature on wildlife laundering and IWT-related money laundering, as well as the first publication to examine these issues in the Brazilian context. The compiled evidence indicates a marked increase in international research on these topics over the past decade and underscores their global relevance and far-reaching implications for biodiversity. Money laundering associated with IWT has distinctive features that require focused attention from financial and environmental authorities. Efforts to address IWT-linked money laundering are starting to take shape on a global scale. The growing relevance of this issue calls for proactive countermeasures and closer integration between financial investigation bodies and environmental agencies. Wildlife laundering is a sophisticated mechanism within IWT and is closely intertwined with money laundering. From conceptual and legal perspectives, the two practices are analogous: because trafficked wildlife specimens and products constitute

proceeds of crime, laundering these animals, plants, and their parts or by-products is effectively equivalent to laundering the profits derived from them. Given its complexity, including its improper entanglement with formal wildlife production, breeding, management, and trade sectors, wildlife laundering demands a special approach from environmental law enforcement agencies.

On the international stage, it is imperative that all countries recognize IWT as a serious crime and a predicate offence to money laundering, thereby strengthening prosecutions at the national level and facilitating more effective cross-border collaboration. In Brazil's domestic context, the current legal framework recognizes IWT as a predicate offence for money laundering and treats wild animals, native plants, and their parts or by-products as assets derived from crime for laundering purposes. Nonetheless, Brazilian law does not yet categorize IWT as a serious crime. Addressing this gap is therefore urgent to strengthen the effectiveness of prosecution measures aimed at dismantling the gangs and criminal organizations that threaten the country's biodiversity. As part of this legislative reform, wildlife laundering should be defined as an aggravating circumstance for the crime of IWT, with penalty aligned with those established in the Brazilian Money Laundering Act. Finally, tackling wildlife laundering and IWT-related money laundering must be a central component of a unified, comprehensive national policy to effectively address IWT in Brazil.

Link to one of the publications derived from this chapter:
https://rgsa.openaccesspublications.org/rgsa/article/view/14182

1.5 – References

Aguiar R, Gray R, Gallo-Cajiao E, Ruckert A, Astbury CC, Labonté R, Tsasis P, Viens AM, Wiktorowicz M. 2025. Preventing zoonotic spillover through regulatory frameworks governing wildlife trade: A scoping review. *PLoS ONE* 20. DOI: 10.1371/journal.pone.0312012.

Alonso AI, van Uhm DP. 2023. Wildlife laundering and "black-washing": green criminological insights into the interactions between legal and illegal trade in European eels and black caviar. *Revista Espanola de Investigacion Criminologica* 21. DOI: 10.46381/REIC.V21I2.837.

Alves RRN, Lima JR de F, Araújo HFP. 2013. The live bird trade in Brazil and its conservation implications: an overview. *Bird Conservation International* 23:53–65. DOI: 10.1017/S095927091200010X.

Alves RRN, Nogueira EEG, Araujo HFP, Brooks SE. 2010. Bird-keeping in the Caatinga, NE Brazil. *Human Ecology* 38:147–156. DOI: 10.1007/s10745-009-9295-5.

Anagnostou M. 2021. Synthesizing knowledge on crime convergence and the illegal wildlife trade. *Environmental Challenges* 5. DOI: 10.1016/j.envc.2021.100222.

Anagnostou M, Doberstein B. 2022. Illegal wildlife trade and other organised crime: A scoping review. *Ambio* 51:1615–1631. DOI: 10.1007/s13280-021-01675-y.

Anderson RS. 1995. The Lacey Act: America's Premier Weapon in the Fight Against Unlawful Wildlife Trafficking. *Pub. Land L. Rev.* 16:27–85.

Andersson AA, Gibson L, Baker DM, Cybulski JD, Wang S, Leung B, Chu LM, Dingle C. 2021a. Stable isotope analysis as a tool to detect illegal trade in critically endangered cockatoos. *Animal Conservation* 24:1021–1031. DOI: 10.1111/acv.12705.

Andersson AA, Tilley HB, Lau W, Dudgeon D, Bonebrake TC, Dingle C. 2021b. CITES and beyond: Illuminating 20 years of global, legal wildlife trade. *Global Ecology and Conservation* 26. DOI: 10.1016/j.gecco.2021.e01455.

Ataíde Jr. V de P. 2024. Notas aos projetos de lei sobre tráfico de animais silvestres. In: Brasil. Conselho Nacional do Ministério Público. ed. *Manual de combate ao tráfico de animais da fauna silvestre brasileira*. Brasília: CNMP, 237–252.

Auliya M, Nijman V, Altherr S, Aguilera WT, Ariano-Sanchéz D, Cantu JC, Colosimo G, Gentile G, Gerber G, Grant T, Henningheim E, Hughes A, Knapp CR, Lieberman S, Malone C, Pasachnik SA, Petrossian G, Sevilla C, Sosnowski M, Weissgold B. 2025. Trafficking of Galápagos iguanas as an example of a global problem: CITES permits, laundering and the role of transit countries in Europe and Africa. *Biological Conservation* 305. DOI: 10.1016/j.biocon.2025.111104.

Batt C, Feltham J, Becker D. 2017. Enhancing the Detection, Investigation and Disruption of Illicit Financial Flows from Wildlife Crime - APG & UNODC Report. *Available at https://www.unodc.org/roseap/uploads/archive/documents/Publications/2017/FINAL_-_UNODC_APG_Wildlife_Crime_report.pdf* (accessed June 24, 2025).

BCB. 2025. Prevenção à lavagem de dinheiro e ao financiamento do terrorismo. *Available at https://www.bcb.gov.br/estabilidadefinanceira/lavagemdinheiro* (accessed June 29, 2025).

Boyd CE, McNevin AA, Davis RP. 2022. The contribution of fisheries and aquaculture to the global protein supply. *Food Security* 14:805–827. DOI: 10.1007/s12571-021-01246-9.

Brancalion PHS, de Almeida DRA, Vidal E, Molin PG, Sontag VE, Souza SEXF, Schulze MD. 2018. Fake legal logging in the Brazilian Amazon. *Science Advances* 4. DOI: 10.1126/sciadv.aat1192.

Brandis KJ, Meagher PJB, Tong LJ, Shaw M, Mazumder D, Gadd P, Ramp D. 2018. Novel detection of provenance in the illegal wildlife trade using elemental data. *Scientific Reports* 8. DOI: 10.1038/s41598-018-33786-0.

Brandis KJ, Zawada K, Meagher P, Ramp D, Francis R. 2025. Development of tiliqua species provenance models for use in combating the illegal wildlife trade. *Frontiers in Ecology and Evolution* 13. DOI: 10.3389/fevo.2025.1526584.

Brasileiro L, Mayrink RR, Pereira AC, Costa FJV, Nardoto GB. 2023. Differentiating wild from captive animals: an isotopic approach. *PeerJ* 11. DOI: 10.7717/peerj.16460.

Cardoso P, Amponsah-Mensah K, Barreiros JP, Bouhuys J, Cheung H, Davies A, Kumschick S, Longhorn SJ, Martínez-Muñoz CA, Morcatty TQ, Peters G, Ripple WJ, Rivera-Téllez E, Stringham OC, Toomes A, Tricorache P, Fukushima CS. 2021. Scientists' warning to humanity on illegal or unsustainable wildlife trade. *Biological Conservation* 263. DOI: 10.1016/j.biocon.2021.109341.

Charity S, Ferreira JM. 2020. *Wildlife Trafficking in Brazil*. Cambridge: TRAFFIC International.

Chatain P-L, Willebois E van der D de, Bökkerink M. 2022. *Preventing Money Laundering and Terrorist Financing, Second Edition: A Practical Guide for Bank Supervisors*. The World Bank. DOI: 10.1596/978-1-4648-1851-6.

CITES. 2025. The CITES species. *Available at https://cites.org/eng/disc/species.php* (accessed August 6, 2025).

COAF. 2024. O que faz o Coaf? *Available at https://www.gov.br/coaf/pt-br/centrais-de-conteudo/publicacoes/publicacoes-do-coaf-1/OquefazoCoaf.pdf* (accessed June 29, 2025).

Costa CET, Mendes H dos S, Garcia PRM. 2007. Crimes contra o meio ambiente: crimes contra a fauna – participação dos criadores de fauna silvestre no tráfico ilegal de animais. Monografia apresentada como requisito para conclusão do XV Curso Especial de Polícia. Brasília: Academia Nacional de Polícia.

Dick V. 2019. Dirty Money and Wildlife Trafficking: Using the Money Laundering Control Act to Prosecute Illegal Wildlife Trade. *Envtl. L. Rep. News & Analysis* 49:10334–10343.

Dickinson H. 2022. Caviar matter(s): The material politics of the European caviar grey market. *Political Geography* 99. DOI: 10.1016/j.polgeo.2022.102737.

ECOFEL. 2021. Financial investigations into wildlife crime. *Available at https://egmontgroup.org/wp-content/uploads/2021/09/2021_ECOFEL_-_Financial_Investigations_into_Wildlife_Crime.pdf* (accessed July 1, 2025).

Egmont Group. 2025. About the Egmont Group. *Available at https://egmontgroup.org/about/* (accessed August 5, 2025).

Elliott LM, Schaedla WH. 2016. *Handbook of transnational environmental crime*. Edward Elgar Pub.

ENCCLA. 2021. XVIII Reunião Plenária da Estratégia Nacional de Combate à Corrupção e à Lavagem de Dinheiro ENCCLA 2021. *Available at https://www.gov.br/mj/pt-br/assuntos/sua-protecao/lavagem-de-dinheiro/enccla/acoes-enccla/acoes-de-2021* (accessed June 29, 2025).

ENCCLA. 2022. Resumo das recomendações aprovadas no grupo de trabalho da Ação 10/2022. *Available at https://www.gov.br/mj/pt-br/assuntos/sua-protecao/lavagem-de-dinheiro/enccla/acoes-enccla/arquivos-enccla-2022/acao-10-2022-resumo-recomendacoes.pdf* (accessed August 4, 2025).

ENCCLA. 2025a. XXII Reunião Plenária da Estratégia Nacional de Combate à Corrupção e à Lavagem de Dinheiro ENCCLA 2024. *Available at https://www.gov.br/mj/pt-br/assuntos/sua-protecao/lavagem-de-dinheiro/enccla/acoes-enccla/* (accessed August 4, 2025).

ENCCLA. 2025b. *Relatório da Ação 10/2025 - Prevenção e Combate ao Tráfico de Fauna Silvestre com Foco Anticorrupção e Antilavagem*.

Erken E, Türkşen U. 2024. *Anti-Money Laundering and the Law - Comparative Approaches to Countering Predicate Crimes*. London: Routledge. DOI: 10.4324/9781003466680.

European Union. 2018. Directive (EU) 2018/1673 of the European Parliament and of the Council of 23 October 2018 on combating money laundering by criminal law. *Available at https://eur-lex.europa.eu/eli/dir/2018/1673/oj/eng* (accessed December 5, 2025).
FAO. 2022. *Global forest sector outlook 2050: Assessing future demand and sources of timber for a sustainable economy*. FAO. DOI: 10.4060/cc2265en.
FATF. 2020a. Money Laundering and the Illegal Wildlife Trade. *Available at https://www.fatf-gafi.org/publications/methodandtrends/documents/money-laundering-illegal-wildlife-trade.html* (accessed April 15, 2025).
FATF. 2020b. Financial Action Task Force - Annual Report 2019-2020. *Available at https://www.fatf-gafi.org/en/publications/fatfgeneral/documents/annual-report-2019-2020.html* (accessed July 1, 2025).
FATF. 2020c. How can private sector help stop money laundering from illegal wildlife trade? *Available at https://www.fatf-gafi.org/content/dam/fatf-gafi/brochures/Private-sector-and-iwt.pdf* (accessed May 19, 2025).
FATF. 2020d. Following the money of the illegal wildlife trade to stop the trade in endangered species and the laundering of profits. *Available at https://www.fatf-gafi.org/content/dam/fatf-gafi/brochures/Following-the-money-IWT-lea-fiu.pdf* (accessed May 19, 2025).
FATF. 2021. Money Laundering from Environmental Crime. *Available at https://www.fatf-gafi.org/content/dam/fatf-gafi/reports/Money-Laundering-from-Environmental-Crime.pdf* (accessed June 24, 2025).
FATF. 2025a. FATF Member Countries, Associate Members and Observers. *Available at https://www.fatf-gafi.org/en/countries/fatf.html* (accessed May 19, 2025).
FATF. 2025b. The FATF. *Available at https://www.fatf-gafi.org/en/the-fatf.html* (accessed May 19, 2025).
Fukushima CS, Mammola S, Cardoso P. 2020. Global wildlife trade permeates the Tree of Life. *Biological Conservation* 247. DOI: 10.1016/j.biocon.2020.108503.
Giagkazoglou Z, Loukovitis D, Gubili C, Chatziplis D, Symeonidis A, Imsiridou A. 2024. Untangling the cephalopod market: Authentication of seafood products in Greece with DNA-barcoding. *Food Control* 163. DOI: 10.1016/j.foodcont.2024.110523.
Gilmour N, Hicks T. 2023. The obsession with defining money laundering. In: Gilmour N, Hicks T eds. *The War on Dirty Money*. Bristol: Bristol University Press, 66–83.
Golban A. 2021. Money laundering within the illegal wildlife trade: how can financial institutions play a role in combatting this negative phenomenon? *Lucrări Ştiinţifice* 64.
Goodell JW, Muckley CB, Neelakantan P, Ryan D, Yu PS. 2025. AI culture 'profiling' and anti-money laundering: Efficacy vs ethics. *International Review of Financial Analysis* 101. DOI: 10.1016/j.irfa.2025.103980.
Harfoot M, Glaser SAM, Tittensor DP, Britten GL, McLardy C, Malsch K, Burgess ND. 2018. Unveiling the patterns and trends in 40 years of global trade in CITES-listed wildlife. *Biological Conservation* 223:47–57. DOI: 10.1016/j.biocon.2018.04.017.
Haris BS. 2024. Added Value and Challenges of the Follow-the-Money Approach in Environmental Crimes. *AML/CFT Journal The Journal of Anti Money Laundering and Countering the Financing of Terrorism* 2:111–125. DOI: 10.59593/amlcft.2024.v2i2.71.
Hinsley A, Hughes A, Margulies J. 2024. Creating a more inclusive approach to wildlife trade management. *Conservation Biology* 38. DOI: 10.1111/cobi.14360.
Hinsley A, Roberts DL. 2018. The wild origin dilemma. *Biological Conservation* 217:203–206. DOI: 10.1016/j.biocon.2017.11.011.
Holden C. 1979. Cracking Down on Illegal Wildlife Trade. *Science* 206:801–802. DOI: 10.1126/science.206.4420.801.
Huang Y. 2025. Paradigm Reconstruction of the Protected Legal Interests in China's Crime of Money Laundering. *Studies in Law and Justice* 4:32–39. DOI: 10.56397/SLJ.2025.04.04.
IBAMA. 2020. A criação amadorista de passeriformes no Brasil: Diagnóstico da Criação de 2004 a 2020. *Available at https://www.gov.br/ibama/pt-br/centrais-de-*

conteudo/publicacoes/arquivos/livros/2022-10-17_criacao_de_passerifomes_diagnostico_2004_2020.pdf (accessed November 30, 2024).
Johnson J. 2001. In Pursuit of Dirty Money: Identifying Weaknesses in the Global Financial System. *Journal of Money Laundering Control* 5:122–132. DOI: 10.1108/eb027298.
Kanthaswamy S. 2024. Review: Wildlife forensic genetics—Biological evidence, DNA markers, analytical approaches, and challenges. *Animal Genetics* 55:177–192. DOI: 10.1111/age.13390.
Kazmar JP. 2000. The international illegal plant and wildlife trade: biological genocide. *UC Davis J. Int'l L. & Pol'y* 6:105–129.
Korejo MS, Rajamanickam R, Md. Said MH. 2021. The concept of money laundering: a quest for legal definition. *Journal of Money Laundering Control* 24:725–736. DOI: 10.1108/JMLC-05-2020-0045.
Kuhnen VV, Remor JO, Lima R. 2012. Breeding and trade of wildlife in Santa Catarina state, Brazil. *Brazilian Journal of Biology* 72:59-64.
Lavorgna A, Sajeva M. 2021. Studying Illegal Online Trades in Plants: Market Characteristics, Organisational and Behavioural Aspects, and Policing Challenges. *European Journal on Criminal Policy and Research* 27:451–470. DOI: 10.1007/s10610-020-09447-2.
Longa FEA. 2025. Cryptocurrency and Money Laundering. *American Journal of Industrial and Business Management* 15:362–371. DOI: 10.4236/ajibm.2025.152017.
Lupton C. 2023. Illegal wildlife trade: the critical role of the banking sector in combating money laundering. *Journal of Money Laundering Control* 26:181–196. DOI: 10.1108/JMLC-06-2023-0105.
Lyons JA, Natusch DJD. 2011. Wildlife laundering through breeding farms: Illegal harvest, population declines and a means of regulating the trade of green pythons (Morelia viridis) from Indonesia. *Biological Conservation* 144:3073–3081. DOI: 10.1016/j.biocon.2011.10.002.
Mallapaty S. 2025. What sparked the COVID pandemic? Mounting evidence points to raccoon dogs. *Nature* 639:14–15. DOI: 10.1038/d41586-025-00426-3.
Margulies JD, Bullough LA, Hinsley A, Ingram DJ, Cowell C, Goettsch B, Klitgård BB, Lavorgna A, Sinovas P, Phelps J. 2019. Illegal wildlife trade and the persistence of "plant blindness." *Plants People Planet* 1:173–182. DOI: 10.1002/ppp3.10053.
Mayrink RR. 2016. Exame pericial para detecção de fraudes em anilhas oficiais de passeriformes: uma ferramenta para o combate ao tráfico de animais silvestres. Florianópolis: Universidade Federal de Santa Catarina.
Meeks D, Morton O, Edwards DP. 2024. Wildlife farming: Balancing economic and conservation interests in the face of illegal wildlife trade. *People and Nature* 6:446–457. DOI: 10.1002/pan3.10588.
Mora C, Tittensor DP, Adl S, Simpson AGB, Worm B. 2011. How Many Species Are There on Earth and in the Ocean? *PLoS Biology* 9:e1001127. DOI: 10.1371/journal.pbio.1001127.
Morton O, Nijman V, Edwards DP. 2024. Assessing and improving the veracity of international trade in captive-bred animals. *Journal of Environmental Management* 354. DOI: 10.1016/j.jenvman.2024.120240.
Mozer A, Prost S. 2023. An introduction to illegal wildlife trade and its effects on biodiversity and society. *Forensic Science International: Animals and Environments* 3. DOI: 10.1016/j.fsiae.2023.100064.
Nellemann C, Henriksen R, Pravettoni R, Stewart D, Kotsovou M, Schlingemann MAJ, Shaw M, Reitano T. 2018. World Atlas of Illicit Funds - A RHIPTO-INTERPOL-GI Assessment. *Available at https://globalinitiative.net/wp-content/uploads/2018/09/Atlas-Illicit-Flows-FINAL-WEB-VERSION-copia-compressed.pdf* (accessed June 24, 2025).
Nellemann C, Kreilhuber A, Stewart D, Kotsovou M, Raxter P, Mrema E, Barrat S. 2016. The rise of environmental crime: a growing threat to natural resources, peace, development and security. *Available at https://www.unep.org/resources/report/rise-environmental-*

crime-growing-threat-natural-resources-peace-development-and (accessed July 8, 2025).
Osorio CP. 2024. Battling the Illegal Wildlife Trade Through Regulatory Finance: The Southeast Asian Context. *Research Paper Journal of Academics Stand Against Poverty* 5:44–74. DOI: 10.5281/zenodo.11536683.
Oyanedel R, Levi M, Furci G. 2024. A call to include fungi in wildlife trade research and policy. *Conservation Biology* 38. DOI: 10.1111/cobi.14340.
Petrossian GA, Marteache N, Viollaz J. 2015. Where do "Undocumented" Fish Land? An Empirical Assessment of Port Characteristics for IUU Fishing. *European Journal on Criminal Policy and Research* 21:337–351. DOI: 10.1007/s10610-014-9267-1.
Regueira RFS, Bernard E. 2012. Wildlife sinks: Quantifying the impact of illegal bird trade in street markets in Brazil. *Biological Conservation* 149:16–22. DOI: 10.1016/j.biocon.2012.02.009.
Reid A, Keatinge T. 2020. Case closed? Why we should review historic wildlife trafficking cases from a financial perspective. *Available at https://static.rusi.org/20200327_lao_web.pdf* (accessed July 8, 2025).
Riccardi M, Reuter P. 2024. The Varieties of Money Laundering and the Determinants of Offender Choices. *European Journal on Criminal Policy and Research*. DOI: 10.1007/s10610-024-09603-y.
Roe D, Lee TM. 2021. Possible negative consequences of a wildlife trade ban. *Nature Sustainability* 4:5–6. DOI: 10.1038/s41893-020-00676-1.
Saraiva AS. 2021. A atuação de organizações criminosas na exploração ilegal de madeira como principal vetor do desmatamento da Amazônia. Manaus: Universidade Federal do Amazonas.
Scheffers BR, Oliveira BF, Lamb I, Edwards DP. 2019. Global wildlife trade across the tree of life. *Science* 366:71–76. DOI: 10.1126/science.aav5327.
Shaffer Y. 2024. Editorial: The FATF criminalization of money laundering – much room for improvement. *Journal of Money Laundering Control* 27:225–227. DOI: 10.1108/JMLC-03-2024-180.
Smith RD. 1977. The Monkey Business. *The Sciences* 17:15–19. DOI: 10.1002/j.2326-1951.1977.tb01539.x.
Stassart JS, Cardoso Jr. D. 2024. *A lavanderia de fauna silvestre: como riscos de fraude, corrupção e lavagem viabilizam o tráfico de vida silvestre*. São Paulo: Transparência Internacional Brasil. 137 p.
STF. 2012. Habeas Corpus n. 111.762-RO, Relatora: Min. Cármen Lúcia. *Available at https://www.stf.jus.br/arquivo/informativo/documento/informativo691.htm* (accessed August 13, 2025).
Sullivan K. 2023. Beyond the Basic Predicate Crimes. In: Sullivan K ed. *Anti-Money Laundering in a Nutshell*. Apress, 231–242. DOI: 10.1007/979-8-8688-0066-5.
Sultan N, Passas N, Mohamed N, Hussain D, Sulaiman S. 2025. The nexus of environmental crimes and money laundering/terrorist financing: effectiveness of the FATF recommendations against green criminology in developing jurisdictions. *Journal of Money Laundering Control*. DOI: 10.1108/JMLC-08-2024-0142.
Traffic. 2021. Initial analysis of the financial flows and payment mechanisms behind wildlife and forest crime. *Available at https://www.traffic.org/site/assets/files/13685/case-digest-financial-flows-analysis-v2022.pdf* (accessed July 8, 2025).
UfW. 2025. United for Wildlife Financial Taskforce - Illegal wildlife trade is transnational organised crime with a significant financial element. *Available at https://unitedforwildlife.org/taskforces/financial-taskforce/* (accessed July 4, 2025).
van Uhm D, South N, Wyatt T. 2021. Connections between trades and trafficking in wildlife and drugs. *Trends in Organized Crime* 24:425–446. DOI: 10.1007/s12117-021-09416-z.
United Nations. 1988. United Nations Convention against Illicit Traffic in Narcotic Drugs and Psychotropic Substances. *Available at*

https://treaties.un.org/doc/Treaties/1990/11/19901111%2008-29%20AM/Ch_VI_19p.pdf (accessed May 12, 2025).
United Nations. 2015. UN General Assembly Resolution A/RES/69/314 - Tackling illicit trafficking in wildlife. *Available at https://docs.un.org/en/A/res/69/314* (accessed October 17, 2024).
United Nations. 2023. Report A/77/933 - Tackling illicit trafficking in wildlife - Report of the Secretary-General. *Available at https://docs.un.org/en/A/77/933* (accessed June 9, 2025).
United Nations. 2025. UN General Assembly Resolution A/RES/79/313 - Tackling illicit trafficking in wildlife. *Available at https://documents.un.org/doc/undoc/gen/n25/177/66/pdf/n2517766.pdf* (accessed August 5, 2025).
UNODC. 2018. Guide on drafting legislation to combat wildlife crime. *Available at https://www.unodc.org/documents/Wildlife/Legislative_Guide.pdf* (accessed June 8, 2025).
UNODC. 2024. World Wildlife Crime Report 2024: Trafficking in Protected Species. *Available at https://www.unodc.org/documents/data-and-analysis/wildlife/2024/Wildlife2024_Final.pdf* (accessed October 18, 2024).
UNODC. 2025. Money Laundering. *Available at https://www.unodc.org/unodc/en/money-laundering/overview.html* (accessed December 4, 2025).
US. 1986. 18 US Code § 1956 - Laundering of monetary instruments. *Available at https://www.law.cornell.edu/uscode/text/18/1956* (accessed December 5, 2025).
Varrà MO, Ghidini S, Husáková L, Ianieri A, Zanardi E. 2021. Advances in troubleshooting fish and seafood authentication by inorganic elemental composition. *Foods* 10. DOI: 10.3390/foods10020270.
Vice D. 1997. Implementation of Biodiversity Treaties: Monitoring, Fact-Finding, and Dispute Resolution. *N.Y.U. J. INT'l L. & POL.* 4:557–640.
Viollaz J, Graham J, Lantsman L. 2018. Using script analysis to understand the financial crimes involved in wildlife trafficking. *Crime, Law and Social Change* 69:595–614. DOI: 10.1007/s10611-017-9725-z.
Wingard J, Pascual M. 2018. Following the Money: Wildlife crimes in anti-money laundering laws. *Available at https://www.legal-atlas.com/uploads/2/6/8/4/26849604/following_the_money.pdf* (accessed June 10, 2025).
World Bank. 2019. Illegal logging, fishing, and wildlife trade: the costs and how to combat it. *Available at https://documents1.worldbank.org/curated/en/422101574414576772/pdf/Illegal-Logging-Fishing-and-Wildlife-Trade-The-Costs-and-How-to-Combat-it.pdf* (accessed July 8, 2025).

CAPÍTULO 2

TROPHIC DISCRIMINATION FACTORS ($\Delta^{13}C$ and $\Delta^{15}N$) AND TISSUE ISOTOPIC TURNOVER ($\delta^{13}C$) IN GIANT SOUTH AMERICAN RIVER TURTLE – *Podocnemis expansa (Schweigger, 1812)*

Abstract

Stable isotope analysis ($\delta^{13}C$, $\delta^{15}N$) is widely used to reconstruct trophic pathways and habitat use, yet quantitatively reliable inference depends on diet-, species-, and tissue-specific estimates of trophic discrimination factors (TDFs) and isotopic turnover variables. These parameters are also relevant to wildlife forensics, as time-explicit interpretation of dietary transitions can help reconstruct captivity histories in illegal trade investigations. The giant South American river turtle (*Podocnemis expansa*) is a threatened species with a long history of overexploitation and persistent illegal trade in the Brazilian Amazon. Despite the existence of licensed breeding operations, concerns remain about wildlife laundering, whereby illegally captured wild individuals are misrepresented as captive-bred. We conducted a controlled feeding experiment with juvenile *P. expansa* to estimate TDFs ($\Delta^{13}C$, $\Delta^{15}N$) and to characterize tissue-specific ^{13}C incorporation dynamics in whole blood, scute keratin, claw, and skin after a diet shift from a C_4-influenced commercial ration to a C_3-based diet, over a period of up to 1,290 days. TDFs were strongly tissue dependent: $\Delta^{13}C$ ranged from depletion in whole blood, claw, and skin to enrichment in scute keratin, whereas $\Delta^{15}N$ was consistently positive but varied among matrices. Turnover modeling indicated slow incorporation overall and tissue differences: estimated isotopic half-lives were ~64 days for claw, ~166 days for whole blood, ~171 days for scute keratin, and ~186 days for skin. Removal of growth effects and allometric scaling further indicated that incorporation timescales may vary substantially with growth dynamics and body mass. Collectively, these parameters provide a temporal framework for interpreting field $\delta^{13}C$ values, inform tissue selection across different integration windows, and reduce bias arising from generic TDFs and turnover assumptions in ecological studies. They also strengthen isotope-based forensic inference by defining tissue-specific detection windows following transfer from the wild to captive feeding and by providing diet-specific TDFs for evaluating suspected wildlife-laundering cases.

Keywords: stable isotope turnover; trophic discrimination factors; *Podocnemis expansa*; illegal wildlife trade; wildlife laundering

Highlights

- Quantifying isotopic incorporation dynamics and trophic discrimination factors (TDFs) is essential for stable isotope–based trophic ecology studies and wildlife forensic applications.
- The giant South American river turtle (*Podocnemis expansa*) is a threatened Amazonian freshwater species highly impacted by illegal trade.
- We estimated TDFs and isotopic turnover parameters for four tissues of juvenile *P. expansa* (whole blood, scute keratin, claw, and skin).
- Both TDFs and turnover parameters were markedly tissue-dependent.
- Growth and body mass influenced incorporation rates, supporting extrapolation across ontogenetic stages and body sizes.

2.1 – Introduction

Stable isotope analysis (SIA), especially using carbon ($\delta^{13}C$) and nitrogen ($\delta^{15}N$), is widely applied to trace energy pathways and trophic interactions because consumer tissues integrate the isotopic composition of assimilated resources over time (Martínez del Rio & Carleton, 2012). In most ecological applications, $\delta^{13}C$ discriminates among basal carbon sources and habitat-linked production pathways, whereas $\delta^{15}N$ is commonly used to infer trophic position and nitrogen flow through food webs (Peterson & Fry, 1987). However, converting tissue isotope values into quantitative ecological inference requires explicit calibration of two mechanistic parameters that vary with diet, tissue, and taxon: trophic discrimination factors (TDFs; diet–tissue offsets) and tissue incorporation (turnover) rates. Together, these parameters determine, respectively, the expected isotopic fractionation between tissues and the dietary baseline and the temporal window associated with isotopic incorporation in each tissue (Caut *et al*., 2009; Martínez del Rio & Carleton, 2012; Vander Zanden *et al*., 2015; Stephens *et al*., 2023). Controlled diet-shift experiments are therefore essential because they provide the empirical basis for estimating isotopic incorporation parameters – turnover rates and their derived residence times and isotopic half-lives – as well as TDFs (Carter *et al*., 2019). This need is particularly acute in ectotherms, where turnover can be slow and somatic growth can contribute significantly to isotopic change, potentially altering apparent incorporation dynamics and, in some contexts, observed diet–tissue offsets (Reich *et al*., 2008; Murray & Wolf, 2012).

Beyond trophic ecology, reliable turnover estimates are increasingly relevant for wildlife forensic applications (Sung *et al*., 2025). In wildlife laundering – the illegal practice whereby wild-caught animals are fraudulently marketed as captive-bred – stable isotopes can help distinguish between wild and captive provenance because diets used in breeding farms usually differ isotopically from natural food sources (Brasileiro *et al*., 2023). The strength of this inference, however, depends on both tissue-specific turnover rates and TDFs: turnover determines how long pre-capture isotopic signatures remain detectable following captivity-induced diet shifts, whereas TDFs quantitatively link tissue isotope values to the isotopic composition of the captive diet. Recent studies have demonstrated the utility of stable isotopes for separating wild *versus* captive provenance of freshwater turtles in the context of illegal trade (Hill *et al*., 2020; Hopkins *et al*., 2022, 2023; Sung *et al*., 2025; Chatfield *et al*., 2026), underscoring the need for experimentally derived turnover parameters to support robust, temporally explicit forensic inference.

Despite the widespread use of stable isotope analysis in trophic ecology, experimentally derived TDFs and tissue-specific turnover rates remain relatively scarce for reptiles, particularly when compared with the extensive literature available for birds and mammals (Warne *et al*., 2010; Lattanzio & Miles, 2016). More specifically within chelonians, studies of isotopic turnover and TDFs have historically been concentrated in marine turtles, in which carbon and nitrogen diet–tissue discrimination, incorporation dynamics, and tissue-to-tissue relationships have been quantified across species, tissues, and life stages [studies compiled by Soto *et al*. (2025)], and additional isotope systems have been explored under controlled feeding (Barceló *et al*., 2021). In contrast, stable isotope turnover and TDF information for freshwater and terrestrial chelonians remains extremely limited worldwide, with very few controlled studies available (Seminoff *et al*., 2007; Murray & Wolf, 2012, 2013; Sung *et al*., 2025).

For the giant South American river turtle (*Podocnemis expansa*), and more broadly for Amazonian freshwater chelonians, TDFs, isotopic turnover rates and other experimentally derived tissue-specific parameters remain unquantified. Only a very limited number of field studies have applied stable isotopes to investigate the trophic ecology of *Podocnemis* spp. (e.g., Lara *et al*., 2012). However, the kinetic turnover baselines needed to interpret tissue isotope values – and thus to define the temporal window over which diet is integrated – are still lacking. As a result, the interpretation of isotope values from wild

populations becomes less robust, particularly in heterogeneous natural habitats where diet composition and resource availability can vary across space and time (Cathelin *et al*., 2025).

Podocnemis expansa is a highly ecologically and socioenvironmentally important species in the Amazon. It has been overexploited for centuries, having been driven to the brink of extinction (Forero-Medina *et al*., 2019). Nowadays, poaching and illegal commerce of adult river turtles and their eggs for human consumption likely represents the most significant wildlife trafficking problem in the Brazilian Amazon (Charity & Ferreira, 2020). The farming of Amazonian river turtles is legally permitted in Brazil (Brazil *et al*., 2025); however, despite the existence of licensed producers supplying animals to the formal market, illegal trafficking networks persist (Pantoja-Lima *et al*., 2014) and may overlap with the regulated breeding and trade sector (Polícia Federal, 2014). Therefore, to support isotope forensics in investigations of illegal trade and wildlife laundering involving *P. expansa*, it is essential to quantify tissue-specific incorporation dynamics, including turnover rates, residence times, and isotopic half-lives, together with TDFs, thereby enabling isotope measurements to be interpreted mechanistically in terms of both provenance (wild vs. captive) and time since dietary transition.

The aim of this work was to provide experimentally derived estimates of TDFs ($\Delta^{13}C$ and $\Delta^{15}N$) and tissue-specific isotopic turnover dynamics ($\delta^{13}C$) for giant South American river turtles (*Podocnemis expansa*). We hypothesized that different tissues of *P. expansa* have distinct TDFs and isotopic turnover parameters. Specifically, we (i) quantify $\Delta^{13}C$ and $\Delta^{15}N$ in whole blood, scute keratin, claw, and skin at the onset of the experiment ($t = 0$), and (ii) model the post-shift $\delta^{13}C$ turnover using one- and two-compartment formulations while accounting for growth-driven dilution and allometric scaling. By combining controlled feeding data with growth and allometric scaling considerations, our results establish baseline parameters for interpreting field-derived isotopic values and for supporting both ecological and forensic applications involving *Podocnemis expansa* and potentially other Amazonian freshwater turtles.

2.2 – Theoretical framework

Stable isotope analysis (SIA) underpins much of modern trophic ecology by linking consumer tissue isotope ratios to assimilated resources, enabling inference on diet composition, habitat use, and trophic structure across food webs. Although multiple isotope systems can be informative, applications in trophic studies most frequently rely on $\delta^{13}C$ and $\delta^{15}N$ (Peterson & Fry, 1987; Shipley & Matich, 2020). $\delta^{13}C$ is widely used to distinguish among basal carbon sources and habitat-linked production pathways supporting consumers, whereas $\delta^{15}N$ is commonly interpreted as an indicator of trophic position based on the stepwise enrichment of ^{15}N across trophic levels (Fry, 2006). In practice, SIA supports a wide range of ecological applications and is frequently integrated with quantitative diet reconstruction frameworks such as mixing models (Ballutaud *et al*., 2022), with recent syntheses highlighting its broad applicability across taxa and research questions (Haywood *et al*., 2019; Quinby, Creighton & Flaherty, 2020; Boulêtreau *et al*., 2025; Berto *et al*., 2025; Perga *et al*., 2025).

2.2.1 – Trophic discrimination factor and isotope incorporation

Robust ecological interpretation of isotopic data requires explicit consideration of two coupled processes linking diet to consumer tissues: (i) diet–tissue isotopic discrimination and (ii) the temporal dynamics of isotope incorporation (Cathelin *et al.*, 2025; Ballutaud *et al*., 2022; Martínez del Rio & Carleton, 2012). Diet–tissue discrimination arises because biochemical routing, assimilation, and metabolic processing alter isotope ratios between ingested resources and consumer tissues, generating tissue- and element-specific offsets that are typically expressed as trophic discrimination factors (TDFs; $\Delta^{13}C$ and $\Delta^{15}N$). These offsets are not universal constants; instead, they vary across taxa and tissues and can change with diet composition and isotopic values, as well as with physiological state (Sturtz *et al*., 2026; Flinders *et al.*, 2026; Caut *et al.*, 2009). This variability has direct consequences for diet estimation: inappropriate TDFs, including literature averages or proxies from other species, can bias inferred source contributions even when consumer and source isotope measurements are precise. Bias magnitude and direction depend on isotopic distinctiveness among sources, diet macronutrient composition, and how discrimination uncertainty is propagated, reinforcing the value of species-, tissue-, and diet-matched TDF estimates (Stephens *et al.,* 2023; Caut *et al.*, 2009).

In addition to diet-tissue discrimination, isotope values in animal tissues are inherently time-integrated, as tissues do not instantaneously reflect dietary isotope ratios but instead shift gradually following changes in resource use. This temporal lag is governed by isotopic incorporation, such that each tissue integrates diet over a characteristic timescale determined by its rate of replacement (Vander Zanden *et al*., 2015). Although often used interchangeably, isotope incorporation and isotopic turnover have slightly different meanings: whereas isotope incorporation emphasizes the progressive assimilation of a dietary isotope signal into a tissue through time, isotopic turnover focuses on the replacement kinetics underlying this change, typically summarized by a turnover rate (λ) and its associated isotopic residence (or retention) time and half-life (Martínez del Rio & Anderson-Sprecher, 2008; Martínez del Rio & Carleton, 2012).

The isotopic turnover rate λ (day^{-1}) is a fractional first-order rate constant; for example, λ = 0.01 day^{-1} implies an exponential replacement of ~1% of the tissue pool per day (exactly, $1 - e^{-\lambda}$). It is closely related to two other key parameters of tissue isotopic incorporation kinetics: the isotopic residence (or retention) time and the isotopic half-life. Isotopic residence time is the characteristic timescale (i.e., the mean time) over which atoms of a given element remain in a tissue undergoing turnover before being replaced by newly incorporated atoms (Martínez del Rio & Carleton, 2012). Mathematically, it is expressed as the inverse of the isotopic turnover rate:

$$\tau = \frac{1}{\lambda} \quad (1)$$

The isotopic half-life, in turn, is defined as the time required for the tissue undergoing turnover to reach 50% of the isotopic equilibrium relative to the new diet (Vander Zanden *et al*., 2015) and can be mathematically expressed as:

$$t_{1/2} = \frac{\ln(2)}{\lambda} \quad (2)$$

It can also be interpreted as the median residence time of the atoms of an element within a tissue (Martínez del Rio & Carleton, 2012). This metric is mathematically related to the mean residence time as follows:

$$t_{1/2} = \ln(2)\tau \quad (3)$$

Isotopic incorporation rates are often assumed to track overall energy metabolism; however, experimental evidence indicates that they are more directly driven by tissue replacement processes – particularly protein turnover associated with macromolecular synthesis and catabolism – than by whole-organism energetic expenditure (Carleton & Del Rio, 2005; Carleton *et al*., 2008; Bauchinger *et al*., 2010). Metabolically active tissues with rapid protein turnover, such as blood plasma, liver, and other viscera, incorporate isotopes over relatively short timescales and thus reflect the isotopic composition of the diet consumed over days to weeks. Intermediate incorporation dynamics are observed in blood cells and skin, which integrate dietary isotopic signals over weeks to months. By contrast, more slowly replaced structural tissues, including muscle, bone, and tooth dentine, retain isotopic information over longer time windows, ranging from months in muscle to years in bone and teeth. Metabolically inert tissues, such as claws, feathers, hair, and other keratinized structures, record the isotopic composition present at the time of formation and therefore preserve a point-in-time isotopic signature from the past (Seminoff *et al.,* 2007; Hahn *et al*., 2012; Vander Zanden *et al*., 2015; Giménez *et al*., 2016; Curtis *et al*., 2022). Because different tissues integrate dietary information over distinct temporal windows, multi-tissue sampling can be particularly informative for reconstructing diet through time. By combining tissues with contrasting turnover rates, researchers can use a multi-tissue "isotopic clock" to distinguish between recent and longer-term resource use and to detect dietary shifts that would be obscured by any single tissue (Carter *et al*., 2019). Nonetheless, this advantage also entails an important interpretive constraint: comparisons among tissues, individuals, or populations can be misleading if tissue-specific integration times are not explicitly accounted for, particularly when diets are dynamic or when consumers have not reached isotopic equilibrium with their current resources (Vander Zanden *et al*., 2015; Ballutaud *et al*., 2022; Soto *et al*., 2025).

Taken together, trophic discrimination factors and turnover rates define both the isotopic offset between diet and consumer tissues and the timescale over which dietary signals are integrated. Accordingly, controlled experiments that estimate these parameters for the focal organism and tissue provide a robust basis for interpreting isotopic datasets, designing biologically appropriate sampling windows, and avoiding consequential bias from adopting generic literature values (Ballutaud *et al*., 2022; Stephens *et al*., 2023; Cathelin *et al*., 2025).

2.2.2 – Growth and allometry

Isotopic turnover arises from two distinct mechanisms: tissue growth and catabolic replacement (or catabolic turnover) (Fry & Arnold, 1982). When an animal is not growing, the rate of isotopic turnover depends solely on catabolism, i.e., the replacement of old tissue by newly synthesized tissue. In contrast, when an animal grows while undergoing a dietary shift, new biomass is added to tissues carrying the isotopic signature of the new diet, producing a dilution effect on the isotopic composition derived from the previous diet (Martínez del Rio & Carleton, 2012). In rapidly growing animals, the contribution of growth-driven isotopic incorporation can represent a substantial fraction of total turnover, accounting for up to 100% of the observed rate in some cases (Reich *et al*., 2008). Conversely, in mature animals with low or no growth rates, tissue isotopic replacement is driven primarily by catabolic turnover (Matley *et al*., 2016). The dilution effect caused by growth can obscure catabolic replacement rates, thereby hindering comparisons of turnover rates across tissues (Dalerum & Angerbjörn, 2005). If the animal is growing exponentially, the turnover rate (λ) can be interpreted as the sum of the catabolic turnover rate (k_c) and the growth rate (k_g) (Martínez del Rio & Carleton, 2012).

In addition to the growth-related effect, isotopic turnover rates also vary systematically with body size; as a general rule, smaller organisms exhibit faster isotopic replacement than larger organisms (Vander Zanden *et al*., 2015; Thomas & Crowther, 2015). This allometric relationship is consistent with predictions from metabolic scaling theory, in which the rates at which elements enter and leave tissues – and therefore the rate at which the isotopic signature of a tissue pool is replaced – depend on body mass. Beyond its isotopic interpretation, the turnover rate (λ) can also be chemically defined as the ratio between the net influx of an element into a tissue and the size of the tissue elemental pool, as expressed by the following equation (Martínez del Rio & Carleton, 2012):

$$\lambda = \frac{\dot{v}}{A_T} \tag{4}$$

where $\dot{v}$ is the net influx of the element into the tissue (in moles time^{-1}) and A_T represents the size of the elemental pool in the tissue (in moles). Tissue size – and therefore A_T – is expected to scale isometrically with total body mass (M^1), while the influx ($\dot{v}$) is assumed to

increase with tissue (pool) size with an exponent of 0.75 ($M^{0.75}$):

$$\lambda \propto \frac{M^{0.75}}{M^{1}} = M^{-0.25} \quad (5)$$

Thus, the fractional isotopic incorporation rate is expected to decrease with body mass with an exponent close to −0.25 (Martínez del Rio & Carleton, 2012).

Empirical results from meta-analyses support this general pattern, although the estimated exponent varies somewhat among syntheses. For example, Vander Zanden *et al*. (2015), compiling data from diet-shift experiments and testing body-mass effects, reported an allometric slope of ~0.22 for the relationship between body mass and isotopic half-life in ectotherms, which corresponds to an exponent of −0.22 when expressed as an incorporation rate. They proposed that the half-life for ectotherms can be estimated as:

$$\ln(\text{half-life}) = 0.22 \ln(\text{body mass}) + \text{a group-specific intercept} \quad (6)$$

demonstrating that isotopic half-life increases (i.e., turnover rate decreases) with increasing body mass. Thomas & Crowther (2015), in a macroevolutionary synthesis, obtained a slightly less negative exponent, suggesting that turnover scales with body mass to the power of −0.19. In comparative terms, $M^{-0.19}$, $M^{-0.22}$, and $M^{-0.25}$ describe the same directional pattern (slower turnover in larger organisms) while differing in effect size. These differences are plausible because aggregated estimates from meta-analyses (Vander Zanden *et al*., 2015; Thomas & Crowther, 2015) depend on the taxa included, tissue types (and possible deviations from the assumed isometry in the scaling of elemental pool size with body mass), environmental conditions like experimental temperatures, as well as methodological heterogeneity across studies. Nevertheless, the numerical proximity of these indices indicates that the theoretical −0.25 scaling provides a useful and biologically interpretable approximation for predicting the order of magnitude of turnover as a function of body size (Vander Zanden *et al*., 2015).

Body mass and growth rate do not necessarily covary. For instance, two individuals from different species may have similar body sizes, yet be in different life stages: one may have already attained asymptotic size, whereas the other may still be a fast-growing juvenile. In that case, the juvenile would be expected to show substantially faster isotopic turnover, because its isotopic change reflects both new tissue addition associated with

growth and ongoing catabolic turnover, while the adult's turnover is essentially driven by catabolic processes (Vander Zanden *et al*., 2015).

From an applied perspective, a key implication is that comparisons among size classes (or among species with widely different body masses) may confound true dietary variations with allometry-driven differences in incorporation rate. Accordingly, when interpreting isotopic values in trophic ecology studies – particularly for ectotherms and long-lived vertebrates – body mass should be treated as a relevant determinant of the temporal window integrated by tissues, and allometric relationships should be considered when appropriate.

Podocnemis expansa spans a wide allometric range, with hatchling body mass typically between 20 and 30 g and adult females that can exceed 45 kg (Andrade, 2012). Given this size variation, it is essential to recognize that both growth and body size may directly influence incorporation rates and, consequently, the temporal window integrated by each tissue. This reinforces the need for controlled, species-specific experimental estimates for this species, particularly when the goal is to support robust inference in future field-based trophic ecology studies and forensic investigations.

2.2.3 – Compartment models of isotopic turnover

Isotopic turnover can be modelled with a first-order, one-compartment exponential function, which assumes that the tissue behaves as a single, well-mixed elemental pool that follows simple first-order kinetics (Cerling *et al*., 2007). This model is based on the equation:

$$\delta_t = \delta_{eq} - \left(\delta_{eq} - \delta_{init}\right) e^{-\lambda t} \quad (7)$$

where δ_t is the isotopic value of the tissue at a given time t, δ_{init} is the initial isotopic composition of the tissue, δ_{eq} is the asymptotic value of the tissue (after its isotopic composition reaches steady state with the new diet), and λ is the turnover constant. However, tissues undergoing isotopic turnover frequently behave as multi-pool (or multi-compartment) systems. This can occur when bulk isotope measurements integrate subcomponents with different replacement rates, or when underlying physiological processes interact in complex ways, reflecting such complexity in tissue isotopic turnover

dynamics (Martínez del Rio & Anderson-Sprecher, 2008). A multi-pool model is mathematically defined by the equation:

$$\delta_t = \delta_{eq} - \left(\delta_{eq} - \delta_{init}\right)\left[\sum_{i=1}^{n-1} p_i\, e^{-\lambda_i t} + \left(1 - \sum_{i=1}^{n-1} p_i\right) e^{-\lambda_n t}\right] \quad (8)$$

In general, the multi-pool models best supported by empirical isotopic turnover data include at most two compartments (Martínez del Rio & Carleton, 2012). Therefore, Eq. 8 for a two-compartment model can be written as:

$$\delta_t = \delta_{eq} - \left(\delta_{eq} - \delta_{init}\right)\left[p\, e^{-\lambda_1 t} + (1-p)\, e^{-\lambda_2 t}\right] \quad (9)$$

where p and $1 - p$ are the mixing weights (fractions) that show how much each exponential component contributes to the total change toward equilibrium: p is the fraction (between 0 and 1) associated with the fast component (λ_1) and $(1 - p)$ is automatically the remaining fraction, associated with the slow component (λ_2).

Selecting the model that best describes isotopic turnover under a given experimental context (taxon, element, tissue, diet, growth, allometry, etc.) is essential to obtain accurate and robust estimates of turnover kinetic parameters.

2.3 – Methods

2.3.1 – Experimental design

Eight juvenile giant South American river turtles (*Podocnemis expansa*; ~2 years old) were obtained from a licensed commercial breeding facility located in the municipality of Iranduba, Amazonas State, Brazil, where they were fed a commercial fish feed with a high maize content and consequently a strong C_4 signal ($\delta^{13}C$ = −14.6‰, $\delta^{15}N$ = 3.7‰). The turtles were then transferred to the Aquatic Chelonian Center of the National Institute for Amazonian Research (Cequa/INPA) in Manaus (Amazonas State, Brazil) and housed in an enclosure providing access to both land and water, with partial sun exposure. Manaus has long-term annual mean temperatures ranging from ~24°C (minimum) to ~32°C (maximum), with an overall mean of ~27.4°C, and a mean relative humidity of ~81%.

The turnover experiment was conducted from December 2018 to July 2022 (1,290 days or 43 months ≈ 3.6 years). From day 1 onward, the animals were switched to a

C_3-based diet consisting primarily of commercial textured soy protein ($\delta^{13}C$ = −26.2‰; $\delta^{15}N$ = −1.3‰) offered ad libitum twice per week, and supplemented C_3 vegetables (mean ± SD: $\delta^{13}C \approx -28.6 \pm 2.3$‰; $\delta^{15}N \approx 4.4 \pm 3.4$‰). Whole blood samples were collected monthly through day 1,290, whereas scute keratin and claw were sampled every two months through day 1,230. Bimonthly skin sampling was conducted only through day 180. Morphometric measurements (body mass, straight-line carapace length and width, straight-line plastron length and width, and carapace height) were recorded at two-month intervals. At the start of the experiment, individuals had a mean body mass of 203.3 g (SD = 43.5) and a mean straight carapace length (SCL) of 122.0 mm (SD = 11.3). One individual died during the study and was excluded from the turnover analyses; however, its day-0 isotopic values were retained for calculating TDFs relative to the pre-experimental diet.

2.3.2 – Sample collection and processing

We collected blood, scute keratin, claw, and skin samples using minimally invasive methods. Blood was sampled monthly, whereas the other tissues were sampled every two months. Blood samples were obtained by venipuncture of the dorsal coccygeal vein and transferred onto glass slides, which were immediately air-dried and stored in appropriate slide boxes. In the laboratory, blood samples were scraped from the slides into microtubes and dried in an oven at 60 °C for 48 h. Scute samples were taken by excising a small fragment from the keratinized layer at the distal end of the marginal scutes of the carapace, and claws were sampled by clipping their distal tips. Both scute and claw samples were stored dry in individual, sealable plastic bags. Skin was sampled by cutting a small superficial fragment of the interdigital membrane and was preserved in absolute ethanol. In the laboratory, scute, claw, and skin samples were cleaned in a 2:1 chloroform:methanol solution for 1 h and dried in an oven at 60 °C for 48 h. All tissue samples were then encapsulated in tin capsules (approximately 0.5 – 0.6 mg per sample) for subsequent SIA analysis.

2.3.3 – Stable isotope analysis

The isotopic ratios of carbon and nitrogen were determined by combustion using an elemental analyzer (Carlo Erba, CHN-1100) coupled to an isotope ratio mass spectrometer (Thermo Finnigan Delta Plus) at the Isotope Ecology Laboratory of the Nuclear Energy Center in Agriculture, University of São Paulo (CENA/USP), Piracicaba/SP, Brazil.

Relative isotope abundance values were expressed in delta notation (δ) in parts per thousand (‰), using the following equation:

$$\delta^{h}E_{sample/standard} = [(R_{sample} - R_{standard})/R_{standard}] = [(R_{sample}/R_{standard})-1] \quad (10)$$

where R is the ratio of the heavier isotope to the lighter isotope of a given element (E) for samples and standards (Meier-Augenstein, 2019) (for example, as in the case of this study, $^{13}C/^{12}C$ or $^{15}N/^{14}N$). The outcome of this equation is numerically less than zero, with significant figures up to the second or third decimal place. To facilitate the interpretation of isotopic analysis data, it is internationally standardized to multiply the results of the equation by 1000. Consequently, the delta notation is expressed in parts per thousand (‰) and represents a relative value rather than an absolute measure.

$\delta^{13}C$ was reported relative to the Vienna Pee Dee Belemnite standard (VPDB; $^{13}C/^{12}C$ ratio = 0.01118), and $\delta^{15}N$ was reported relative to atmospheric air (AIR; $^{15}N/^{14}N$ ratio = 0.0036765). Laboratory internal standard samples (sugarcane leaves) are routinely interspersed with target samples to correct the effects of mass and instrumental drift during and between runs (one standard sample for every ten target samples). The long-term analytical errors for internal standards are 0.2‰ for both $\delta^{13}C$ and $\delta^{15}N$. The sugarcane internal standard is regularly calibrated against IAEA standards NBS18 and NBS22 for carbon and IAEA N1 and N2 for nitrogen. To ensure comparability of $\delta^{13}C$ and $\delta^{15}N$ values with the international reference scales, we applied a two-point (double-standard) normalization using multiple certified reference materials spanning a broad isotopic range. The reference materials used to derive the normalization equations were measured in a separate analytical session from the study samples because the sample analyses had been completed earlier. Although standards and samples were not analyzed in the same session, this correction remains valid because it addresses the instrument scale definition (linearity and intercept) used to express results on the VPDB (for $\delta^{13}C$) and AIR (for $\delta^{15}N$) scales, rather than short-term within-run drift. Carbon reference materials included NBS 19, NBS 22, and USGS 61, USGS 62, USGS 63, and USGS 89; nitrogen reference materials included IAEA-N1, IAEA-N2, and the same USGS materials. To strengthen the scale transfer, five carbon standards and five nitrogen standards were analyzed (more than is typical in routine practice). The resulting relationships were: $\delta^{13}C\_true = 1.01626 \times \delta^{13}C\_measured + 0.84085$ ($R^2 = 0.99$) and $\delta^{15}N\_true = 0.99278 \times \delta^{15}N\_measured - 0.72202$ ($R^2 = 0.99$). Reported $\delta^{13}C$ and $\delta^{15}N$ values were adjusted using these equations. The raw $\delta^{13}C$ and $\delta^{15}N$ analytical

dataset used to generate all figures and tables is available as supplementary material (Mendeley Data, V1, doi: 10.17632/5y2fzh2wp3.1).

2.3.4 – Data analysis

2.3.4.1 – Determination of trophic discrimination factors ($\Delta^{13}C$ and $\Delta^{15}N$)

We determined diet–tissue trophic discrimination factors (TDFs) for carbon ($\Delta^{13}C$) and nitrogen ($\Delta^{15}N$) by subtracting the isotopic value of the pre-shift diet from the corresponding tissue value measured at day 0 ($\Delta X = \delta X_{tissue} - \delta X_{diet}$). Because the turtles had been maintained on a single commercial feed for approximately two years prior to the experiment, we assumed that tissues were at isotopic equilibrium with this baseline diet at the start of the study. Differences among tissues were tested using a within-individual repeated-measures ANOVA (rmANOVA)[8], with Greenhouse–Geisser correction when applicable.

2.3.4.2 – Modeling and analysis of isotopic turnover data

2.3.4.2.1 – Exploratory visualization and data filtering

As an initial exploratory step to visualize overall turnover trajectories, we plotted the $\delta^{13}C$ data and fitted monoexponential (one-compartment) curves for each tissue. Data were presented both as individual observations and as time-point means with 95% confidence intervals, the latter to facilitate visualization of temporal trends. Then, following the recommendations of Martínez del Rio & Anderson-Sprecher (2008), we used the reaction progress variable proposed by Cerling *et al*. (2007) as a preliminary diagnostic of whether tissue turnover was likely to follow one- or two-compartment dynamics. This approach applies a logarithmic transformation to isotopic data using the following equation:

$$ln\,(1-F) = ln\left[\frac{\delta^{t}-\delta^{eq}}{\delta^{init}-\delta^{eq}}\right] = -\lambda t \qquad (11)$$

where $(1-F)$ represents the fractional approach to equilibrium, i.e., the fraction of the turnover reaction that has yet to occur, assuming that the total turnover amplitude (i.e., the difference between δ^{init} and δ^{eq} is equal to 1). $F = 0$ at the beginning of the reaction e $F =$

[8] Assumptions for rmANOVA were evaluated by confirming a complete within-subject design (one observation per individual × tissue), testing sphericity with Mauchly's test and applying Greenhouse–Geisser correction when violated; and inspecting residual normality using Q–Q plots and the Shapiro–Wilk test prior to Tukey-adjusted post hoc comparisons (emmeans).

1, at equilibrium (the asymptote). If the turnover reaction follows first-order kinetics (a single compartment), the plot of $ln\ (1 - F)$ *versus* time is a decreasing straight line, and its slope corresponds to λ.

The reaction progress variable highlighted a pattern already suggested by the original turnover plots, which indicated departures from the expected smooth, monotonic exponential decay, including intermittent plateaus and occasional reversals in $\delta^{13}C$ trajectories. These patterns are not consistent with the assumptions of classical isotopic turnover models and are most likely attributable to circumstantial constraints at the research facility, which may have resulted in unintended intermittent intake of C_4-derived items during the intermediate phase of the experiment. Such dietary perturbations can violate the assumption of a single, sustained diet switch and, if included in model fitting, may confound tissue incorporation kinetics with externally imposed dietary variability, potentially biasing estimates of turnover rates and derived residence times. To reduce this risk and preserve the interpretability of turnover parameters, analyses were restricted to periods when the C_3 diet appeared most consistent. We therefore retained observations from 0–180 days, which primarily capture the initial post-switch incorporation phase, and from ≥1140 days, which characterize the long-term approach to isotopic equilibrium. This restriction represents a conservative modeling choice intended to approximate as closely as possible the conditions originally assumed by the experimental design.

2.3.4.2.2 – Equilibrium assumptions and kinetic model fitting

Isotopic turnover of $\delta^{13}C$ was modeled using one- (1C) and two-compartment (2C) exponential models (Martínez del Rio & Anderson-Sprecher, 2008; Carleton *et al*., 2008) fitted to the filtered dataset (observations in t ≤ 180 days and ≥ 1140) designed to capture the early response to the diet shift (the fastest $\delta^{13}C$ decay) and the late-time approach to equilibrium. For tissues with late-time observations (blood, scute keratin, and claw), the asymptotic value (δ_{eq}) was first computed empirically from late-time $\delta^{13}C$ (≥ 1140 days; mean per individual followed by a grand mean across individuals). This empirical δ_{eq} was compared with a model-estimated δ_{eq}. To do so, we fitted the 2C model with δ_{eq} either fixed or estimated as a free parameter and then compared model support using AICc (ΔAICc) and Akaike weights. This comparison was performed under the 2C formulation because this model has greater flexibility to fit turnover trajectories; therefore, if freely estimated δ_{eq} remain similar to the late-time fixed value even in this more flexible model, fixing δ_{eq} can

be considered a robust and conservative assumption for subsequent analyses. Because δ_{eq} estimates were very close between fixed and freely estimated δ_{eq} for all tissues and AICc-based support favored fixed δ_{eq} for most cases, δ_{eq} was treated as an empirically anchored constant (i.e., not estimated as a free model parameter) in subsequent kinetic fits to ensure methodological uniformity. Skin contained only early-time data, so its asymptote (δ_{eq}) could not be estimated empirically and was fixed at -24.7‰, an intermediate proxy based on late-time values of the keratinized tissues (scute and claw) measured at the end of the experiment.

2.3.4.2.3 – Model selection and parameter reporting

Model structure was then assessed under fixed δ_{eq} by comparing one- (1C) and two-compartment (2C) formulations using AICc (ΔAICc) and Akaike weights. The AICc-based model selection test was performed for the dataset restricted to early observations (≤ 180 days) and late observations approaching an asymptote (≥ 1140 days), anchoring δ_{eq} from late values. The test resulted in distinct outcomes for the tissues. The 2C model was strongly supported for blood $\delta^{13}C$ ($AICc_{1C}$ = -128.4 vs. $AICc_{2C}$ = -137.5; ΔAICc = 9.11; w_{1C} = 0.01, w_{2C} = 0.99), and the fitted solution was robust to multiple sets of starting parameter values, converging to a stable two-timescale structure. In contrast, scute $\delta^{13}C$ supported the 1C model over the 2C alternative ($AICc_{1C}$ = 40.2 vs. $AICc_{2C}$ = 44.9; ΔAICc = 4.65; w_{1C} = 0.91, w_{2C} = 0.09), with 2C fits showing poor stability across starting values and frequent convergence to boundary or effectively mono-exponential solutions. For claw $\delta^{13}C$, 1C and 2C received nearly equivalent support ($AICc_{1C}$ = 11.5 vs. $AICc_{2C}$ = 10.9; ΔAICc = 0.58; w_{1C} = 0.43, w_{2C} = 0.57), indicating no meaningful advantage of the more complex formulation; therefore, inference for claw $\delta^{13}C$ under this subset was based on 1C by parsimony. For skin $\delta^{13}C$, fixing δ_{eq} at -24.8‰ yielded apparent AICc support for 2C; however, because only early-time observations were available and 2C tended toward parameter degeneracy[9], we treated skin as an assumption-based fit and retained the 1C curve.

[9] Parameter degeneracy refers to a lack of parameter identifiability that occurs when a model has more parameters than the information content of the data can support. In this situation, many different parameter combinations yield virtually indistinguishable fitted curves, so the model may reproduce the trajectory well, but individual parameter estimates are not uniquely or stably determined and should not be interpreted mechanistically. In isotope turnover models – particularly two-compartment (2C) formulations – degeneracy commonly manifests as convergence to boundary solutions (e.g., $p \to 0$ or $p \to 1$; k approaching an imposed lower bound such as 10^{-6}), collapse of the biphasic structure when $k_1 \approx k_2$ (effectively reducing the 2C model to a mono-exponential, 1C-like behavior), or strong parameter trade-offs in which changes in δeq are offset by compensatory changes in p and/or k_2, leaving the predicted curve largely unchanged.

2.3.4.2.4 – Uncertainty estimation

Uncertainty in turnover model fits was quantified using a nonparametric bootstrap with individual-level resampling (B = 1,200). For each replicate, the model was refitted, and 95% pointwise confidence intervals were derived for each sampling time from the empirical distribution of bootstrap-predicted δ^{13}C values (2.5th–97.5th percentiles; percentile method). Marginal 95% confidence intervals for δ_{eq} were obtained from its bootstrap distribution, whereas confidence intervals for rate constants (λ for 1C; λ1 and λ2 for 2C) were obtained from the bootstrap distributions of refitted model parameters using the percentile method. Convergence was high across models (valid refits: blood 2C = 1177/1200; scute 1C = 1200/1200; claw 1C = 1200/1200; skin 1C = 1200/1200), and only converged refits were included in bootstrap summaries. To propagate uncertainty in the empirically anchored equilibrium value, δ_{eq} was re-estimated from late-time observations within each bootstrap replicate ($t \geq 1140$ d; mean of individual means), and the kinetic model was then refitted with δ_{eq} fixed at that replicate-specific value. For skin, δ_{eq} was fixed a priori; thus, bootstrap uncertainty reflects only the fitted trajectory and turnover rate conditional on that fixed δ_{eq}.

2.3.4.2.5 – Estimation of turnover rates (λ)*, isotopic residence times* (τ)*, half-lives (T50) and near-asymptotic equilibrium (T95 and T99)*

Turnover rate constants were derived from the models fitted to the data, and the corresponding isotopic residence times were calculated using Eq. 1. For 1C tissues (scute, claw and skin), half-lives (T50) and near-asymptotic equilibrium (T95 and T99) were estimated using Eq. 11 [$\ln(1 - F) = -\lambda t$], which yields T50 = ln(2)/λ, T95 = ln(20)/λ, and T99 = ln(100)/λ. For 2C tissue (whole blood), these parameters were obtained from the following equation (adapted from Eq. 9):

$$(1 - F) = pe^{-\lambda_1 t} + (1 - p)e^{-\lambda_2 t} \quad (12)$$

In both cases (1C and 2C), $(1 - F)$ – the fractional approach to equilibrium – equals 0.50 at T50, 0.05 at T95, and 0.01 at T99.

For whole blood, fitted by a 2C model, we estimated the contribution of the fast component (λ_1) to total turnover across different time points along the incorporation trajectory using the following equation:

$$share\_rate\_\lambda_{1(t)} = \frac{p\lambda_1 e^{-\lambda_1 t}}{p\lambda_1 e^{-\lambda_1 t} + (1-p)\lambda_2 e^{-\lambda_2 t}} \quad (13)$$

2.3.4.3 – Assessment of growth and allometric effects

We compared animal growth in terms of body mass and body size (straight carapace length, SCL). A quadratic polynomial regression provided the best fit for this relationship, according to AICc. Using the body-mass time series, we subsequently fitted an exponential growth curve, which was also supported by AICc. After estimating the growth rate (k_g) from this exponential model, we subtracted it from the tissue-specific turnover rates (λ in 1C; λ_1 and λ_2 in 2C) to separate the contribution of growth-related isotopic dilution from catabolic turnover (k_c).

Because our study animals were juveniles, we applied allometric scaling corrections based on Eq. 5 to extrapolate turnover kinetics to larger conspecifics. According to this equation, if body mass increases by a factor of X, the turnover rate is expected to scale as $X^{-0.25}$. However, we used the –0.22 exponent reported by Vander Zanden *et al*. (2015) because it is an ectotherm-specific value derived from empirical data. So, because the allometric relationship is expressed as a power law ($\lambda \propto M^{-0.22}$), reference mass of the study cohort was defined as the geometric mean of body mass observations (356.5 g), which corresponds to the arithmetic mean on the log scale and provides a representative central tendency under multiplicative scaling. For projections to larger animals, we considered three body-mass categories: 5 kg (typical market weight for commercially farmed *P. expansa*), 8 kg (approximate mean mass of wild adult males), and 25 kg (approximate mean mass of wild adult females). Based on Eq. 5, we derived a scaling factor (s) to multiply turnover rates and a time multiplier ($1/s$) to scale residence times and half-lives.

In commercial farms, *Podocnemis expansa* around the 5-kg body-mass range are still in a fattening phase and undergo non-negligible somatic growth. We therefore estimated an exponential specific growth rate (k_g) for the 5-kg mass class from captive-rearing data reported by Melo *et al*. (2003), who observed an increase in mean body mass from 3.609 kg

to 6.338 kg over a 12-month interval (between 24 and 36 months of rearing). The rate was calculated as:

$$k_g = \frac{\ln (W_2 \,/\, W_1)}{\Delta t} \tag{14}$$

where k_g is the exponential specific growth rate (time –1), W_1 is the initial body mass, W_2 is the final body mass, and Δt is the time interval between W_1 and W_2 (Crane, Ogle & Shoup, 2020). Because the source reported only mean body masses with no measure of dispersion, we approximated a 95% confidence interval by propagating uncertainty under a conservative coefficient of variation (CV = 25%). We then added this growth rate to the catabolic turnover constant estimated in our experiment and propagated uncertainty by combining their respective uncertainty bounds. For the other two body-mass categories (adult males at 8 kg and females at 25 kg), *P. expansa* growth is approximately 0.24 g day^{-1} (Andrade, 2012), which corresponds to ~0.00003 d^{-1} for an 8-kg animal and ~0.00001 d^{-1} for a 25-kg animal. Because these rates are very low, we treated growth-driven dilution as negligible for these projections and approximated λ as the catabolic rate constant alone.

2.4 – Results

2.4.1 – Trophic discrimination factors (TDFs)

Trophic discrimination factors differed among tissues for both elements (Table 1; Fig. 1). For carbon, $\Delta^{13}C$ values spanned both enrichment and depletion relative to diet. Whole blood showed the largest ^{13}C depletion (median $\Delta^{13}C$ = –1.9‰), followed by claw (–1.3‰) and skin (–0.4‰). In contrast, scute keratin showed a slight ^{13}C enrichment ($\Delta^{13}C$ = +0.6‰). All pairwise contrasts among tissues for $\Delta^{13}C$ differed significantly (different letter groups in Table 1). For nitrogen, all tissues were ^{15}N-enriched relative to diet, with median $\Delta^{15}N$ values ranging from +1.8‰ in whole blood to +3.1‰ in skin, whereas the other two keratinized tissues (scute and claw) had similar median $\Delta^{15}N$ values (+2.7‰) (Table 1, Fig. 1). Significant differences were detected among tissues, except for scute keratin, which did not differ significantly from either claw or skin.

Table 1 – Isotopic values (median $\delta^{13}C$ and $\delta^{15}N$, ‰) and trophic discrimination factors (median $\Delta^{13}C$ and $\Delta^{15}N$, ‰) for juvenile *Podocnemis expansa* (n = 8) at the start of the experiment, immediately before the diet switch (d = 0). Trophic discrimination factors were calculated as $\Delta = \delta_{tissue} - \delta_{diet}$. Values are presented as medians and CI95%. Different letters indicate statistically significant differences (α = 0.05).

Tissue/diet	^{13}C		^{15}N	
	$\delta^{13}C$ (‰)	$\Delta^{13}C$ (‰)	$\delta^{15}N$ (‰)	$\Delta^{15}N$ (‰)
diet	-14.6	–	+3.7	–
whole blood	-16.5 (-16.7 – -16.3)	-1.9^{a} (-2.1 – -1.6)	+5.5 (5.5 – 5.7)	+1.8^{e} (1.8 – 2.0)
scute keratin	-14.0 (-14.4 – -13.1)	+0.6^{b} (0.2 – 1.5)	+6.4 (6.2 – 6.9)	+2.7^{fg} (2.5 – 3.1)
claw	-15.9 (-16.2 – -15.8)	-1.3^{c} (-1.6 – -1.2)	+6.4 (6.1 – 6.4)	+2.7^{f} (2.4 – 2.7)
skin	-15.0 (-15.1 – -14.9)	-0.4^{d} (-0.5 – -0.3)	+6.8 (6.5 – 6.9)	+3.1^{g} (2.9 – 3.2)

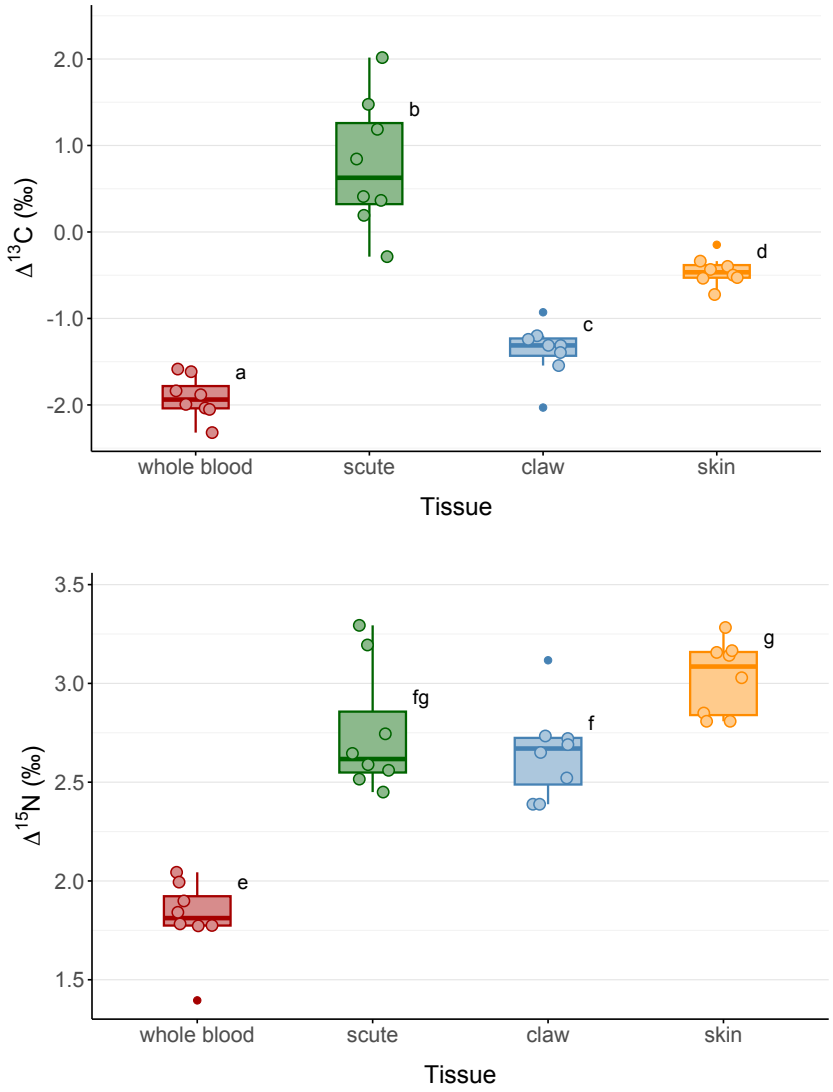

Figure 1. Comparison of tissue-specific trophic discrimination factors for carbon ($\Delta^{13}C$, ‰) and nitrogen ($\Delta^{15}N$, ‰) in juvenile *Podocnemis expansa* (n = 8) at the start of the experiment, immediately before the diet switch (d = 0). Circles represent individual Δ estimates calculated relative to the baseline diet; filled dots indicate outliers. Different letters denote statistically significant differences (α = 0.05).

2.4.2 – Isotopic turnover

Exploratory visualization of the full $\delta^{13}C$ time series (Fig. 2) revealed that turnover data trajectories departed from the expected smooth, monotonic approach to equilibrium, exhibiting unusually shallow curvature, intermittent plateaus, and occasional reversals, particularly in whole blood, scute, and claw. For skin, observations extended only to 180 days, limiting evaluation of longer-term turnover dynamics. These artifacts were likely influenced by contamination of the experimental diet with isotopically C4 food items, as described in the Methods. Data in Fig. 2 are shown both as individual observations (left panels) and as time-point means with 95% confidence intervals (CI95%) (right panels). Fitted curves and model equations are reported only for the individual-level dataset to avoid aggregation bias (curves were overlaid on the mean ± CI95% plots for illustrative purposes).

When we restricted the analyses to the early response to the diet shift (0–180 days) and the late-time approach to equilibrium (≥ 1140 days), the fitted trajectories aligned more consistently with plausible incorporation kinetics (plots in Fig. 3). In these plots, light blue marks the observations excluded from model fitting, whereas dark blue dots are the retained data. Data filtering reduced the amount of usable information and widened uncertainty intervals, particularly during the late incorporation phase for whole blood, scute, and claw (for skin, we fixed δ_{eq} because late-time observations were unavailable, so uncertainty was concentrated mainly in the mid-trajectory portion of the curve). Consequently, confidence in estimates of asymptotes, turnover rates, isotopic residence times, and isotopic half-lives was certainly lower than it would have been with a full, uncontaminated dataset.

Even using filtered data, isotopic turnover rates remained low, resulting in long residence times and half-lives as expected for ectothermic organisms (Tables 2 and 3). These parameters also varied markedly among tissues and were strongly influenced by growth (Fig. 5, Tables 5 and 6). Prior to removal of growth effects (Table 3), claw showed the fastest response to the dietary shift (half-life ≈ 64 days), followed by whole blood (half-life ≈ 166 days), scute keratin (half-life ≈ 171 days), and skin (half-life ≈ 186 days) (values rounded to the nearest integer).

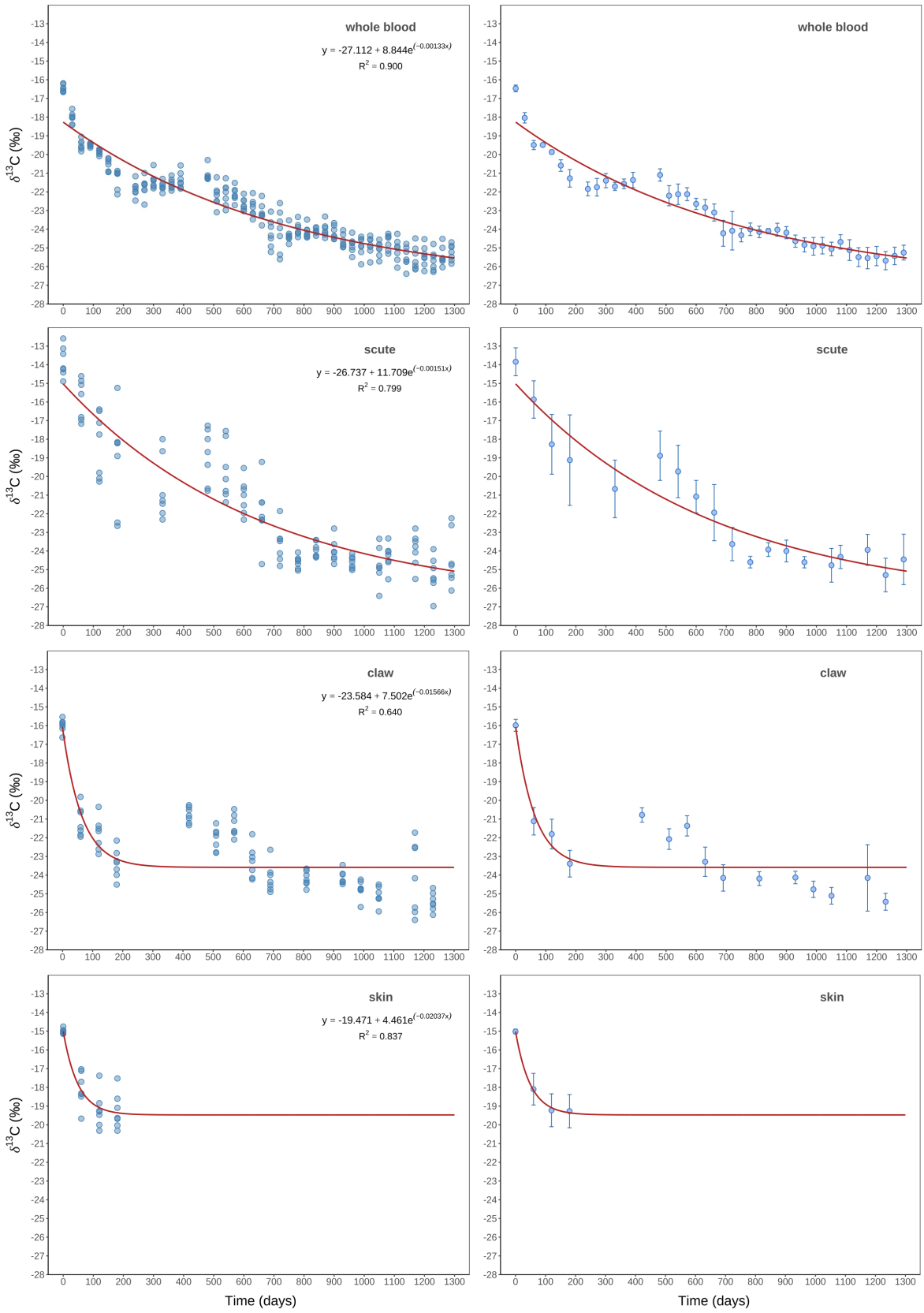

Figure 2 – Preliminary isotopic turnover plots for each tissue fitted with monoexponential curves (one compartment models). Left-hand panels show individual observations, whereas right-hand panels summarize the data as time-point means with 95% confidence intervals, to facilitate visualization of overall patterns. To avoid aggregation bias, the fitted curves shown in the mean + CI95% plots were overlaid from the corresponding individual-level fits for each tissue, solely for illustrative purposes.

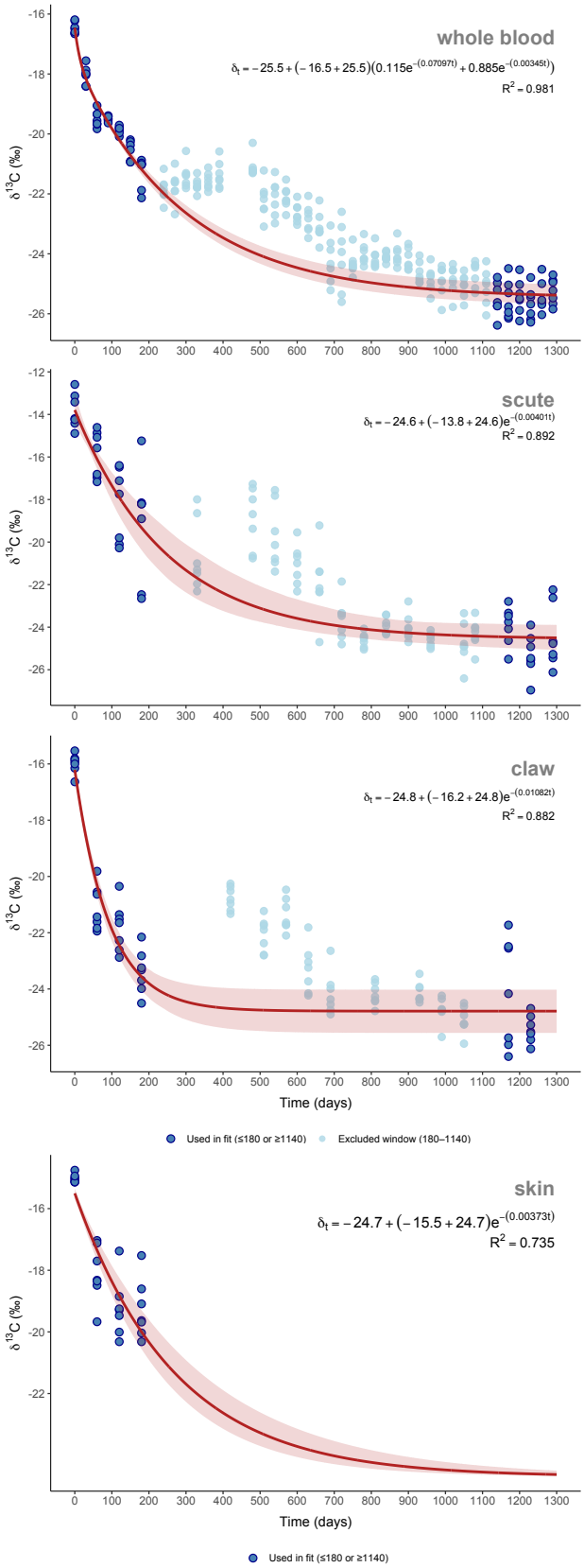

Figure 3 – ^{13}C turnover in juvenile *Podocnemis expansa* tissues following the dietary shift. Dots are individual measurements; dark blue indicates observations used for model fitting (t = 0–180 days and t ≥ 1140 days); light blue indicates excluded observations. Lines show best-fit first-order kinetic models (two-compartment for whole blood; one-compartment for scute, claw, and skin). Shaded ribbons represent 95% bootstrap confidence bands.

Whole blood was the only tissue that required a two-compartment (2C) model. In contrast, claw, scute, and skin were more parsimoniously described by one-compartment (1C) models. For whole blood, the 2C model was consistent with the presence of two carbon pools with contrasting turnover rates. The fast component had $\lambda_1 = 0.07077$ day^{-1}, while the slow component had $\lambda_2 = 0.00344$ day^{-1}, with a relatively small mixing weight for the fast component ($p = 0.115$) (Table 2). The two-timescale structure translated into markedly different residence times ($\tau_1 \approx 14$ days and $\tau_2 \approx 291$ days; Table 3). Composite turnover progression in whole blood reached the half-life (T50) at ~166 days and the near-asymptotic equilibrium (T95) at ~836 days. The fractional contribution of the fast component to the overall composite rate declined rapidly during incorporation (Table 4). The contribution of λ_1 was ~71% at day 1 and ~58% at day 10, but declined to ~26% by day 30 and to near-zero by days 60–83, indicating that the fast pool dominated whole-blood turnover only during the initial incorporation phase, after which the slow pool entirely governed the turnover kinetics. At the isotopic half-life (T50 ≈ 166 days), λ_1 accounted cumulatively for about 23% of total whole-blood turnover; by near-equilibrium (T95 ≈ 836 days), its contribution had declined to around 12% of the overall isotopic replacement.

Among the 1C tissues, turnover rates differed substantially (Table 2). Claw stood out by exhibiting the highest rate, followed by scute and skin. These differences were reflected in turnover times: claw reached half-life at ~64 days and T95 at ~276 days, whereas scute keratin and skin exhibited markedly longer timescales (scute half-life ≈ 171 days, T95 ≈ 738 days; skin half-life ≈ 186 days, T95 ≈ 804 days) (Table 3).

Table 2 – Model parameters for turnover kinetics of the experimental cohort. Parameters are reported as medians with 95% confidence intervals (95% CI). For skin, δ_{eq} was fixed a priori due to the absence of late-time observations; thus, uncertainty in skin parameters is conditional on the assumed δ_{eq}.

Tissue	δ_{eq} (‰)	λ (day^{-1})	p	λ_1 (day^{-1})	λ_2 (day^{-1})	R^2
whole blood	-25.5 (-25.8 – -25.1)	–	0.115 (0.093 – 0.142)	0.07077 (0.05154–0.13393)	0.00344 (0.00328–0.00363)	0.981
scute keratin	-24.6 (-25.3 – -23.9)	0.00406 (0.00260–0.00594)	–	–	–	0.892
claw	-24.8 (-25.6 – -24.0)	0.01086 (0.00909–0.01275)	–	–	–	0.882
skin	-24.7 (fixed)	0.00373 (0.00295–0.00445)	–	–	–	0.735

Table 3 – Isotopic residence times (τ) and turnover progression across tissues. Turnover estimated at 50% incorporation (T50 = half-life) and near-asymptotic equilibrium [95% incorporation (T95) and 99% incorporation (T99)]. Values are presented as medians and 95% CI. For scute, claw, and skin (one-compartment fits), turnover times were calculated from Eq. 11 as $t = -\ln(1 - F)/\lambda$; thus, $T50 = \ln(2)/\lambda$, $T95 = \ln(20)/\lambda$, and $T99 = \ln(100)/\lambda$. For whole blood (two-compartment fit), T50, T95 and T99 were defined as solutions to Eq. 12.

Tissue	τ (days)	τ_1 (days)	τ_2 (days)	T50 (days)	T95 (days)	T99 (days)
whole blood	–	14.1 (7.5–19.4)	290.7 (275.6–305.0)	166.0 (155.4–174.5)	835.5 (792.9–874.3)	1303.5 (1236.4–1364.0)
scute keratin	246.4 (168.3–384.9)	–	–	170.8 (116.6–266.8)	738.3 (504.1–1153.0)	1134.9 (775.0–1772.4)
claw	92.1 (78.4–110.0)	–	–	63.8 (54.4–76.2)	275.8 (235.0–329.5)	423.9 (361.2–506.5)
skin	268.3 (224.7–338.9)	–	–	186.0 (155.8–234.9)	803.7 (673.2–1015.4)	1235.4 (1034.8–1560.9)

Table 4 – Fractional contribution of the fast-component rate (λ_1) to the overall rate (λ) in whole blood turnover during the early phase of the incorporation trajectory (values computed using Eq. 13; $p = 0.115$, $\lambda_1 = 0.07077$, $\lambda_2 = 0.00344$).

Turnover time	Fractional contribution of λ_1
day 1	~ 71%
day 10	~ 58%
day 30	~ 26%
day 60	~ 4%
day 83	< 1%

Juveniles grew substantially during the experiment (Figs. 4–5), and the fitted growth rate from the cohort was $k_g = 0.00127\ day^{-1}$. We used this rate to partition observed turnover into growth-driven isotopic dilution and catabolic replacement (Tables 5 and 6). Growth contributed a non-trivial fraction of empirical turnover rate, but its proportional contribution varied among tissues (Table 5). Among the one-compartment tissues, the fraction attributable to growth (k_g/λ) was broadly similar for scute keratin (~31%) and skin (~34%), but substantially lower for claw, in which growth accounted for only ~12% of the empirical turnover. A growth contribution comparable to scute keratin and skin also characterized the long-timescale pool in whole blood: growth accounted for ~37% of the slow component (λ_2), but only ~2% of the fast component (λ_1). This pattern indicates that growth-driven isotopic dilution influenced whole-blood turnover throughout the intermediate and late phases of incorporation, after the brief fast-component phase (~83 days). After removing growth effects, the resulting lower catabolic turnover rates (Table 5)

led to longer residence times and slower turnover progression across all tissues (Table 6). Scute keratin half-life increased from ~171 days to ~249 days and T95 from ~738 days to ~1075 days, while skin half-life increased from ~186 to ~282 days and T95 from ~804 to ~1219 days. Whole-blood composite turnover likewise slowed after removal of growth effects (half-life from ~166 to ~263 days; T95 from ~836 to ~1325 days). Claw showed the smallest absolute shift because the growth rate was relatively small compared with its λ; nevertheless, half-life increased from ~64 to ~72 days and T95 from ~276 to ~312 days.

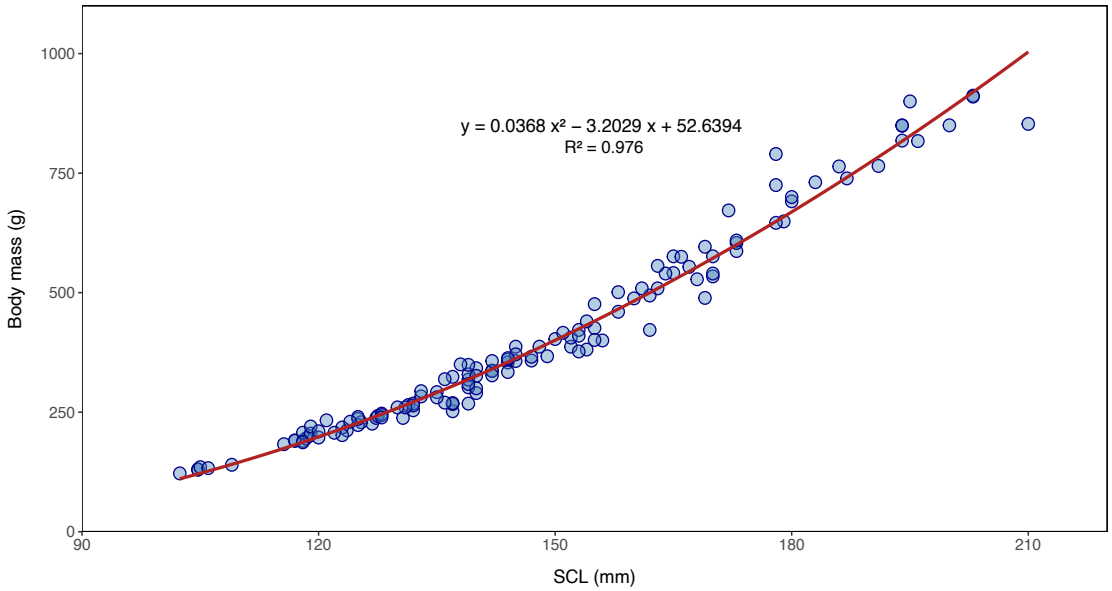

Figure 4 – Allometric relationship between straight carapace length (SCL) and body mass of juvenile *Podocnemis expansa* throughout the turnover experiment.

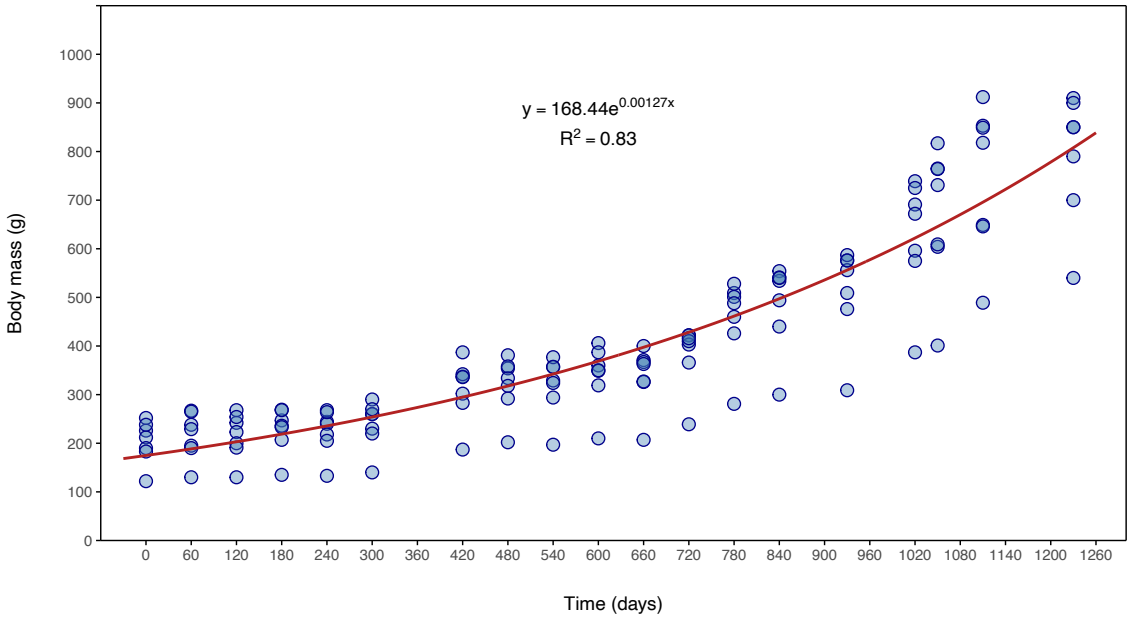

Figure 5 – Exponential growth trajectory of juvenile *Podocnemis expansa* throughout the turnover experiment.

Table 5 – Catabolic turnover rates after removing growth effect (k_g = 0.00127 day^{-1}) from the overall turnover rates λ (1C models – scute, claw and skin), λ_1 and λ_2 (2C model – whole blood). Values are presented as medians and 95% CI, along with the corresponding percentage contribution of growth to the total turnover rate (k_g/λ) for each tissue.

Tissue	k_c (day^{-1})	% growth (k_g/λ)	k_{1c} (day^{-1})	% growth (k_g/λ_1)	k_{2c} (day^{-1})	% growth (k_g/λ_2)
whole blood	–	–	0.06950 (0.05027–0.13266)	1.8% (0.9–2.5%)	0.00217 (0.00201–0.00236)	36.9% (35.0–38.7%)
scute keratin	0.00279 (0.00133–0.00467)	31.3% (21.4–48.9%)	–	–	–	–
claw	0.00955 (0.00782–0.01148)	11.7% (10.0–14.0%)	–	–	–	–
skin	0.00246 (0.00168–0.00318)	34.1% (28.5–43.0%)	–	–	–	–

Table 6 – Growth-corrected isotopic residence times (τ) and turnover progression across tissues (data based on catabolic turnover rates; $k_c = \lambda - k_g$). Turnover estimated at 50% incorporation (T50 = half-life) and near-asymptotic equilibrium [95% incorporation (T95) and 99% incorporation (T99)]. Values are presented as medians and 95% CI. For scute, claw, and skin (one-compartment fits), turnover times were calculated from Eq. 11 as $t = -\ln(1 - F)/\lambda$; thus, T50 = ln(2)/λ, T95 = ln(20)/λ, and T99 = ln(100)/λ. For whole blood (two-compartment fit), T50, T95 and T99 were defined as solutions to Eq. 12.

Tissue	τ (days)	τ_1 (days)	τ_2 (days)	T50 (days)	T95 (days)	T99 (days)
whole blood	–	14.4 (7.5–19.9)	460.9 (424.0–497.9)	262.9 (240.1–282.2)	1324.7 (1219.7–1425.0)	2067.8 (1902.8–2225.4)
scute keratin	358.7 (214.0–752.9)	–	–	248.6 (148.3–521.9)	1074.6 (641.1–2255.5)	1651.9 (985.6–3467.2)
claw	104.2 (87.1–127.8)	–	–	72.3 (60.4–88.6)	312.3 (261.0–383.0)	480.1 (401.2–588.7)
skin	406.9 (314.4–595.1)	–	–	282.0 (218.0–412.5)	1219.0 (942.0–1782.8)	1873.9 (1448.1–2740.6)

Allometric scaling analyses projected substantially slower $\delta^{13}C$ turnover with increasing body mass (Table 7). As a consequence, scaled catabolic turnover constants decreased across all tissues in the 5-, 8-, and 25-kg scenarios (Table 8), and predicted turnover times increased accordingly (Table 10). Under the 5-kg scenario, incorporating an additional growth term derived from farm growth data produced intermediate turnover times relative to the juvenile estimates and the purely catabolic adult projections (Tables 9–10). In contrast, assuming zero growth for the 8- and 25-kg scenarios led to markedly prolonged turnover, with predicted T50 and especially T95 reaching multi-month to multi-year scales in whole blood, scute keratin, and skin (Table 10). Across all body-mass classes, claw consistently exhibited the fastest incorporation, with the highest scaled turnover rates among

tissues and, consequently, the shortest predicted half-life and T95 values (Tables 8 and 10). This pattern was consistent under both the 5-kg scenario including growth and the 8-kg and 25-kg zero-growth scenarios (Table 10).

Table 7 – Rate-scaling factors (s) and corresponding time multipliers (1/s) derived from $\lambda \propto M^{-0.22}$ for three projected body-mass scenarios in *Podocnemis expansa*: 5 kg (typical market mass of farmed individuals), 8 kg (approximate mean mass of wild adult males), and 25 kg (approximate mean mass of wild adult females).

Scenario	Mass (g)	Rate scaling factor (s)	Time multiplier (1/s)
5 kg	5,000	0.5593	1.7878
8 kg	8,000	0.5044	1.9826
25 kg	25,000	0.3926	2.5474

Table 8 – Allometrically scaled catabolic turnover rates (medians and 95% CI).

Tissue	Scenario	k_c (day^{-1})	k_{1c} (day^{-1})	k_{2c} (day^{-1})
whole blood	5 kg	–	0.03887 (0.02811–0.07420)	0.00121 (0.00112–0.00132)
	8 kg	–	0.03506 (0.02536–0.06691)	0.00109 (0.00101–0.00119)
	25 kg	–	0.02729 (0.01974–0.05208)	0.00085 (0.00079–0.00093)
scute keratin	5 kg	0.00156 (0.00074–0.00261)	–	–
	8 kg	0.00141 (0.00067–0.00236)	–	–
	25 kg	0.00109 (0.00052–0.00183)	–	–
claw	5 kg	0.00537 (0.00437–0.00642)	–	–
	8 kg	0.00484 (0.00395–0.00579)	–	–
	25 kg	0.00377 (0.00307–0.00451)	–	–
skin	5 kg	0.00137 (0.00094–0.00178)	–	–
	8 kg	0.00124 (0.00085–0.00160)	–	–
	25 kg	0.00096 (0.00066–0.00125)	–	–

Table 9 – Overall turnover rates (catabolic turnover + growth) projected for *Podocnemis expansa* in the 5-kg body-mass range. Values were obtained by adding the catabolic turnover rate estimated for this mass range (Table 8) to the growth rate inferred from Melo *et al*. (2003) ($0.00154\ \text{day}^{-1} \pm 0.00020$). Reported intervals incorporate uncertainty from both rate constants.

Tissue	(λ day^{-1})	λ_{1c} (day^{-1})	λ_{2c} (day^{-1})
whole blood	–	0.04041 (0.02969–0.07573)	0.00275 (0.00253–0.00298)
scute keratin	0.00309 (0.00226–0.00418)	–	–
claw	0.00691 (0.00593–0.00797)	–	–
skin	0.00292 (0.00244–0.00336)	–	–

Table 10 – Allometrically scaled isotopic residence times (τ) and turnover progression across tissues. Turnover estimated at 50% incorporation (T50 = half-life) and near-asymptotic equilibrium [95% incorporation (T95) and 99% incorporation (T99)]. Values are presented as medians and 95% CI. For scute, claw, and skin (one-compartment fits), turnover times were calculated from Eq. 11 as $t = -\ln(1 - F)/\lambda$; thus, $T50 = \ln(2)/\lambda$, $T95 = \ln(20)/\lambda$, and $T99 = \ln(100)/\lambda$. For whole blood (two-compartment fit), T50, T95 and T99 were defined as solutions to Eq. 12. For the 5-kg category, turnover times were calculated combining the catabolic turnover rate obtained in this experiment with the growth rate inferred from Melo *et al*. (2003) (Table 9). For the remaining categories, only the catabolic turnover rate was considered, assuming zero growth.

Tissue	Scenario	τ (days)	τ_1 (days)	τ_2 (days)	T50 (days)	T95 (days)	T99 (days)
whole blood	5 kg	–	24.7 (13.2–33.7)	363.2 (335.8–394.9)	207.3 (189.7–226.2)	1044.0 (966.1–1136.5)	1628.4 (1506.6–1772.6)
	8 kg	–	28.5 (14.9–39.4)	913.8 (840.6–987.2)	521.2 (475.9–559.6)	2626.3 (2418.2–2825.2)	4099.6 (3772.4–4412.0)
	25 kg	–	36.6 (19.2–50.7)	1174.0 (1080.0–1268.3)	669.6 (611.4–718.9)	3374.2 (3106.8–3629.7)	5267.0 (4846.6–5668.4)
scute keratin	5 kg	323.1 (239.4–442.7)	–	–	224.0 (165.9–306.8)	967.9 (717.2–1326.2)	1488.0 (1102.5–2038.6)
	8 kg	711.2 (424.3–1492.6)	–	–	492.9 (294.1–1034.6)	2130.5 (1271.1–4471.6)	3275.1 (1954.0–6873.9)
	25 kg	913.7 (545.1–1917.7)	–	–	633.3 (377.9–1329.3)	2737.2 (1633.1–5744.9)	4207.7 (2510.4–8831.4)
claw	5 kg	144.6 (125.5–168.6)	–	–	100.2 (87.0–116.9)	433.3 (375.8–505.1)	666.0 (577.8–776.4)
	8 kg	206.7 (172.7–253.5)	–	–	143.3 (119.7–175.7)	619.1 (517.4–759.3)	951.8 (795.3–1167.2)
	25 kg	265.5 (221.9–325.6)	–	–	184.1 (153.8–225.7)	795.5 (664.7–975.5)	1222.8 (1021.8–1499.6)
skin	5 kg	342.9 (297.5–409.1)	–	–	237.7 (206.2–283.6)	1027.2 (891.1–1225.5)	1579.1 (1369.9–1883.9)
	8 kg	806.7 (623.4–1179.8)	–	–	559.2 (432.1–817.8)	2416.7 (1867.6–3534.5)	3715.0 (2870.9–5433.4)
	25 kg	1036.4 (800.9–1515.8)	–	–	718.4 (555.2–1050.7)	3104.9 (2399.4–4541.0)	4773.0 (3688.4–6980.6)

2.5 – Discussion

2.5.1 – Trophic discrimination factors

Our results show that TDFs in *Podocnemis expansa* are strongly tissue-specific, reinforcing the pronounced taxonomic and among-tissue variability documented in ectotherms (Soto *et al*., 2025) and underscoring the limitations of adopting fixed literature values [e.g., 0‰ – 1.0‰ for $\Delta^{13}C$ and 3.0‰ – 4.0‰ for $\Delta^{15}N$ (DeNiro & Epstein, 1978; Deniro & Epstein, 1981; Post, 2002)] that have been widely used in isotopic mixing models (Caut *et al*., 2009; Stephens *et al*., 2023). Both carbon and nitrogen discrimination varied among tissues, with differences not only in magnitude but also, for carbon, in direction. $\Delta^{13}C$ was negative in whole blood (−1.9‰), claw (−1.3‰), and skin (−0.4‰), but positive in scute keratin (+0.6‰). By contrast, $\Delta^{15}N$ was consistently positive across tissues, although still tissue dependent ($\Delta^{15}N$ = +1.8‰ in whole blood; +2.7‰ in scute keratin and claw; +3.1‰ in skin). Such within-species heterogeneity indicates that tissue type is a major determinant of TDFs. Accounting for this variation can improve quantitative isotopic inference by supporting the use of tissue- and species-specific TDFs, particularly when sources are isotopically similar or when sampling design and analytical resolution constrain effective source discrimination (Caut *et al*., 2009; Stephens *et al*., 2023).

Although the literature on TDFs in turtles is limited, discrimination factors clearly vary not only across reptile orders but also within chelonians. Soto *et al*. (2025) compiled the available literature reporting $\Delta^{13}C$ and $\Delta^{15}N$ for multiple tissues in reptiles. Compared with that dataset, $\Delta^{13}C$ values for whole blood, claw, and skin in *P. expansa* were more negative than the overall ranges reported for other taxa, whereas scute keratin values overlapped with published ranges. For $\Delta^{15}N$, scute keratin and claw were more positive than those reported for other species or groups, while whole blood and skin showed overlapping ranges (Tables 11 and 12, Figure 6).

Table 11 – Comparison of $\Delta^{13}C$ (‰) values for *Podocnemis expansa* (this study) with mean values reported in the literature by reptile taxon. Literature ranges were summarized from the synthesis of Soto *et al*. (2025), which compiled species-specific estimates, associated standard deviations, diet information, and the corresponding original sources.

	Testudines				Squamata	Crocodilia
	Continental (non-marine) chelonians				Small terrestrial reptiles (lizards, snakes and iguanas)	Crocodilians
	Freshwater turtles		Terrestrial chelonians	Sea turtles		
Tissue	*Podocnemis expansa*	*Trachemys scripta*	*Gopherus agassizii, Terrapene ornata luteola*	*Chelonia mydas, Caretta caretta, Dermochelys coriacea*	*Crotaphytus collaris, Sceloporus undulatus, Elaphe guttata guttata, Cyclura* spp.	*Crocodylus niloticus, Alligator mississippiensis, Caiman latirostris*
plasma	–	–	+0.3 – +3.7	–0.6 – +1.2	–0.5 – +0.2	–1.7 – +0.2
whole blood/ red blood cells (RBC)	–1.9	–	–2.5 – +4.1	–1.1 – +1.5	–1.1 – +2.5	–1.6 – +0.7
scute/ scute keratin	+0.6	–	–0.9 – +5.1	–0.9 – +1.8	–	–0.9 – +0.9
claw/ nail	–1.3	–	–	–	+1.2	–0.8 – +1.2
skin/dermis/ epidermis	–0.4	–	–	+0.2 – +2.6	–0.8 – +4.5	–

Table 12 – Comparison of $\Delta^{15}N$ (‰) values for *Podocnemis expansa* (this study) with mean values reported in the literature by reptile taxon. Literature ranges were summarized from the synthesis of Soto *et al*. (2025), which compiled species-specific estimates, associated standard deviations, diet information, and the corresponding original sources.

	Testudines				Squamata	Crocodilia
	Continental (non-marine) chelonians				Small terrestrial reptiles (lizards, snakes and iguanas)	Crocodilians
	Freshwater turtles		Terrestrial chelonians	Sea turtles		
Tissue	*Podocnemis expansa*	*Trachemys scripta*	*Gopherus agassizii, Terrapene ornata luteola*	*Chelonia mydas, Caretta caretta, Dermochelys coriacea*	*Crotaphytus collaris, Sceloporus undulatus, Elaphe guttata guttata, Cyclura* spp.	*Crocodylus niloticus, Alligator mississippiensis, Caiman latirostris*
plasma	–	+2.5 – +3.8	–	+0.3 – +4.2	+2.7 – +3.5	–2.2 – +1.2
whole blood/ red blood cells (RBC)	+1.8	–0.8 – +2.2	–	–0.3 – +2.5	+2.8 – +4.1	–0.9 – +1.5
scute/ scute keratin	+2.7	–	–	–0.6 – +0.6	–	+0.8 – +1.5
claw/ nail	+2.7	–	–	–	+0.7	+1.1 – +1.8
skin/dermis/ epidermis	+3.1	–	–	+1.6 – +4.9	+4.2 – +6.0	–

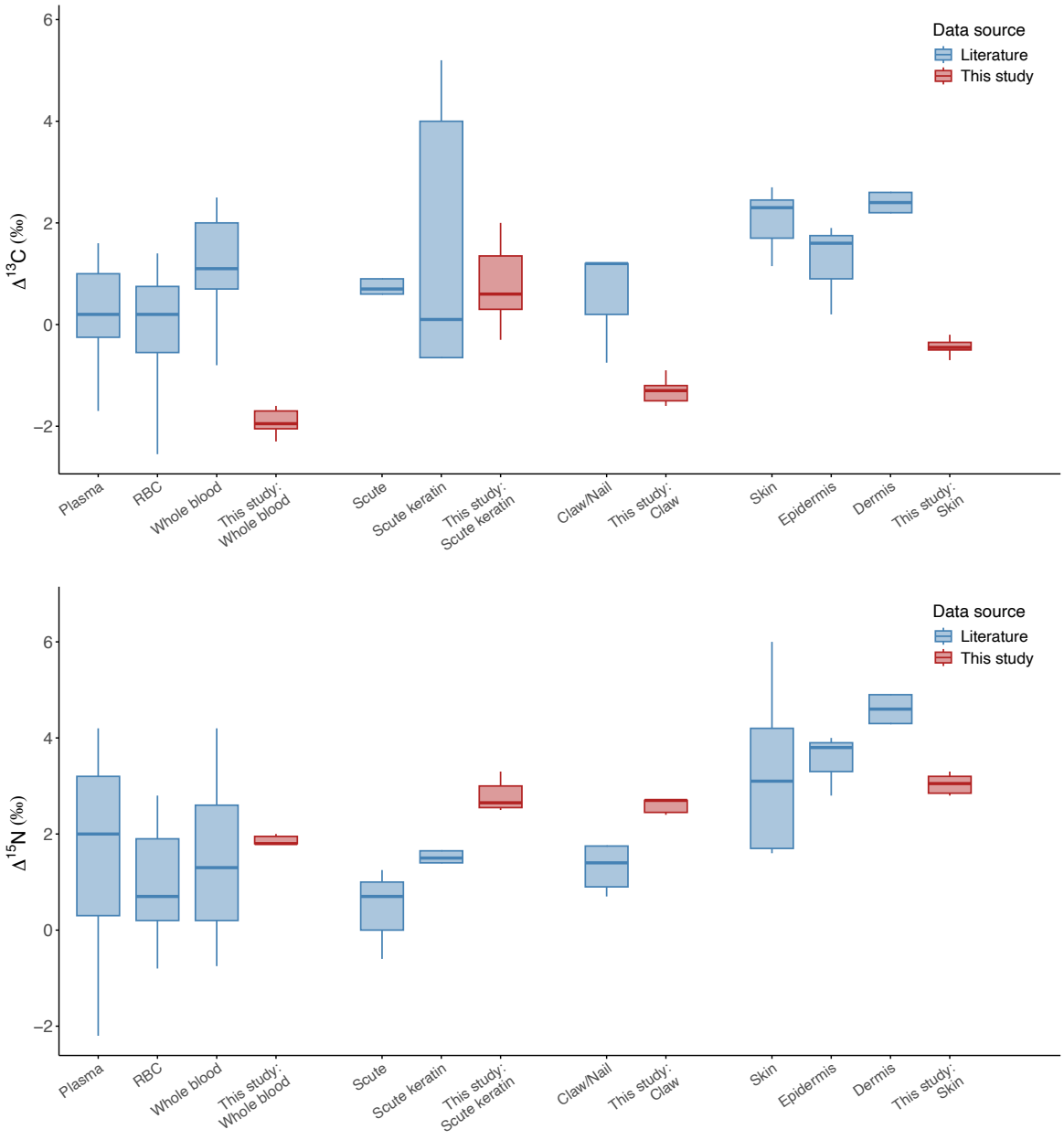

Figure 6 – Graphical comparison of $\Delta^{13}C$ and $\Delta^{15}N$ values for *Podocnemis expansa* (this study, red boxplots) and literature values for reptiles (blue boxplots), based on the dataset compiled by Soto *et al*. (2025).

In the compilation by Soto *et al*. (2025), only three studies addressed continental (non-marine) chelonians – one on a freshwater turtle and two on desert-dwelling species (one tortoise and one terrestrial turtle). Regarding the freshwater turtle study, the whole-blood $\Delta^{15}N$ value of *Podocnemis expansa* (+1.8‰) closely matched the whole-blood (+2.2‰) and red-blood-cell (RBC) (+1.9‰) values reported for *Trachemys scripta*, a temperate freshwater turtle native to North America (Seminoff *et al*., 2007). However, this similarity was observed under only one of the two experimental diets used in that study (a ^{15}N-depleted diet, $\delta^{15}N$ = +4.8‰) [the diet used in our experiment would also be classified,

under that paper's criteria, as ^{15}N-depleted (δ^{15}N = +3.7‰)]. Under a second diet (^{15}N-enriched, δ^{15}N = 10.3‰), whole-blood Δ^{15}N differed markedly (−0.8‰), both in magnitude and in direction (RBC were not analyzed under this second diet). The similarity in TDFs observed by those authors under one of the diets between whole blood and RBC supports the practical assumption that RBC-based estimates provide the closest available analogue for whole-blood comparisons, a pattern also reported by Seminoff *et al*. (2006). By contrast, the discrepancies observed in whole blood values between the two diets demonstrate the strong influence of diet on TDFs, in line with the syntheses presented by Caut *et al*. (2009) and Stephens *et al*. (2023).

Compared with desert chelonians studied by Murray and Wolf, whole-blood Δ^{13}C in *P. expansa* (−1.9‰) differed markedly from most RBC Δ^{13}C values reported for *Gopherus agassizii* (Murray & Wolf, 2012) and *Terrapene ornata luteola* (Murray & Wolf, 2013), approximating the value reported for only one of the experimental groups evaluated across both studies. In *G. agassizii*, RBC Δ^{13}C values were slightly positive, reaching +0.2‰ under a ^{13}C-enriched diet and +0.8‰ under a ^{13}C-depleted diet [notably, the diet used in our experiment was likewise ^{13}C-enriched (δ^{13}C = −14.6‰)]. In *T. ornata luteola*, RBC Δ^{13}C values showed much broader variation across two experimental cohorts, ranging from negative under the enriched diet (−2.5‰ and −0.5‰) to strongly positive under the depleted diet (+3.2‰ and +4.1‰). The same studies also reported scute-keratin values. In *G. agassizii*, scute-keratin Δ^{13}C remained positive under both enriched (+0.8‰) and depleted (+0.6‰) diets and was closely aligned with the value observed in *P. expansa* (+0.6‰). In *T. ornata luteola*, by contrast, scute-keratin Δ^{13}C again ranged from negative values under the enriched diet (−0.2‰ and −0.9‰) to strongly positive values under the depleted diet (+5.1‰ and +4.0‰), differing from *P. expansa* under both dietary treatments.

Concerning sea turtles, small terrestrial reptiles, and crocodilians, a similar pattern emerges, with substantial variation linked to taxon, tissue, diet, ontogenetic stage, and experimental conditions. In some groups, however, Δ^{13}C and Δ^{15}N values are consistently positive. For example, Δ^{13}C in adult iguanas of the genus *Cyclura* was +2.5‰ in whole blood and +4.5‰ in skin, whereas Δ^{15}N was +4.1‰ in whole blood and +6.0‰ in skin (Steinitz *et al*., 2016). In contrast, crocodilians studied by several authors generally displayed lower TDFs, with Δ^{13}C ranging from −1.7‰ to +1.2‰ depending on tissue (plasma, whole blood, scute, and claw) (Table 11) and Δ^{15}N varying between −2.2‰ and +1.8‰ across the same tissues (Table 12).

Collectively, these comparisons indicate that the variability observed in *Podocnemis expansa* points to a combination of dietary, physiological, ontogenetic, and biochemical drivers. Several non-mutually exclusive mechanisms may underlie the negative $\Delta^{13}C$ values observed in whole blood, claw, and skin, the positive $\Delta^{13}C$ value observed in scute keratin, and the intermediate but tissue-dependent $\Delta^{15}N$ values documented here.

Diet isotopic composition is a well-established determinant of trophic discrimination. Experimental syntheses have demonstrated negative relationships between diet $\delta^{15}N$ and $\Delta^{15}N$, and, in some contexts, between diet $\delta^{13}C$ and $\Delta^{13}C$ (Caut *et al*., 2009; Stephens *et al*., 2023). This is one possible hypothesis to explain, for example, the relatively low $\Delta^{15}N$ values reported for crocodilians, which occupy high trophic positions [studies included in Soto *et al*. (2025), with values summarized in Table 12]. The experimental diet used in our study can be classified as relatively ^{15}N-depleted when compared to higher $\delta^{15}N$ diets used in other reptile TDF experiments (e.g., fish- or insect-based diets with $\delta^{15}N$ frequently exceeding 6–10‰). Within this diet-dependent scaling framework, the relatively low baseline $\delta^{15}N$ of our experimental diet may have contributed to comparatively elevated TDFs in *P. expansa* relative to other reptiles, particularly in scute keratin and claw and, to a lesser extent, in whole blood. At the same time, because the individuals were juveniles undergoing sustained growth, growth-mediated dilution may have exerted an opposing downward influence on $\Delta^{15}N$ by increasing the proportional contribution of tissue accretion to isotopic incorporation. Thus, the observed $\Delta^{15}N$ values likely reflect the net effect of these countervailing processes, with enrichment associated with the dietary baseline being partially offset by growth-related reductions in discrimination.

Similarly, the ^{13}C-enriched diet ($\delta^{13}C = -14.6$‰, reflecting a strong C_4 signature) may have contributed to the reduced $\Delta^{13}C$ observed in all tissues of our cohort, particularly the negative discrimination values in whole blood, claw, and skin. Meta-analytic evidence indicates that variation in diet isotopic composition explains a substantial fraction of cross-taxon differences in $\Delta^{13}C$, supporting that diet-dependent biochemical processes can yield reduced or even negative $\Delta^{13}C$ values across feeding regimes (Stephens *et al*., 2023).

In addition to isotopic baseline, dietary macronutrient composition – especially protein quantity and quality – can influence discrimination factors. Experimental studies have shown that low-protein or amino acid–imbalanced diets may increase $\Delta^{15}N$ through enhanced deamination, nitrogen recycling, and increased reliance on de novo synthesis of non-essential amino acids, whereas high-quality, well-balanced protein sources may reduce

isotopic diet-tissue fractionation (Pearson *et al*., 2003; Robbins, Felicetti & Sponheimer, 2005; Stephens *et al*., 2022; Stephens *et al*., 2023). Although the amino acid profile and digestible protein fraction of the diet used in the present study were not directly quantified, it is plausible that diet's protein content and quality interacted with its isotopic composition to shape the observed TDFs.

Regarding carbon, $\Delta^{13}C$ is strongly influenced by dietary macronutrient composition and substrate routing during tissue synthesis (Stephens *et al*., 2022). Mixed diets, such as the commercial feed provided prior to the turnover experiment, can reduce $\Delta^{13}C$ through differential metabolic routing (Stephens *et al*., 2022). Commercial feeds such as the one used in our pre-experimental diet typically contain soybean meal, a protein-rich ingredient with a C_3 carbon isotopic signature, and maize, a lower-protein ingredient with a C_4 signature (Andrade, 2008). When C_3-derived protein is consumed alongside C_4-derived carbohydrates, dietary amino acids are preferentially incorporated into tissue synthesis, whereas C_4 carbohydrates are predominantly oxidized for energy or diverted to lipid storage. As a result, tissues tend to reflect the C_3 protein signature rather than the isotopic composition of the bulk diet, yielding reduced or even negative $\Delta^{13}C$ values (Stephens *et al*., 2022). It is therefore plausible that such routing mechanisms contributed to the comparatively low $\Delta^{13}C$ observed across tissues in *P. expansa*.

Ontogenetic stage likely also influenced the observed TDFs in *P. expansa*. Tissue accretion during juvenile growth reduces the relative contribution of catabolic replacement to isotopic incorporation (Reich *et al*., 2008). In juvenile growing ectotherms, a substantial fraction of assimilated nutrients is directly incorporated from the diet into newly synthesized tissue. Consequently, tissue isotopic composition more closely reflects that of the diet, resulting in reduced isotopic discrimination, particularly in protein-rich tissues (Martínez del Rio *et al*., 2009). It is therefore possible that, in the absence of growth-related dilution, $\Delta^{15}N$ values – and potentially $\Delta^{13}C$ values to a lesser extent – could have been higher than those observed in our experiment.

Although additional physiological variables can modulate trophic discrimination factors, only a subset appears relevant under the present experimental conditions. Lipids are known to be depleted in ^{13}C, so tissue samples with high lipid content can be biased toward lower $\Delta^{13}C$ (DeNiro & Epstein, 1977). Bulk C:N ratios of tissues in our experiment ranged from 2.58 to 3.03, values typical of protein-dominated matrices, indicating minimal lipid contribution and making substantial lipid-driven bias in $\Delta^{13}C$ unlikely. Therefore, the

negative $\Delta^{13}C$ values observed are more plausibly explained by dietary composition and substrate routing than by lipid effects.

Nitrogen excretion patterns also vary across chelonians and other reptiles and are often associated with habitat: many aquatic taxa excrete significant proportions of nitrogen as ammonia and urea, whereas most terrestrial reptiles – particularly those from arid environments – are predominantly uricotelic (Moyle, 1949). Because these pathways differ in the degree of metabolic processing prior to nitrogen elimination, they may influence the magnitude of preferential ^{14}N loss and thus modulate $\Delta^{15}N$. This hypothesis is supported by a meta-analysis showing significantly lower consumer–diet $\Delta^{15}N$ in ammonotelic organisms compared with ureotelic and uricotelic species, consistent with additional biochemical processing steps in urea/uric acid formation providing further opportunities for isotopic fractionation (Vanderklift & Ponsard, 2003). In this context, the freshwater aquatic habit of *P. expansa* suggests a mixed ammonotelic–ureotelic pattern rather than the strongly uricotelic strategy typical of xeric terrestrial reptiles, potentially contributing to interspecific variation in $\Delta^{15}N$ alongside dietary and growth-related effects.

Elevated environmental temperatures may accelerate somatic growth in ectotherms, thereby increasing the contribution of tissue accretion to isotopic incorporation and reducing apparent TDFs through growth-mediated dilution (Reich *et al*., 2008). However, higher temperatures may also increase metabolic rate and nutrient flux (Gillooly *et al*., 2001), potentially elevating $\Delta^{15}N$ through enhanced protein turnover, particularly when metabolic processing outweighs the diluting influence of tissue accretion (Martínez del Rio *et al*., 2009; Stephens *et al*., 2022; Stephens *et al*., 2023). In the present study, juveniles exhibited sustained growth under tropical thermal conditions, suggesting that both mechanisms likely operated simultaneously, although the dominant effect remains uncertain.

Taken together, these processes highlight the mechanistic complexity underlying TDF values and indicate that their magnitude and direction cannot be predicted from any single physiological or environmental variable. Instead, they emphasize the need for precise, tightly controlled species-, tissue-, and diet-specific measurements when estimating discrimination factors for ecological applications (Caut *et al*., 2009; Stephens *et al*., 2023).

2.5.2 – Turnover

2.5.2.1 – Data filtering

Restricting analyses to the early post-switch phase (t = 0–180 d) and the long-term approach to isotopic equilibrium (t ≥ 1140 d) represented a cautious compromise between temporal completeness and biological interpretability of the turnover parameters. This choice explicitly acknowledges the dataset's limitations and follows systematic data exploration showing that key model premises were not uniformly satisfied across the complete time series (Zuur *et al*., 2010). From a causal modeling perspective, parameter estimates are scientifically meaningful only when the model reflects the underlying causal process generating the data; when that process changes, inference may remain mathematically feasible but lose biological meaning and interpretation (Shipley, 2000). Classical isotopic turnover models are mechanistic representations of tissue incorporation following a single, sustained dietary shift, and their parameters are most informative when this assumption is reasonably met (Martínez del Rio & Anderson-Sprecher, 2008). In the present study, possible intermittent dietary perturbations during the intermediate phase likely altered the underlying data-generating process, resulting in non-monotonic turnover trajectories that are not well captured by first-order incorporation models assuming a constant diet. Such patterns suggest departures from diet stability and can compromise the biological interpretability of turnover parameters (Martínez del Rio & Anderson-Sprecher, 2008; Vander Zanden *et al*., 2015). Including these segments could therefore conflate incorporation kinetics with externally imposed dietary variability, biasing turnover rates downward and inflating derived residence times and half-lives. Therefore, prioritizing periods in which dietary conditions appeared most consistent with model requirements was intended to preserve more reliable parameter estimation and physiological interpretability. In summary, the filtering was not intended to artificially "improve" the results but to isolate time windows in which the assumption of an approximately constant diet was more plausible. Accordingly, the estimated parameters should be interpreted as describing turnover under idealized conditions of dietary stability, rather than as a full reconstruction of the contaminated experimental trajectory.

2.5.2.2 – Isotopic incorporation dynamics and tissue-specific variation

Even after restricting model fits to intervals with the most consistent dietary conditions, turnover in juvenile *Podocnemis expansa* remained slow, as generally expected for ectotherms (Warne *et al*., 2010; Vander Zanden *et al*., 2015), and was clearly tissue

dependent. Claw exhibited the fastest apparent incorporation, with a half-life of approximately 64 d before removal of growth effects, whereas whole blood (≈ 166 d), scute keratin (≈ 171 d), and skin (≈ 186 d) were markedly slower.

The contrast between claw and scute keratin is particularly informative. Although both are keratinized tissues, the comparatively slower incorporation of scute keratin – at least at this ontogenetic stage in *P. expansa* – likely reflects the accretionary mode of scute growth in chelonians, in which new keratin is deposited onto pre-existing layers rather than fully remodeled (Alibardi, 2005). Because older layers are retained as new material is added, scutes can preserve isotopic information over extended periods and effectively function as longer temporal archives of dietary history. By contrast, the faster claw-keratin turnover observed here suggests rapid claw growth in juveniles and implies that the segments clipped at successive sampling events included a substantial contribution of recently formed keratin. It is worth noting that juvenile *P. expansa* claws are relatively thin and short, consistent with high growth rates as reflected by our turnover estimates. In adults, which have thicker and longer claws, claw growth – and thus isotopic replacement of the distal portion typically clipped for stable isotope analysis – may be slower. Even so, our claw-turnover results suggest that this tissue may be better suited to track dietary shifts over an intermediate timescale: shorter than that integrated by scute, yet longer than that captured by rapidly turning over tissues such as plasma or visceral organs (Martínez del Rio & Carleton, 2012). Finally, because no other isotope-turnover study has simultaneously quantified claw and scute keratin in chelonians, it remains unclear whether the magnitude of the claw–scute contrast observed here can be generalized across taxa or across ontogenetic stages.

2.5.2.2.1 – Multiple-compartment modeling of whole-blood isotopic incorporation

Multi-compartment models (sometimes described as multiple pools or multiple phases of isotopic incorporation) do not necessarily imply the existence of physically distinct, separable compartments within a tissue. Rather, they are phenomenological mathematical representations that approximate incorporation kinetics as two or more exponential phases, thereby capturing tissue physiological complexity without uniquely identifying underlying mechanisms. Because multiple mechanistic phenomena and/or underlying structures can give rise to the same bi-exponential (or multi-exponential) functional form, parameters such as phase proportions and rate constants should not be interpreted as literal pool sizes and turnover rates of discrete tissue compartments. Rather,

they are more cautiously interpreted as describing kinetically distinct phases of incorporation (Martínez del Rio & Anderson-Sprecher, 2008).

That said, for whole blood, it is reasonable to relate the two kinetic phases to the tissue's dominant fractions, plasma and RBC, which are known to differ markedly in incorporation kinetics (Carleton *et al*., 2008). Although there is no strict one-to-one mapping between these fractions and the model compartments, the rapid phase of whole-blood turnover in our experiment was likely driven largely by plasma turnover, whereas the slow phase primarily reflects the longer residence time of RBC. Chelonian RBC are nucleated and have relatively long lifespans. For the freshwater turtle *Trachemys scripta* estimates are on the order of ~300 days (Frische *et al*., 2001), with even longer values reported for other taxa, such as 600–800 days in *Terrapene* spp. (Altland & Brace, 1962). This prolonged erythrocyte longevity, together with the lower mass-specific metabolic rates characteristic of ectotherms, are widely regarded as key drivers of the relatively slow whole blood and RBC isotopic turnover observed in chelonians (and more generally in reptiles) compared with birds and mammals (Warne *et al*., 2010; Murray & Wolf, 2013).

2.5.2.2.2 – Comparisons with literature data

Isotopic incorporation dynamics in ectotherms are often slower than those reported for endotherms and can be highly variable. This heterogeneity reflects the interacting effects of metabolic rate and its thermal dependence, species-specific physiology, ontogenetic stage, body size, growth rate, tissue type, diet composition, and other biological and ecological factors (Seminoff *et al*., 2007; Warne *et al*., 2010; Rosenblatt & Heithaus, 2013). Beyond this inherent variability, comparisons across studies are further limited by the small number of investigations on closely related taxa performed under comparable experimental designs and environmental conditions.

Among reptiles, published carbon half-lives in whole blood or RBC – the tissues for which a comparatively larger body of work is available – span roughly from ~24 days to ~216 days (e.g., Warne *et al*., 2010; Murray & Wolf, 2012, 2013; Reich *et al*., 2008; Fisk *et al*., 2009; Caut *et al*., 2013; Rosenblatt & Heithaus, 2013). Aside from these blood-based estimates (whole blood/RBC, with plasma also frequently reported), very few investigations have quantified carbon turnover in other reptile tissues.

The whole-blood half-life of *P. expansa* (~166 d) was relatively similar in order of magnitude to RBC half-life in collared lizards [*Crotaphytus collaris*; ~216 d; (Warne *et al*., 2010)] and to RBC turnover in the American alligator [*Alligator mississippiensis*; ~142 d; (Rosenblatt & Heithaus, 2013)]. However, it exceeded the RBC half-lives reported for juvenile desert tortoises [*Gopherus agassizii*; 88 d; (Murray & Wolf, 2012)] and juvenile desert box turtles [*Terrapene ornata luteola*; 69 d; (Murray & Wolf, 2013)]. It was also substantially longer than the whole-blood half-life reported for juvenile loggerhead sea turtles [*Caretta caretta*; 32 d; (Reich *et al*., 2008)]. Notably, the individuals studied by Reich *et al*. (2008) were rapidly growing juveniles, with growth rates roughly an order of magnitude higher than in our experiment. Even after accounting for growth effects, however, the estimated isotopic half-lives for *C. caretta* remained substantially shorter than those observed for *P. expansa*.

For keratinized tissues, scute carbon half-life in *P. expansa* (~171 d) was relatively close to the estimate reported for the American alligator [*Alligator mississippiensis*; ~148 d; (Rosenblatt & Heithaus, 2013)], but substantially longer than the value reported for juvenile loggerhead turtles [*Caretta caretta*; ~35 d; (Reich *et al*., 2008)]. In the same study, skin half-life in *C. caretta* (~32 d) was also much shorter than the value observed for *P. expansa* (~186 d). The claw carbon half-life estimated in our study (~64 d) contrasted sharply with both the much shorter value reported by Lattanzio & Miles (2016) for the small-bodied lizard *Urosaurus ornatus* (3.7 d) and, in the opposite direction, the substantially longer estimate reported by Sung *et al*. (2025) for the freshwater turtle *Platysternon megacephalum* (~311 d). Sung *et al*. attributed the exceptionally slow carbon turnover in claw to the species' cold mountain-stream habitat, where low temperatures depress metabolic rate and thereby slow isotopic incorporation into keratinized tissues. Moreover, their estimates were derived from adults, which likely further contributed to slower incorporation relative to juveniles. Nevertheless, even after correcting for the contribution of growth in our cohort, the estimated claw isotopic half-life (~72 d) remained far shorter than that reported for *P. megacephalum*. Environmental temperature, possibly acting in conjunction with species-specific physiological traits, therefore appears to be a plausible explanation for this interspecific contrast, given that *Podocnemis expansa* is a tropical species exposed to much warmer thermal regimes.

Beyond comparisons with other controlled turnover experiments, we evaluated our results against the predictive approach proposed by Vander Zanden *et al*. (2015). In that

study, the authors developed a broad allometric model to predict isotopic half-lives from body mass using an analysis of covariance (ANCOVA), with a common mass-scaling slope (0.22 on a log–log scale) and group-specific intercepts for major tissue–taxon categories (Eq. 6). Table 13 compares the half-lives estimated for our experimental cohort, as well as their allometric projections to larger body-mass classes, with ectotherm predictions from that meta-analytic model. Because that study's relationship was derived from a multi-taxa compilation spanning diverse experimental conditions and analytical approaches, its predictions are best interpreted as a macroecological benchmark rather than tissue- or species-specific expectations. Even so, at our experimental body mass (356.5 g), the half-lives of scute keratin and skin were broadly consistent with those predicted from the "vertebrate ectotherm whole body" intercept in Table 3 of Vander Zanden *et al*. (2015). By contrast, claw exhibited shorter half-lives than expected under that intercept, whereas whole blood half-life was substantially longer-lived than predicted by the "vertebrate ectotherm blood" category. This comparison is necessarily approximate because "whole body" is a general grouping, often used for small organisms analyzed in their entirety, and that study's ectotherm categories do not include keratin-, claw-, or epidermis-specific intercepts. Discrepancies became large in absolute terms at higher projected masses (8,000 and 25,000 g), but these differences primarily reflect baseline calibration (intercept shifts) rather than disagreement in mass scaling, because both approaches imply half-life $\propto M^{+0.22}$ (or $\lambda \propto M^{-0.22}$). Moreover, the two frameworks are not strictly commensurate: our adult-mass projections (8 and 25 kg) assume near–zero growth and therefore reflect catabolic turnover only, whereas the Vander Zanden *et al.* model synthesizes published half-lives across studies with widely varying growth regimes that do not consistently separate growth from catabolism.

Table 13 – Comparison of half-lives estimated for our experimental cohort and three allometric projections with values predicted by the model of Vander Zanden *et al*. (2015) (body mass in grams; half-lives in days; values rounded to the nearest integer).

body mass	Vander Zanden *et al*. (2015)	This study	Vander Zanden *et al*. (2015)	This study		
	blood	whole blood	whole body	scute keratin	claw	skin
356.5	~79	~166	~140	~171	~64	~186
5,000	~142	~207	~251	~224	~100	~238
8,000	~157	~521	~278	~493	~143	~559
25,000	~202	~670	~357	~633	~184	~718

Overall, the divergence at large body masses is best interpreted as arising from the combined effects of cohort-anchored extrapolation, non-equivalence of modeled turnover components, and coarse tissue categorization in the meta-analytic framework. Despite these limitations, comparison with the projections of Vander Zanden *et al*. (2015) remains informative because it situates our species- and tissue-specific turnover estimates within a broader macroecological context, clarifies whether they conform to or depart from cross-taxon expectations for ectotherms, and provides a transparent benchmark for assessing the plausibility of our allometric extrapolations to larger body masses.

2.5.2.3 – Contribution of growth and metabolism to isotopic change (growth dilution)

In growing juvenile ectotherms, such as the *Podocnemis expansa* individuals studied here, changes in tissue isotopic composition are driven by both the accretion of new biomass (growth) and the catabolic replacement of existing tissue (Martínez del Rio *et al*., 2009). Our data allowed the total turnover rate (λ) to be partitioned into growth (k_g) and catabolic (k_c) components. Although growth contributed to isotopic change, the persistence of measurable catabolic turnover (k_c) (Table 5) indicates that baseline metabolic processes continue to play a substantive role in isotopic replacement, even in structural tissues. This contrasts with some observations in hatchling sea turtles (Reich *et al*., 2008), or fish larvae (Hesslein, Hallard & Ramlal, 1993) in which growth dominated turnover almost entirely, but is consistent with findings in larger chelonians in which catabolism remains a non-trivial contributor even during periods of somatic growth. Reich *et al*. (2008) reported that the contribution of growth to carbon incorporation ranged from 31% to 46% across tissues in juvenile loggerhead turtles (*Caretta caretta*), whereas Murray & Wolf (2012) found that growth accounted for ~50% of RBC carbon turnover in juvenile desert tortoises (*Gopherus agassizii*). Overall, the estimated contribution of growth to isotopic incorporation in *P. expansa* was somewhat lower: ~12% for claw, ~31% for scute, ~34% for skin, and ~37% for the slow phase of whole blood. These findings indicate that growth dilution alone cannot explain the observed incorporation dynamics and that metabolically mediated protein replacement remained an important component of tissue turnover.

2.5.2.4 – Allometric effect on isotopic turnover rate

Projections across body-size classes (5 kg, 8 kg, and 25 kg) revealed a substantial increase in isotopic half-lives with increasing body mass (Table 10). For example, the estimated whole-blood T50 increased from ~207 days in 5-kg individuals to ~670 days in 25-kg individuals. This pattern is consistent with allometric theory for isotopic turnover, which predicts that fractional incorporation rates scale negatively with body mass [approximately $M^{-0.22}$ (Vander Zanden *et al*., 2015)], reflecting declines in mass-specific metabolic rate and protein synthesis in larger animals (Martínez del Rio & Carleton, 2012). The ecological implications are substantial: adult *P. expansa* likely exhibit a very long "isotopic memory", such that tissues sampled from adults may reflect resources assimilated months to years prior to capture. Consequently, when comparing juveniles and adults in the wild, it is critical to recognize that their tissues integrate diet over markedly different temporal windows – a central issue to interpreting trophic ecology (Thomas & Crowther, 2015; Carter *et al*., 2019).

Ambient and water temperatures at our experimental facility were likely lower than in more open, sun-exposed settings because the enclosure that housed the animals experienced shading during part of the day. By contrast, large commercial rearing ponds are typically under near-continuous solar exposure, and many natural habitats used by wild turtles (e.g., large Amazonian rivers and floodplain lakes) also experience more persistent insolation and warmer thermal regimes. In ectotherms, lower temperatures depress both growth and catabolic metabolism, reducing tissue replacement and slowing isotopic incorporation; as a consequence, empirical isotopic half-lives increase (Gillooly *et al*., 2001; Wolf *et al*., 2009; Vander Zanden *et al*., 2015; Thomas & Crowther, 2015). This temperature dependence offers a biologically plausible explanation for part of the exceptionally high half-lives projected under the body-mass scenarios (5 kg, 8 kg, and 25 kg). If our cohort were maintained under warmer, more sun-exposed conditions resembling commercial farms or the thermal regimes of large Amazonian waterbodies, they would be expected to grow faster and also exhibit higher catabolic turnover, thereby increasing their isotopic incorporation rates and consequently reducing half-lives. As a result, projected half-lives for larger turtles would be lower in absolute terms, although the allometric scaling with body mass ($k \propto M^{-0.22}$) would remain unchanged.

2.5.2.5 – Whole-blood turnover under an alternative fitting interval (0–60 d vs. 0–180 d)

Visual inspection of the plots in Figure 3 suggests that, within the 0–180 d interval, some observations still exhibit a degree of departure from the expected exponential turnover pattern, appearing right-shifted relative to an otherwise smooth decay trajectory. Despite these visual indications of mild disturbance, we retained the 0–180 d window – rather than restricting the analysis to a shorter segment to avoid such deviations (e.g., 0 – 60 d) – in the interest of methodological rigor. This decision prioritized preserving parameter identifiability over further minimizing potential bias from early irregularities. Restricting scute, claw, and skin to 0–60 d would leave only two sampling occasions per tissue, a design under which the asymptote (δ_{eq}) and the turnover rate (λ) are often weakly identified and may become strongly correlated, resulting in fragile fits and unstable inference. This concern is consistent with general identifiability limitations in isotopic incorporation models: when early data are sparse, multiple parameter combinations can yield similarly plausible trajectories, particularly when δ_{eq} is not tightly constrained by late observations (Martínez del Rio & Anderson-Sprecher, 2008; Carleton *et al*., 2008). For whole blood, the 0–60 d interval still provides three time points (0, 30, and 60 d), offering somewhat stronger anchoring of the initial slope; however, it would remain a restricted window relative to the full dynamics expected under multi-pool kinetics (Carleton *et al*., 2008).

Nevertheless, as an exploratory comparison, we fit an alternative model using whole-blood data from $t = 0–60$ d and $t \geq 1140$ d to quantify how derived turnover parameters would change, compared with the primary model based on 0–180 d and ≥1140 d observations. When whole-blood $\delta^{13}C$ turnover was modeled using only 0–60 d and ≥1140 d observations under a 1-compartment model, the resulting empirical turnover rate ($\lambda = 0.00678\ d^{-1}$) implied an isotopic half-life of ~102 d for the experimental cohort, instead of ~166 d under the broader 0–180 d window. Under this shorter-window fit, the time to near-asymptotic equilibrium (T95) was also reduced from ~836 d to ~442 d, nearly halving the time required to approach completion of isotopic turnover. Deriving the corresponding catabolic rate from this λ and applying the same allometric scaling used in Tables 7 to 10 yielded projected half-lives of ~150 d at 5 kg, ~249 d at 8 kg, and ~321 d at 25 kg. These projections were substantially lower than the corresponding half-lives obtained from the 0–180 d-based modeling (~207 d, ~521 d, and ~670 d, respectively; Table 10) and were more consistent with the magnitude of half-life expectations derived from the allometric framework reported by Vander Zanden *et al*. (2015) (~142 d, ~157 d and ~212 d, respectively;

Table 13). Importantly, the higher λ inferred from the 0–60 d window also markedly shortened the projected time to near-equilibrium (T95) across the body-mass scenarios: from ~1044 d (~2.9 years) to ~648 d (~1.8 years) at 5 kg, from ~2626 d (~7.2 years) to ~1078 d (~2.9 years) at 8 kg, and from ~3374 d (~9.2 years) to ~1387 d (~3.8 years) at 25 kg. These results suggest that isotopic half-lives and times to near-equilibrium estimated from the 0–180 d and ≥1140 d intervals may still be somewhat overestimated due to residual perturbations in the $\delta^{13}C$ time series used for model fitting.

2.5.2.6 – Ecological and forensic implications

From an ecological perspective, the turnover parameters estimated here provide the temporal calibration required to interpret field $\delta^{13}C$ dynamics in *Podocnemis expansa* in terms of when, rather than simply what, resources are assimilated. Tissue-specific incorporation rates define the integration window represented by each tissue, allowing investigators to distinguish recent dietary or habitat use from longer-term assimilative history and to place seasonal shifts, ontogenetic niche changes, and habitat transitions on a biologically meaningful timescale (Martínez del Rio & Carleton, 2012). In practice, the estimated turnover rates, along with the derived residence times and half-lives, support mechanistic interpretation of tissue $\delta^{13}C$ trajectories following natural dietary shifts. They also inform sampling design by guiding the selection of tissues with temporal resolution suited to specific ecological questions and help reduce bias arising from the use of generic, non-taxon-specific turnover values.

Relatedly, because TDFs vary among taxa, tissues and diets, specific estimates are essential for accurately translating tissue isotope values into inferences about dietary baselines (Stephens *et al*., 2023). These calibrations refine interpretation of the timing of seasonal or ontogenetic diet shifts and habitat-use transitions. When interpreting diet shifts in natural habitats, however, it is important to recognize that our study was based on a commercial captive diet with a C_4–derived $\delta^{13}C$ signature markedly different from that of natural C_3–based Amazonian food webs. This difference may limit the applicability of the carbon TDF estimates obtained here to studies of free-ranging animals. In contrast, $\delta^{15}N$ differences between captive and wild diets are likely to be less pronounced than those observed for carbon (Ometto *et al*., 2006; Nardoto *et al*., 2014), suggesting that the nitrogen TDFs estimated here may be more transferable to ecological studies of wild populations.

Beyond this, somatic growth is ecologically relevant for isotope ecology because it affects how rapidly tissues incorporate dietary isotopic signals (Reich *et al*., 2008). By focusing on growing juveniles, the present study makes this particularly clear for *P. expansa*. Somatic accretion represented a non-trivial component of isotopic incorporation across tissues, as quantified by the growth contribution estimates. Accordingly, growth must be treated explicitly when interpreting tissue $\delta^{13}C$ dynamics in the field, either by incorporating growth into turnover models or by using growth-corrected turnover parameters, as done here.

For forensic inference, turnover parameters and species-, tissue- and diet-specific TDFs for *P. expansa* strengthen isotope-based approaches for detecting wildlife laundering (i.e., illegally captured wild animals falsely marketed as captive-bred). Brazilian Amazonian turtle farms typically rely on standardized commercial fish feeds containing maize (Andrade *et al*., 2021), which have a C_4-derived $\delta^{13}C$ signature that contrasts markedly with the C_3-based diets of free-ranging animals. Thus, carbon turnover rates and isotopic half-lives can determine how long pre-capture isotopic signals remain detectable in turtle tissues after wild animals are transferred to captivity and switched to commercial feed. Together, these parameters define an evidentiary "detection window" for estimating time since capture or transfer to commercial facilities and for interpreting suspected cases of illegal wildlife trade and laundering. In practical terms, given the contrast in $\delta^{13}C$ between natural and captive diets, we suggest that the wild dietary signal can be detected with greater confidence for roughly one isotopic half-life, that is, until the tissue has moved about halfway from the original wild $\delta^{13}C$ composition toward the captive diet equilibrium value. As tissues approach near-asymptotic equilibrium, their $\delta^{13}C$ values converge on the captive endpoint, and uncertainty in source attribution increases markedly (Sung *et al*., 2025). Based on Table 3, we estimate that, after a juvenile *P. expansa* is captured in the wild and transferred to captivity on a C_4-signature diet, the original forest-derived isotopic signal may remain detectable for around two months in claw and for approximately five to six months in whole blood, scute keratin, and skin. In larger specimens, these windows would be expected to extend, potentially reaching around six months in claw and about 20 to 24 months in the other tissues for a 25-kg individual (Table 10).

In this study, TDFs were calibrated against a captive ration with a pronounced C_4 influence, yielding diet-specific discrimination values that are particularly relevant to forensic investigations in commercial production systems. Once the isotopic composition of the feed used at a questioned farm is known, these TDFs allow $\delta^{13}C$ and $\delta^{15}N$ values in turtle

tissues to be interpreted relative to that dietary baseline, facilitating comparison between observed tissue signatures and those expected under sustained captive feeding. Combined with turnover-based detection windows, this feed-specific calibration provides a more robust evidentiary basis for evaluating whether a questioned turtle has plausibly remained on commercial feeds for a sufficient period to exhibit the expected diet–tissue offsets, thereby supporting forensic inference in suspected wildlife-laundering cases.

2.6 – Conclusion

This study provides the first experimental estimates of carbon turnover parameters and nitrogen TDFs for a tropical freshwater turtle species, as well as the first report of carbon TDFs for any freshwater turtle. It characterizes $\delta^{13}C$ incorporation kinetics in *Podocnemis expansa* and establishes tissue-specific baselines for $\Delta^{13}C$ and $\Delta^{15}N$ across four tissues (whole blood, scute keratin, claw, and skin), thereby helping to fill a major empirical gap in the isotopic ecology of tropical freshwater chelonians.

TDFs were tissue-dependent for both elements: carbon discrimination differed among tissues not only in magnitude but also in direction, whereas nitrogen discrimination remained consistently positive although still tissue-specific. These results reinforce the growing consensus that TDFs are not universal constants and should instead be treated as species-, tissue-, and ideally diet-specific parameters in isotope-based inference.

Turnover analyses showed that incorporation kinetics also differed among tissues and required different model structures, with whole blood best described by a two-compartment formulation and the other tissues adequately represented by one-compartment models. Incorporation was slow overall, with estimated isotopic half-lives of ~64 days for claw, ~171 days for scute keratin, ~166 days for whole blood, and ~186 days for skin, highlighting the long integration windows represented by these tissues in this ectotherm. Partitioning isotopic change into growth-mediated and catabolic components further demonstrated that somatic accretion can be a non-trivial driver of incorporation in juveniles, underscoring the need to account for growth when interpreting tissue isotope trajectories in growing individuals. Allometric projections likewise indicated that turnover is expected to slow substantially with increasing body mass, extending residence times and half-lives into multi-month to multi-year windows in larger turtles, with direct implications for the temporal interpretation of field isotope data.

These calibrated parameters strengthen ecological and forensic inference in *Podocnemis expansa* and potentially in other Amazonian freshwater turtles. They provide the temporal framework needed to interpret field $\delta^{13}C$ values in relation to when resources were assimilated and which habitats contributed to tissue formation, thereby improving understanding of the timing of dietary shifts, habitat transitions, and seasonal changes in resource use. They also provide tissue- and element-specific TDFs that allow isotope values to be interpreted more accurately relative to dietary sources and trophic baselines, reducing bias associated with the use of generic discrimination factors. From a forensic perspective, these calibrations enable time-explicit evaluation of isotopic trajectories following transfer from wild diets to captive feeds and provide a stronger basis for assessing whether tissue signatures are consistent with feeding regimes used in commercial production systems. They also improve the capacity of isotope-based approaches to detect suspected wildlife laundering by distinguishing turtles consistent with prolonged captive feeding from those more plausibly sourced from the wild. More broadly, the results underscore that reliable isotope-based inference in freshwater turtles depends on experimentally derived, species-, tissue-, and diet-specific calibration of both turnover parameters and TDFs, ideally with explicit consideration of ontogenetic stage and growth dynamics.

2.7 – References

Alibardi L. 2005. Proliferation in the epidermis of chelonians and growth of the horny scutes. *Journal of Morphology* 265:52–69. DOI: 10.1002/jmor.10337.

Altland PD, Brace KC. 1962. Red cell life span in the turtle and toad. *American Journal of Physiology-Legacy Content* 203:1188–1190. DOI: 10.1152/ajplegacy.1962.203.6.1188.

Andrade PCM. 2008. *Criação e Manejo de Quelônios no Amazonas*. Manaus: Ibama/Pró-Varzea.

Andrade PCM. 2012. *Manejo Comunitário de Quelônios - Projeto Pé-de-pincha*. Manaus: Moderna.

Andrade PCM, Garcez JR, Lima AC, Duarte JAM, Anízio TLF, Rodrigues WS, Oliveira AB, Alves HRB. 2021. Panorama da quelonicultura no Brasil – uma estratégia para conservação das espécies e geração de renda. *Aquaculture Brasil*:34–40.

Ballutaud M, Travers-Trolet M, Marchal P, Dubois SF, Giraldo C, Parnell AC, Nuche-Pascual MT, Lefebvre S. 2022. Inferences to estimate consumer's diet using stable isotopes: Insights from a dynamic mixing model. *PLoS ONE* 17. DOI: 10.1371/journal.pone.0263454.

Barceló LP, Seminoff JA, Zanden HBV, Jones TT, Bjorndal KA, Bolten AB, Mustin W, Busquets-Vass G, Newsome SD. 2021. Hydrogen isotope assimilation and discrimination in green turtles. *Journal of Experimental Biology* 224. DOI: 10.1242/jeb.231431.

Bauchinger U, Keil J, McKinney RA, Starck JM, McWilliams SR. 2010. Exposure to cold but not exercise increases carbon turnover rates in specific tissues of a passerine. *Journal of Experimental Biology* 213:526–534. DOI: 10.1242/jeb.037408.

Berto D, Fanelli E, Vizzini S, Rampazzo F, Da Ros Z, Noventa S, Fortibuoni T, Antonini C, Cilluffo G, Signa G, Premici A, Bardelli R, Raicevich S. 2025. ISOMED - A Stable ISOtope database of MEDiterranean marine food web components. *Scientific Data* 12. DOI: 10.1038/s41597-025-05981-y.

Boulêtreau S, Vagnon C, Comte L, Sagouis A, Pool T, Stiling RR, Harrod C, South J, McIntosh AR, Perga M-E, Sánchez-Hernández J, Roussel J-M, Tunney TD, Jackson M, Olden JD, Cucherousset J. 2025. IsoFresh: A global stable isotope database of freshwater food webs. *Knowledge & Management of Aquatic Ecosystems*:15. DOI: 10.1051/kmae/2025010.

Brasileiro L, Mayrink RR, Pereira AC, Costa FJV, Nardoto GB. 2023. Differentiating wild from captive animals: an isotopic approach. *PeerJ* 11. DOI: 10.7717/peerj.16460.

Brazil MVS, Chaves WA, Vidal MD, Tavares AS, Wilcove DS. 2025. The potential and limitations of turtle farming to contribute to conservation in the Brazilian Amazon. *Biological Conservation* 304:111055. DOI: 10.1016/j.biocon.2025.111055.

Carleton SA, Kelly L, Anderson-Sprecher R, Del Rio CM. 2008. Should we use one-, or multi-compartment models to describe 13C incorporation into animal tissues? *Rapid Communications in Mass Spectrometry* 22:3008–3014. DOI: 10.1002/rcm.3691.

Carleton SA, Del Rio CM. 2005. The effect of cold-induced increased metabolic rate on the rate of 13C and 15N incorporation in house sparrows (Passer domesticus). *Oecologia* 144:226–232. DOI: 10.1007/s00442-005-0066-8.

Carter WA, Bauchinger U, McWilliams SR. 2019. The Importance of Isotopic Turnover for Understanding Key Aspects of Animal Ecology and Nutrition. *Diversity* 11:84. DOI: 10.3390/d11050084.

Cathelin E, Lefebvre S, Giraldo C. 2025. From static to dynamic: Embracing dynamics in isotopic diet estimation. *PLOS One* 20:e0330327. DOI: 10.1371/journal.pone.0330327.

Caut S, Angulo E, Courchamp F. 2009. Variation in discrimination factors (Δ15N and Δ13C): The effect of diet isotopic values and applications for diet reconstruction. *Journal of Applied Ecology* 46:443–453. DOI: 10.1111/j.1365-2664.2009.01620.x.

Cerling TE, Ayliffe LK, Dearing MD, Ehleringer JR, Passey BH, Podlesak DW, Torregrossa AM, West AG. 2007. Determining biological tissue turnover using stable isotopes: The reaction progress variable. *Oecologia* 151:175–189. DOI: 10.1007/s00442-006-0571-4.
Charity S, Ferreira JM. 2020. *Wildlife Trafficking in Brazil*. Cambridge: TRAFFIC International.
Chatfield MWH, Frederick CA, Yorks D, Pollock E, Hopkins JB. 2026. Combating the illegal turtle trade using chemical markers. *The Journal of Wildlife Management* 90. DOI: 10.1002/jwmg.70141.
Crane DP, Ogle DH, Shoup DE. 2020. Use and misuse of a common growth metric: guidance for appropriately calculating and reporting specific growth rate. *Reviews in Aquaculture* 12:1542–1547. DOI: 10.1111/raq.12396.
Curtis MJ, Beaumont J, Elamin F, Wilson AS, Koon HEC. 2022. Method of micro-sampling human dentine collagen for stable isotope analysis. *Rapid Communications in Mass Spectrometry* 36. DOI: 10.1002/rcm.9305.
Dalerum F, Angerbjörn A. 2005. Resolving temporal variation in vertebrate diets using naturally occurring stable isotopes. *Oecologia* 144:647–658. DOI: 10.1007/s00442-005-0118-0.
DeNiro MJ, Epstein S. 1977. Mechanism of Carbon Isotope Fractionation Associated with Lipid Synthesis. *Science* 197:261–263. DOI: 10.1126/science.327543.
DeNiro MJ, Epstein S. 1978. Influence of diet on the distribution of carbon isotopes in animals. *Geochimica et Cosmochimica Acta* 42:495–506. DOI: 10.1016/0016-7037(78)90199-0.
DeNiro MJ, Epstein S. 1981. Influence of diet on the distribution of nitrogen isotopes in animals. *Geochimica et Cosmochimica Acta* 45:341–351. DOI: 10.1016/0016-7037(81)90244-1.
Flinders JM, Clement A, Magoulick DD. 2026. Effects of prey and tissue type on δ13C and δ15N discrimination and turnover rates of rainbow trout. *Hydrobiologia*. DOI: 10.1007/s10750-025-06097-5.
Forero-Medina G, Ferrara CR, Vogt RC, Fagundes CK, Balestra RAM, Andrade PCM, Lacava R, Bernhard R, Lipman AJ, Lenz AJ, Ferrer A, Calle A, Aponte AF, Calle-Rendón BR, Santos Camilo C, Perrone E, Miraña E, Cunha FAG, Loja E, Del Rio J, Vera Fernandez JL, Hermández OE, Del Aguila R, Pino R, Cueva R, Martinez S, Diniz Bernardes VC, Sainz L, Horne BD. 2019. On the future of the giant South American river turtle Podocnemis expansa. *ORYX* 55:73–80. DOI: 10.1017/S0030605318001370.
Frische S, Bruno S, Fago A, Weber RE, Mozzarelli A. 2001. Oxygen binding by single red blood cells from the red-eared turtle *Trachemys scripta*. *Journal of Applied Physiology* 90:1679–1684. DOI: 10.1152/jappl.2001.90.5.1679.
Fry B. 2006. *Stable Isotope Ecology*. New York, NY: Springer New York. DOI: 10.1007/0-387-33745-8.
Fry B, Arnold C. 1982. Rapid 13C/12C turnover during growth of brown shrimp (Penaeus aztecus). *Oecologia* 54:200–204. DOI: 10.1007/BF00378393.
Gillooly JF, Brown JH, West GB, Savage VM, Charnov EL. 2001. Effects of Size and Temperature on Metabolic Rate. *Science* 293:2248–2251. DOI: 10.1126/science.1061967.
Giménez J, Ramírez F, Almunia J, G. Forero M, de Stephanis R. 2016. From the pool to the sea: Applicable isotope turnover rates and diet to skin discrimination factors for bottlenose dolphins (Tursiops truncatus). *Journal of Experimental Marine Biology and Ecology* 475:54–61. DOI: 10.1016/j.jembe.2015.11.001.
Hahn S, Hoye BJ, Korthals H, Klaassen M. 2012. From food to offspring down: Tissue-specific discrimination and turn-over of stable isotopes in herbivorous waterbirds and other avian foraging guilds. *PLoS ONE* 7. DOI: 10.1371/journal.pone.0030242.
Haywood JC, Fuller WJ, Godley BJ, Shutler JD, Widdicombe S, Broderick AC. 2019. Global review and inventory: how stable isotopes are helping us understand ecology and inform

conservation of marine turtles. *Marine Ecology Progress Series* 613:217–245. DOI: 10.3354/meps12889.

Hesslein RH, Hallard KA, Ramlal P. 1993. Replacement of Sulfur, Carbon, and Nitrogen in Tissue of Growing Broad Whitefish (Coregonus nasus) in Response to a Change in Diet Traced by δ34S, δ13C, and δ15N. *Canadian Journal of Fisheries and Aquatic Sciences* 50:2071–2076. DOI: 10.1139/f93-230.

Hill KGW, Nielson KE, Tyler JJ, Mcinerney FA, Doubleday ZA, Frankham GJ, Johnson RN, Gillanders BM, Delean S, Cassey P. 2020. Pet or pest? Stable isotope methods for determining the provenance of an invasive alien species. *NeoBiota* 59:21–37. DOI: 10.3897/NEOBIOTA.59.53671.

Hopkins JB, Frederick CA, Yorks D, Pollock E, Chatfield MWH. 2022. Forensic Application of Stable Isotopes to Distinguish between Wild and Captive Turtles. *Biology* 11. DOI: 10.3390/biology11121728.

Hopkins JB, Frederick CA, Yorks D, Pollock E, Chatfield MWH. 2023. Advancing Forensic Chemical Analysis to Classify Wild and Captive Turtles. *Diversity* 15. DOI: 10.3390/d15101056.

Lara NRF, Marques TS, Montelo KM, de Ataídes AG, Verdade LM, Malvásio A, de Camargo PB. 2012. A trophic study of the sympatric amazonian freshwater turtles podocnemis unifilis and podocnemis expansa (testudines, podocnemidae) using carbon and nitrogen stable isotope analyses. *Canadian Journal of Zoology* 90:1394–1401. DOI: 10.1139/cjz-2012-0143.

Lattanzio M, Miles D. 2016. Stable carbon and nitrogen isotope discrimination and turnover in a small-bodied insectivorous lizard. *Isotopes in Environmental and Health Studies* 52:673–681. DOI: 10.1080/10256016.2016.1154854.

Martínez del Rio C, Anderson-Sprecher R. 2008. Beyond the reaction progress variable: The meaning and significance of isotopic incorporation data. *Oecologia* 156:765–772. DOI: 10.1007/s00442-008-1040-z.

Martínez del Rio C, Carleton SA. 2012. How fast and how faithful: The dynamics of isotopic incorporation into animal tissues. *Journal of Mammalogy* 93:353–359. DOI: 10.1644/11-MAMM-S-165.1.

Martínez del Rio C, Wolf N, Carleton SA, Gannes LZ. 2009. Isotopic ecology ten years after a call for more laboratory experiments. *Biological Reviews* 84:91–111. DOI: 10.1111/j.1469-185X.2008.00064.x.

Matley JK, Fisk AT, Tobin AJ, Heupel MR, Simpfendorfer CA. 2016. Diet-tissue discrimination factors and turnover of carbon and nitrogen stable isotopes in tissues of an adult predatory coral reef fish, Plectropomus leopardus. *Rapid Communications in Mass Spectrometry* 30:29–44. DOI: 10.1002/rcm.7406.

Meier-Augenstein W. 2019. From stable isotope ecology to forensic isotope ecology — Isotopes' tales. *Forensic Science International* 300:89–98. DOI: 10.1016/j.forsciint.2019.04.023.

Melo LAS, Izel ACU, Andrade PCM, Silva AV, Hossaine-Lima M das G. 2003. *Criação de Tartaruga da Amazônia (Podocnemis expansa)*. Manaus: Embrapa. 14 p. ISSN 1517-3135.

Moyle V. 1949. Nitrogenous excretion in Chelonian reptiles. *Biochemical Journal* 44:581–584. DOI: 10.1042/bj0440581.

Murray IW, Wolf BO. 2012. Tissue carbon incorporation rates and diet-to-tissue discrimination in ectotherms: Tortoises are really slow. *Physiological and Biochemical Zoology* 85:96–105. DOI: 10.1086/663867.

Murray IW, Wolf BO. 2013. Diet and growth influence carbon incorporation rates and discrimination factors (Δ13C) in Desert Box Turtles, Terrapene ornata luteola. *Herpetological Conservation and Biology* 8:149–162.

Nardoto GB, Quesada CA, Patiño S, Saiz G, Baker TR, Schwarz M, Schrodt F, Feldpausch TR, Domingues TF, Marimon BS, Marimon Junior B-H, Vieira ICG, Silveira M, Bird MI, Phillips OL, Lloyd J, Martinelli LA. 2014. Basin-wide variations in Amazon forest

nitrogen-cycling characteristics as inferred from plant and soil ^{15}N: ^{14}N measurements. *Plant Ecology & Diversity* 7:173–187. DOI: 10.1080/17550874.2013.807524.
Ometto JPHB, Ehleringer JR, Domingues TF, Berry JA, Ishida FY, Mazzi E, Higuchi N, Flanagan LB, Nardoto GB, Martinelli LA. 2006. The stable carbon and nitrogen isotopic composition of vegetation in tropical forests of the Amazon Basin, Brazil. *Biogeochemistry* 79:251–274. DOI: 10.1007/s10533-006-9008-8.
Pantoja-Lima J, Aride PHR, de Oliveira AT, Félix-Silva D, Pezzuti JCB, Rebêlo GH. 2014. Chain of commercialization of Podocnemis spp. turtles (Testudines: Podocnemididae) in the Purus River, Amazon Basin, Brazil: Current status and perspectives. *Journal of Ethnobiology and Ethnomedicine* 10. DOI: 10.1186/1746-4269-10-8.
Pearson SF, Levey DJ, Greenberg CH, Martínez del Rio C. 2003. Effects of elemental composition on the incorporation of dietary nitrogen and carbon isotopic signatures in an omnivorous songbird. *Oecologia* 135:516–523. DOI: 10.1007/s00442-003-1221-8.
Perga M, Bouletreau S, Cucherousset J, Harrod C, McIntosh A, Olden JD, Vagnon C, Jardine T. 2025. A global estimator of C and N isotope baselines for fresh waters. *Methods in Ecology and Evolution*. DOI: 10.1111/2041-210x.70225.
Peterson BJ, Fry B. 1987. Stable Isotopes in Ecosystem Studies. *Annual Review of Ecology and Systematics* 18:293–320. DOI: 10.1146/annurev.es.18.110187.001453.
Polícia Federal. 2014. Operação Podocnemis combate a prática de crime ambiental em dois estados. *Available at www.pf.gov.br/agencia/noticias/2014/08/operacao-podocnemis-combate-a-pratica-de-crime-ambiental-em-dois-estados* (accessed July 29, 2020).
Post DM. 2002. Using Stable Isotopes to Estimate Trophic Position: Models, Methods, and Assumptions. *Ecology* 83:703–718. DOI: 10.1890/0012-9658(2002)083[0703:USITET]2.0.CO;2.
Quinby BM, Creighton JC, Flaherty EA. 2020. Stable isotope ecology in insects: a review. *Ecological Entomology* 45:1231–1246. DOI: 10.1111/een.12934.
Reich KJ, Bjorndal KA, Martínez del Rio C. 2008. Effects of growth and tissue type on the kinetics of 13C and 15N incorporation in a rapidly growing ectotherm. *Oecologia* 155:651–663. DOI: 10.1007/s00442-007-0949-y.
Robbins CT, Felicetti LA, Sponheimer M. 2005. The effect of dietary protein quality on nitrogen isotope discrimination in mammals and birds. *Oecologia* 144:534–540. DOI: 10.1007/s00442-005-0021-8.
Rosenblatt AE, Heithaus MR. 2013. Slow isotope turnover rates and low discrimination values in the American alligator: Implications for interpretation of ectotherm stable isotope data. *Physiological and Biochemical Zoology* 86:137–148. DOI: 10.1086/668295.
Seminoff JA, Bjorndal KA, Bolten AB. 2007. Stable carbon and nitrogen isotope discrimination and turnover in pond sliders Trachemys scripta: Insights for trophic study of freshwater turtles. *Copeia*:534–542. DOI: 10.1643/0045-8511(2007)2007[534:SCANID]2.0.CO;2.
Seminoff J, Jones T, Eguchi T, Jones D, Dutton P. 2006. Stable isotope discrimination (δ13C and δ15N) between soft tissues of the green sea turtle Chelonia mydas and its diet. *Marine Ecology Progress Series* 308:271–278. DOI: 10.3354/meps308271.
Shipley B. 2000. *Cause and Correlation in Biology: A User's Guide to Path Analysis, Structural Equations and Causal Inference*. Cambridge University Press.
Shipley ON, Matich P. 2020. Studying animal niches using bulk stable isotope ratios: an updated synthesis. *Oecologia* 193:27–51. DOI: 10.1007/s00442-020-04654-4.
Soto DX, Radloff FGT, Bond AL, Hobson KA, Leslie AJ. 2025. In the quest of isotope equilibrium for trophic discrimination estimation: diet–tissue dynamics in Nile crocodiles (Crocodylus niloticus). *Isotopes in Environmental and Health Studies*. DOI: 10.1080/10256016.2025.2535762.
Steinitz R, Lemm JM, Pasachnik SA, Kurle CM. 2016. Diet-tissue stable isotope (Δ13C and Δ15N) discrimination factors for multiple tissues from terrestrial reptiles. *Rapid Communications in Mass Spectrometry* 30:9–21. DOI: 10.1002/rcm.7410.

Stephens RB, Ouimette AP, Hobbie EA, Rowe RJ. 2022. Reevaluating trophic discrimination factors (*Δδ*13C and *Δδ*15N) for diet reconstruction. *Ecological Monographs* 92. DOI: 10.1002/ecm.1525.

Stephens RB, Shipley ON, Moll RJ. 2023. Meta-analysis and critical review of trophic discrimination factors (Δ13C and Δ15N): Importance of tissue, trophic level and diet source. *Functional Ecology* 37:2535–2548. DOI: 10.1111/1365-2435.14403.

Sturtz JM, Peoples B, Goforth R, Cheek C. 2026. Stable isotope analysis shows limited assimilation of carbohydrates in muscle tissue of an omnivorous fish. *Environmental Biology of Fishes* 109. DOI: 10.1007/s10641-025-01783-8.

Sung Y-H, Liew JH, Chan WS, Fok AWL, Leung J, Wong HF, Baker DM, Bonebrake TC, Dingle C, Dudgeon D, Karraker NE, Lau A, Colon VA, Magouras I, Ades G, Crow P, Rose-Jeffreys L, Spencer R, Fong JJ. 2025. Stable isotope analysis successfully identifies wild-caught individuals of threatened Asian freshwater turtles in illegal trade. *Global Ecology and Conservation* 64:e03947. DOI: 10.1016/j.gecco.2025.e03947.

Thomas SM, Crowther TW. 2015. Predicting rates of isotopic turnover across the animal kingdom: A synthesis of existing data. *Journal of Animal Ecology* 84:861–870. DOI: 10.1111/1365-2656.12326.

Vanderklift MA, Ponsard S. 2003. Sources of variation in consumer-diet δ^{15}N enrichment: a meta-analysis. *Oecologia* 136:169–182. DOI: 10.1007/s00442-003-1270-z.

Warne RW, Gilman CA, Wolf BO. 2010. Tissue-carbon incorporation rates in lizards: Implications for ecological studies using stable isotopes in terrestrial ectotherms. *Physiological and Biochemical Zoology* 83:608–617. DOI: 10.1086/651585.

Wolf N, Carleton SA, Martínez del Rio C. 2009. Ten years of experimental animal isotopic ecology. *Functional Ecology* 23:17–26. DOI: 10.1111/j.1365-2435.2008.01529.x.

Vander Zanden MJ, Clayton MK, Moody EK, Solomon CT, Weidel BC. 2015. Stable Isotope Turnover and Half-Life in Animal Tissues: A Literature Synthesis. *PLOS ONE* 10:e0116182. DOI: 10.1371/journal.pone.0116182.

Zuur AF, Ieno EN, Elphick CS. 2010. A protocol for data exploration to avoid common statistical problems. *Methods in Ecology and Evolution* 1:3–14. DOI: 10.1111/j.2041-210x.2009.00001.x.

CAPÍTULO 3

FORENSIC ISOTOPES TRACE ILLEGAL WILDLIFE TRADE IN THE BRAZILIAN AMAZON

Abstract

Illegal wildlife trade is a major threat to global biodiversity, growing increasing attention from governments and international organizations. In this context, forensic services are becoming increasingly involved in cases of wildlife trafficking and wildlife laundering, especially in efforts to determine the origin of seized animals. Among the forensic techniques used for this purpose, stable and radiogenic isotope analyses have shown particular promise. In the Brazilian Amazon, the poaching and illegal trade of freshwater turtles represent a major conservation issue. Among Amazonian freshwater turtle species, *Podocnemis expansa* (the giant South American river turtle) stands out as the most relevant in the context of trafficking and commercial farming. Although commercial turtle farming is legal, illegal trade persists and frequently involves organized smuggling networks, sometimes with suspected involvement of the formal turtle production and trade sector. This article presents a multi-isotopic approach based on carbon ($\delta^{13}C$), nitrogen ($\delta^{15}N$), and strontium ($^{87}Sr/^{86}Sr$) to detect turtles allegedly laundered through commercial breeding facilities and to trace potential trafficking routes of seized animals. We used $\delta^{13}C$ and $\delta^{15}N$ to compare wild and captive turtles, and $^{87}Sr/^{86}Sr$ to investigate the geographic origin of wild individuals. $\delta^{13}C$ revealed significant differences between wild and captive turtles, indicating its potential utility for detecting wildlife laundering. Although $\delta^{15}N$ showed no significant differences between captive and wild turtles, it may still help identify isotopic signatures associated with specific breeding farms. Our $^{87}Sr/^{86}Sr$ results indicate that turtles incorporate the isotopic signatures of water bodies into the bony matrix of their shells. Because the principal Amazonian rivers have already been characterized for $^{87}Sr/^{86}Sr$, it was possible to infer probable trafficking routes for seized turtles. We conclude that this multi-isotopic approach is effective for investigating river turtle trafficking and laundering in the Brazilian Amazon. It may therefore serve as a valuable tool for environmental law enforcement and as a reference for similar wildlife trafficking cases in Brazil and other Amazonian countries.

Keywords: illegal wildlife trade; wildlife laundering; wildlife trafficking; forensic isotopes; stable isotopes; radiogenic isotopes; Amazon; turtles; *Podocnemis expansa*.

Highlights

- Poaching and illegal trade of river turtles represent a major wildlife trafficking issue in the Brazilian Amazon.
- We tested a multi-isotopic approach based on $\delta^{13}C$, $\delta^{15}N$, and $^{87}Sr/^{86}Sr$ to detect wildlife laundering in turtle farms and trace trafficking routes of seized animals.
- $\delta^{13}C$ distinguished wild from captive turtles, whereas $\delta^{15}N$ showed potential for distinguishing farm-specific isotopic signatures.
- Wild turtles reflected the $^{87}Sr/^{86}Sr$ signatures of the water bodies they inhabited, enabling inferences about geographic origin.
- This approach identified potential cases of wildlife laundering and traced likely trafficking routes of seized turtles.

Graphical Abstract

3.1 – Introduction

Biodiversity loss is a major consequence of ongoing global environmental change. Of the nine planetary processes that regulate Earth's environmental stability, biosphere integrity—directly undermined by the decline of wild species populations—has already exceeded the safe threshold required to sustain humanity on Earth (Richardson *et al*., 2023). This phenomenon, also referred to as "Anthropocene defaunation," is driven in part by species overexploitation (Dirzo *et al*., 2014). The illegal wildlife trade, one of the most profitable illicit activities worldwide (Guynup *et al*., 2020), plays a substantial role in accelerating biodiversity decline (Mozer & Prost, 2023). As a result, international concern has intensified. Organizations such as INTERPOL, the United Nations Office on Drugs and Crime (UNODC), the World Bank, and the World Customs Organization (WCO) have increasingly engaged with this issue (UNODC, 2024). Since 2015, the United Nations General Assembly has adopted resolutions recognizing wildlife trafficking as a serious crime and calling for stronger national measures to combat it (United Nations, 2015, 2025). In this context, illegal wildlife trade has become an increasingly important global law enforcement challenge, demanding progressively more specialized scientific support from wildlife forensic services (Haines *et al*., 2021). Beyond identifying seized animals or their derivatives, checking their status against protected-species lists, and detecting mistreatment, one of the most difficult questions faced by wildlife forensic scientists worldwide remains: where do trafficked animals come from?

In pursuit of solutions to this issue, isotope forensics have emerged as a tool for assigning geographical provenance of wildlife, as well as for discriminating between wild and captive origins (Bowen *et al*., 2005; Alexander *et al*., 2019; Jiguet *et al*., 2019). Stable and radiogenic isotopes are well-established techniques in various areas of forensic science, with emerging relevance and applicability for wildlife forensics (Meier-Augenstein, 2019; Pauli & Rodriguez Curras, 2024; Prigge *et al*., 2024). The isotopic technique relies on analyzing the ratio between the heaviest and lightest isotopes of the same element, and how this ratio varies between environmental compartments, organisms, and materials. Although the stable isotopes of the same element have the same chemical properties, the lighter isotopes are more reactive than the heavier ones, i.e. they are more easily moved from the reactant phase to the product. This difference causes a variation in the isotopic ratio (proportion between heavy and light isotopes) between phases of chemical reactions or biological and physical processes, a phenomenon called isotopic fractionation. Each

chemical element has different processes that determine or influence isotopic fractionation (Fry, 2006).

Carbon and nitrogen are among the main stable isotopes used in ecological and forensic studies (Chesson *et al*., 2018). Other elements with relevant stable isotopes for wildlife forensics include oxygen, hydrogen, and sulfur (Bowen *et al*., 2005; Meier-Augenstein, 2019; Sung *et al*., 2025). Because both carbon and nitrogen isotopes are closely related to animals' diet, they have been widely used to differentiate between wild and captive animals, for ecological, forensic and animal-derived food certification purposes (Brasileiro *et al*., 2023). Specifically in the context of trafficking in freshwater and terrestrial chelonians, stable carbon and nitrogen isotope analysis has increasingly been used in recent years to distinguish wild-caught from captive individuals (Hill *et al*., 2020; Hopkins *et al*., 2022, 2023; Brandis *et al*., 2023; Sung *et al*., 2025; Chatfield *et al*., 2026).

For carbon, photosynthesis is the main biological process driving isotopic fractionation. Most plants are C_3 plants, defined by the photosynthetic pathway they use, and preferentially assimilate the lighter isotope (^{12}C) over the heavier isotope (^{13}C) during CO_2 uptake. As a result, their tissues have lower relative abundances of ^{13}C compared to atmospheric CO_2, which results in lower carbon isotopic ratios (lower $\delta^{13}C$ values). Trees, shrubs, and legumes are typical C_3 plants. In contrast, C_4 plants discriminate much less against ^{13}C, resulting in higher carbon isotope ratios than those of C_3 plants. Common examples include maize, sugarcane, and most tropical grasses. Importantly, the $\delta^{13}C$ ranges of C_3 and C_4 plants do not overlap, making this contrast a powerful tool in ecological and forensic studies (Fry, 2006; Chesson *et al*., 2018). Because animals consume plants either directly or indirectly through the food chain, the isotopic composition of the diet is incorporated into their tissues. Thus, the relative contribution of C_3- and C_4-derived foods can produce distinct carbon isotope ratios in animal tissues. In the case of nitrogen, isotopic fractionation is shaped mainly by soil biogeochemical processes, which influence plant isotope composition, and by trophic position, as $\delta^{15}N$ values generally increase along the food chain (Fry, 2006).

In addition to stable isotopes, radiogenic isotopes have also been effectively used in forensic science. Among the elements with radiogenic isotopes of forensic relevance, strontium is particularly prominent due to its capacity to attribute geographic origin (Bataille & Bowen, 2012; Bataille *et al*., 2020; Kafino *et al*., 2024). A radiogenic isotope is generated through the radioactive decay of an unstable (radioactive) parent isotope. For example, strontium has four isotopes, among which ^{87}Sr is formed by the radioactive decay of ^{87}Rb.

The strontium isotope ratio is calculated by the direct ratio between ^{87}Sr and ^{86}Sr, which is a non-radiogenic stable isotope. In older geologic rocks enriched in rubidium, prolonged radioactive decay of ^{87}Rb to ^{87}Sr produces high $^{87}Sr/^{86}Sr$ ratios, a geochemical signature that is also reflected in soils derived from these rocks (Semenishchev & Voronina, 2020). Given that strontium has no metabolic or biological functions, it does not undergo isotopic fractionation in environmental matrices, including soil, water, and plants, nor within animal tissues (Flockhart *et al*., 2015). Consequently, the $^{87}Sr/^{86}Sr$ ratio of soil, plants, animals, and water at a given location generally reflects the isotopic composition of the underlying bedrock (the solid rock beneath loose deposits such as soil or alluvium). Due to its similarity in ionic radius and charge, strontium tends to replace calcium in calcified biological tissues, including teeth, bones, fish scales, and otoliths, where its isotope ratio can be laboratory-measured (Pouilly *et al*., 2014). As a result, strontium isotopes have gained prominence in provenance studies of humans and animals, particularly in forensic applications (Bataille & Bowen, 2012).

The Amazon Basin encompasses different bedrock types (Fig. 1-A), resulting in marked spatial variation in strontium isotope ratios. The Andes Mountains consist predominantly of geologically young Cenozoic volcanic rocks and therefore exhibit low $^{87}Sr/^{86}Sr$ ratios. In contrast, the granitic shields of Guyana and Central Brazil are formed by ancient cratonic rocks, which display substantially higher strontium isotope ratios. Between these extremes, the Amazon Trough, composed of sedimentary rocks, is characterized by intermediate $^{87}Sr/^{86}Sr$ values. As Amazon rivers drain these distinct geological domains, the dissolved strontium in their waters reflects these contrasting isotopic signatures (Santos *et al*., 2015; Mereles *et al*., 2025) (Fig. 1-B). These basin-scale differences in $^{87}Sr/^{86}Sr$ have already been applied to investigate the geographic origin and migration of fish (Pouilly *et al*., 2014; Duponchelle *et al*., 2016; Hauser *et al*., 2019; Pereira *et al*., 2019).

In Brazil, the name Amazon River applies to the stretch extending from its mouth on the Atlantic Ocean to the city of Manaus, where the Negro River meets the Solimões River (Fig. 1-A). The Solimões River is the largest Amazon tributary, accounting for approximately 56% of the total discharge of the Amazon River at its estuary (Palmer & Edmond, 1992; Duponchelle *et al*., 2016). Hereafter, we refer to the Manaus-to-mouth stretch as the Lower Amazon. At a broader spatial scale, the Amazon Basin can be divided into four main sub-basins: Negro, Solimões, Madeira, and Tapajós (Pouilly *et al*., 2014; Santos *et al*., 2015) (Fig. 1-B).

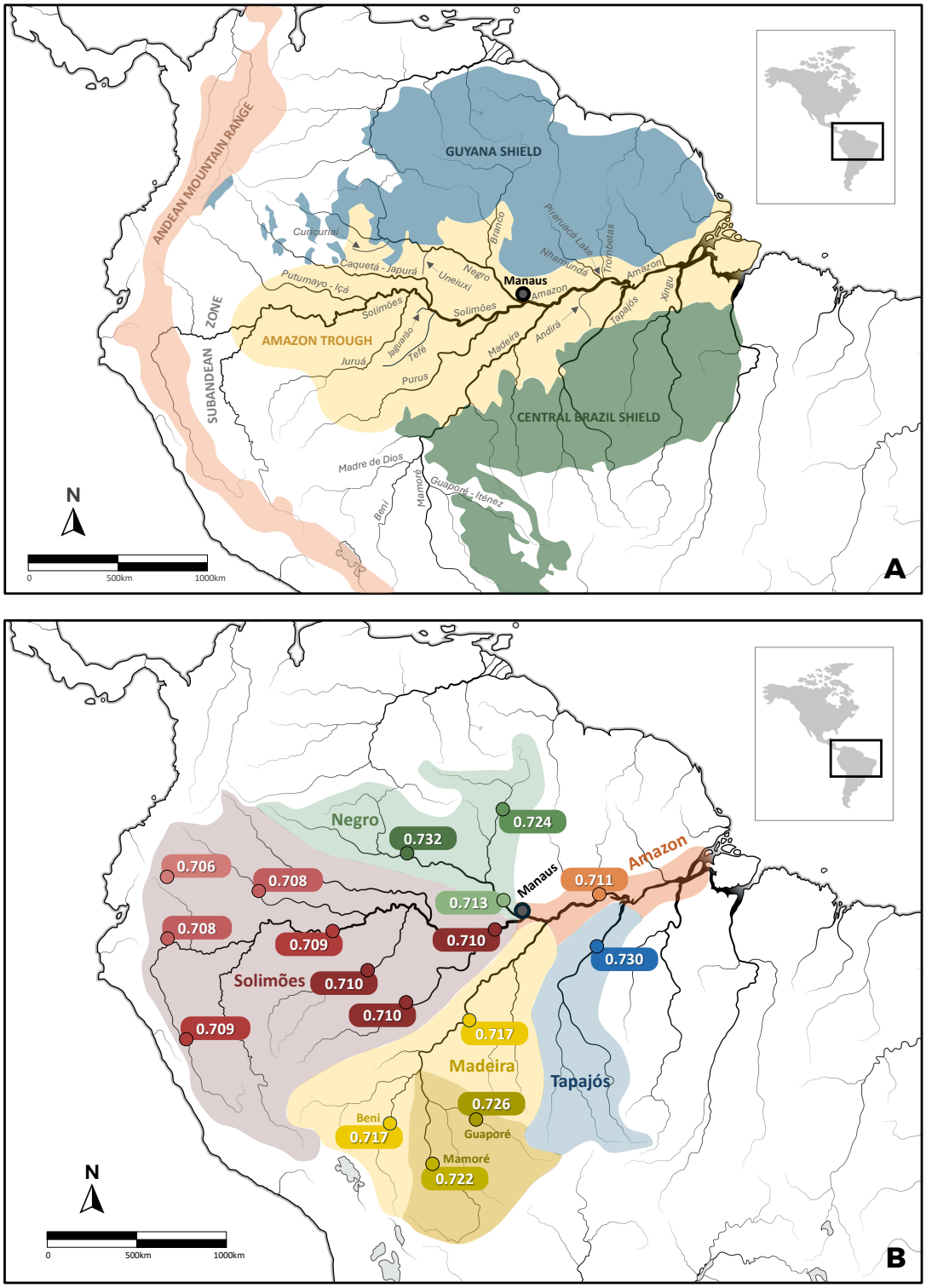

Figure 1-A – Simplified map of the main geological terrains of the Amazon Basin, showing the major rivers and selected tributaries mentioned in the text. The Andes are composed predominantly of geologically young Cenozoic volcanic rocks, whereas the Guiana and Central Brazil Shields consist of geologically old cratonic rocks. Sedimentary rocks of intermediate age form the Amazon Trough. Adapted from Reis *et al*. (2010) and Santos *et al*. (2015).

Figure 1-B – Schematic representation of dissolved $^{87}Sr/^{86}Sr$ ratios across the main Amazon Basin drainages. Rivers draining the Guiana and Central Brazil Shields, such as tributaries of the Negro Sub-basin, the Tapajós River, and part of the Madeira Sub-basin exhibit higher $^{87}Sr/^{86}Sr$ values than rivers draining Andean-derived sediments in the western Solimões Sub-basin. The Amazon mainstem and tributaries draining the sedimentary basin show intermediate $^{87}Sr/^{86}Sr$ values. Adapted from Pouilly *et al*. (2014) and Santos *et al*. (2015).

The Amazon is one of the most biodiverse areas on the planet, encompassing more than half of the world's tropical forests and housing approximately a quarter of all the global wildlife (Malhi *et al*., 2008; Pimm *et al*., 2014). In addition to its vast diversity of mammals, birds, amphibians, and other taxa, the Amazon is distinguished as one of the richest regions globally in terms of continental (both freshwater and terrestrial) chelonian species (Rhodin *et al*., 2017).

Continental chelonians are among the most threatened vertebrate groups globally, with more than 60% of the 356 recognized species either threatened with extinction or already extinct (Lovich *et al*., 2018). In Brazil, the consumption of meat and eggs from Amazonian river turtles, notably the giant South American river turtle (*Podocnemis expansa*), has long been part of the dietary traditions of Indigenous and riverine communities. (Gilmore, 1986). From the 17th century onward, these animals were heavily exploited by both local populations and European settlers, driven by the consumption of meat and eggs and by the extraction of oil from eggs for public lighting. This prolonged overexploitation drastically reduced wild populations of Amazonian river turtles and placed them at risk of extinction (Forero-Medina *et al*., 2019).

In response to this situation, the Brazilian government implemented conservation programs for these species in the latter half of the 20th century. One of the strategies was the establishment of legalized commercial turtle breeding operations, which were planned to alleviate poaching pressure on wild populations (Salera Jr., Balestra & Luz, 2016). However, despite the presence of these authorized farms, poaching and the illegal trade of river turtles persist in the Brazilian Amazon, often involving organized smuggling networks, sometimes with suspected involvement of the formal turtle production and trade sector (Kemenes & Pezzuti, 2007; Pantoja-Lima *et al*., 2014; Polícia Federal, 2014).

Currently, more than 1.7 million chelonians are consumed each year just in the urban areas of Amazonas (the largest state in the Brazilian Amazon), the vast majority from illegal sources (Chaves *et al*., 2021). As an example, more than 3,900 turtles of the genus *Podocnemis* and 122 turtle trawl nets were confiscated in less than two years in just one federal biological reserve on the Middle Purus River, in the state of Amazonas, Brazil (Kemenes & Pezzuti, 2007). This scenario positions the trafficking of river turtles and their eggs as the foremost wildlife trade issue in the Brazilian Amazon, in volume and numbers, with its relevance extending to the domestic market as well as neighboring Amazonian countries (Charity & Ferreira, 2020).

In this paper we present a multi-isotopic approach based on carbon, nitrogen, and strontium to differentiate between wild and captive Amazon river turtles and to identify trafficking routes of these species. Our research had three objectives: (1) to determine the $\delta^{13}C$ and $\delta^{15}N$ signatures of reference wild and captive-bred turtles and assess whether they provide sufficient isotopic contrast for forensic application, particularly for detecting wildlife laundering; (2) to compare $^{87}Sr/^{86}Sr$ ratios in reference wild turtles with strontium isotope ratios in the environments they inhabited, namely the water bodies from which they were collected; and (3) to compare the isotopic signatures of turtles of questioned origin (seized or investigated animals) with these reference datasets to distinguish captive from wild origin and, for wild turtles, to assign geographic provenance.

3.2 – Methods

3.2.1 – Study area

We collected samples from turtles of questioned origin at a retailer in Manaus, at a breeding farm in the municipality of Iranduba, within the Manaus metropolitan area, and during two seizures conducted by the Brazilian Federal Police at the port of Manaus. All these samples were part of an investigation conducted by the Brazilian Federal Police Superintendency in the state of Amazonas into fraudulent activities related to wildlife laundering within the legalized turtle trade sector. Captive reference specimens were collected from two farms in Iranduba, whereas wild reference specimens were obtained from multiple locations across the Amazon Basin and from a site on the Brazilian Atlantic coast (Fig. 2 and Table 1). Additionally, we collected eight samples of commercial feed from seven different breeders in the states of Amazonas and Pará, Brazil, including the two farms where the reference captive animals were sampled.

We selected Manaus as the primary study site because it is the largest urban center in the Amazon (more than 2.5 million inhabitants) and the main consumption hub for these animals, accounting for more than 40% of total consumption in Amazonas state (Chaves *et al*., 2021). The city is located right at the confluence of the two main tributaries that form the Amazon River – The Negro and Solimões rivers – making it a critical hub for turtle trafficking routes originating from various regions within the Amazon (Kemenes & Pezzuti, 2007; Pezzuti *et al*., 2010; Schneider *et al*., 2011; Pantoja-Lima *et al*., 2014). Moreover, Manaus is the capital of Amazonas, the largest Brazilian state in the Amazon region, which contains approximately 79% of Brazil's turtle farms and more than 150,000

animals under commercial production. The Manaus metropolitan area accounts for more than 90% of this production (Andrade *et al*., 2021) and hosts retailers and restaurants authorized to sell turtles for human consumption. Despite its legal status, this formal production and trade chain has already been investigated by the Brazilian Federal Police due to suspicion of wildlife laundering, in which trafficked wild animals are falsely declared as legally farm-raised (Amazonas Atual, 2014; Polícia Federal, 2014; Marques, 2021). This study aims to develop an isotope-based forensic tool for detecting wildlife laundering in Amazonian turtle farms and tracing the trafficking routes of seized animals, particularly those destined for the Manaus metropolitan area.

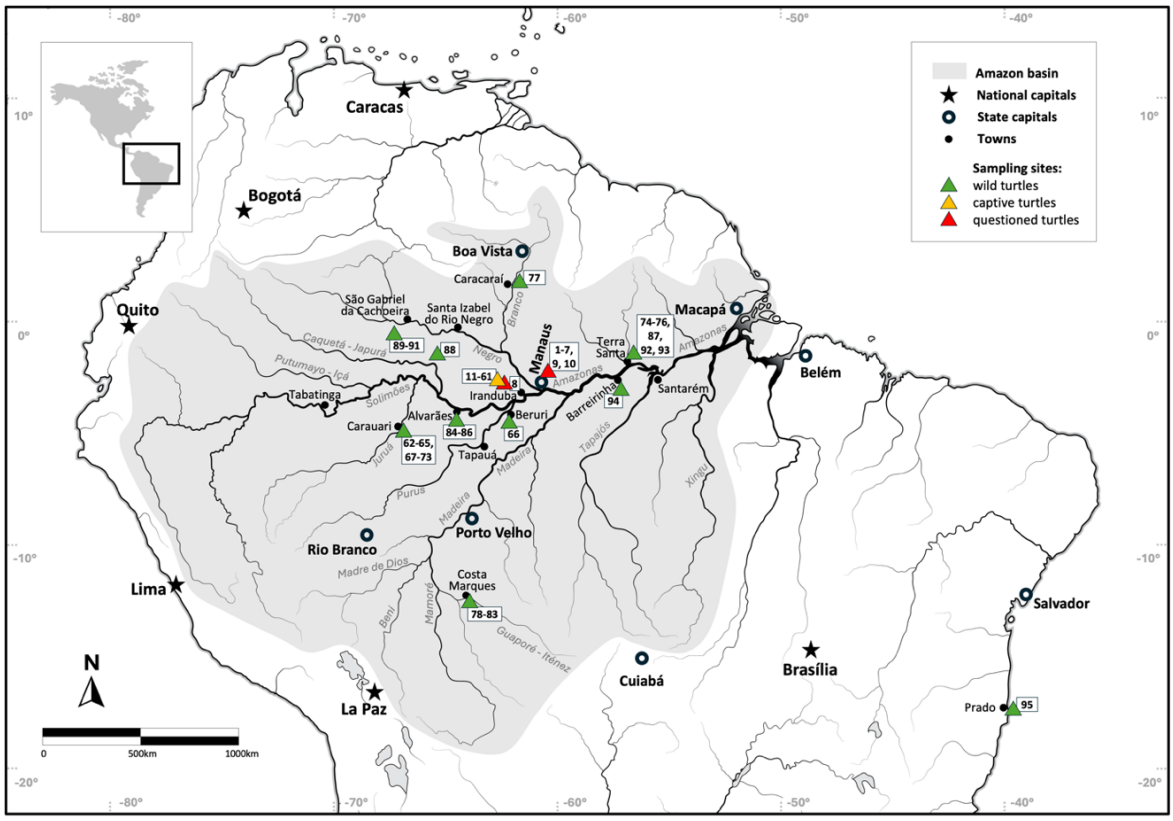

Figure 2 – Hydrographic map of the Amazon Basin showing the sampling sites of wild, captive and questioned turtles. The numbers attached to each site symbol refer to the identification of the samples listed in Table 1.

3.2.2 – Sampling protocol

Carapace scute samples were collected from wild animals, scientific collections, commercial breeders, and batches of animals seized by the Brazilian Federal Police. From each animal or carcass, a sample of approximately 1 cm^2 was collected from the edge of a marginal carapace scute, containing horny (keratinized) and/or bony layers. In live animals, when samples were intended exclusively for carbon and nitrogen analyses, only the horny layer was collected in a painless and non-invasive procedure. When the bony layer was necessary, whenever possible we took advantage of the carapace scute fragments that would already be cut during routine marking. After collection, all the samples were dried and individually packed in evidence bags with specific numbering and description to ensure the chain of custody until laboratory analysis. All the collection procedures in this research complied with the official permissions and guidelines for this research, both from the Brazilian Federal Police (process no. 08350.008500/2020-83), and from ICMBio, the Brazilian federal environmental agency responsible for licensing collection of wildlife biological material for scientific purposes (SisBio licenses nos. 77627-1, 77627-2, 77627-3, and 77627-4). No animals were sacrificed or mutilated during this study.

Table 1 presents a comprehensive summary of the sampled specimens, detailing their geographic origins, types of samples obtained, analytical procedures performed, and additional sampling information. The corresponding isotopic dataset is provided in the supplementary material. Table 2 and Figs. 3 to 6 contain subsets of these data, aligned with the objectives of each analysis or graphical representation. Detailed descriptions are provided in the respective titles of each table and figure.

Table 1 – Identification of samples, relevant aspects of collection, and isotopic analyses conducted.

Sample id	Sample type	Species	Origin (geographical location/collection)					Sampled tissues	Isotopic analyses
			River/ water body	Subbasin	Municipality	State	Description		
1	questioned	*Podocnemis expansa*	--	--	Manaus	Amazonas	Federal Police inspection - licensed retailer	Carapace scute - horny layer	$\delta^{13}C$, $\delta^{15}N$
2	questioned	*Podocnemis expansa*	--	--	Manaus	Amazonas	Federal Police inspection - licensed retailer	Carapace scute - horny layer	$\delta^{13}C$, $\delta^{15}N$
3	questioned	*Podocnemis expansa*	--	--	Manaus	Amazonas	Federal Police inspection - licensed retailer	Carapace scute – horny and bony layers	$\delta^{13}C$, $\delta^{15}N$ and $^{87}Sr/^{86}Sr$
4	questioned	*Podocnemis expansa*	--	--	Manaus	Amazonas	Federal Police inspection - licensed retailer	Carapace scute – horny and bony layers	$\delta^{13}C$, $\delta^{15}N$ and $^{87}Sr/^{86}Sr$
5	questioned	*Podocnemis expansa*	--	--	Manaus	Amazonas	Federal Police inspection - licensed retailer	Carapace scute – horny and bony layers	$\delta^{13}C$, $\delta^{15}N$ and $^{87}Sr/^{86}Sr$
6	questioned	*Podocnemis expansa*	--	--	Manaus	Amazonas	Federal Police inspection - licensed retailer	Carapace scute – horny and bony layers	$\delta^{13}C$, $\delta^{15}N$ and $^{87}Sr/^{86}Sr$
7	questioned	*Podocnemis expansa*	--	--	Manaus	Amazonas	Federal Police inspection - licensed retailer	Carapace scute – horny and bony layers	$\delta^{13}C$, $\delta^{15}N$ and $^{87}Sr/^{86}Sr$
8	questioned	*Podocnemis expansa*	--	--	Iranduba	Amazonas	commercial breeder (large carapace displayed as an ornament)	Carapace scute – horny and bony layers	$\delta^{13}C$, $\delta^{15}N$ and $^{87}Sr/^{86}Sr$
9	questioned	*Podocnemis erythrocephala*	--	--	Manaus	Amazonas	Federal Police seizure 1 – port of Manaus	Carapace scute – horny and bony layers	$\delta^{13}C$, $\delta^{15}N$ and $^{87}Sr/^{86}Sr$
10	questioned	*Podocnemis erythrocephala*	--	--	Manaus	Amazonas	Federal Police seizure 2 – port of Manaus	Carapace scute – horny and bony layers	$\delta^{13}C$, $\delta^{15}N$ and $^{87}Sr/^{86}Sr$
11 to 18	captive	*Podocnemis expansa*	--	--	Iranduba	Amazonas	commercial breeder 1 batch 1 (juveniles)	Carapace scute - horny layer	$\delta^{13}C$, $\delta^{15}N$
19 to 30	captive	*Podocnemis expansa*	--	--	Iranduba	Amazonas	commercial breeder 1 batch 2 (rearing animals)	Carapace scute - horny layer	$\delta^{13}C$, $\delta^{15}N$
31 to 39	captive	*Podocnemis expansa*	--	--	Iranduba	Amazonas	commercial breeder 1 batch 3 (finishing animals)	Carapace scute - horny layer	$\delta^{13}C$, $\delta^{15}N$
40 to 45	captive	*Podocnemis expansa*	--	--	Iranduba	Amazonas	commercial breeder 1 batch 4 (breeding stock)	Carapace scute - horny layer	$\delta^{13}C$, $\delta^{15}N$
46 to 61	captive	*Podocnemis expansa*	--	--	Iranduba	Amazonas	commercial breeder 2	Carapace scute - horny layer	$\delta^{13}C$, $\delta^{15}N$
62 to 65	wild	*Podocnemis expansa*	Middle Juruá River	Solimões	Carauari	Amazonas	Federal Police collection	Carapace scute – horny and bony layers	$\delta^{13}C$, $\delta^{15}N$ and $^{87}Sr/^{86}Sr$
66	wild	*Podocnemis expansa*	Low Purus River	Solimões	Beruri	Amazonas	Federal Police collection	Carapace scute - horny layer	$\delta^{13}C$, $\delta^{15}N$
67 to 72	wild	*Podocnemis expansa*	Middle Juruá River	Solimões	Carauari	Amazonas	UFAM collection	Carapace scute - horny layer	$\delta^{13}C$, $\delta^{15}N$
73	wild	*Podocnemis expansa*	Middle Juruá River	Solimões	Carauari	Amazonas	UFAM collection	Carapace scute – bony layer	$^{87}Sr/^{86}Sr$
74, 75	wild	*Podocnemis expansa*	Piraruacá Lake	Lower Amazon	Terra Santa	Pará	UFAM collection	Carapace scute - horny layer	$\delta^{13}C$, $\delta^{15}N$
76	wild	*Podocnemis expansa*	Piraruacá Lake	Lower Amazon	Terra Santa	Pará	UFAM collection	Carapace scute – horny and bony layers	$\delta^{13}C$, $\delta^{15}N$ and $^{87}Sr/^{86}Sr$
77	wild	*Podocnemis expansa*	Branco River	Negro	Caracaraí	Roraima	UFAM collection	Carapace scute – bony layer	$^{87}Sr/^{86}Sr$
78 to 82	wild	*Podocnemis expansa*	Guaporé River	Madeira	Costa Marques	Rondônia	WCS collection	Carapace scute - horny layer	$\delta^{13}C$, $\delta^{15}N$
83	wild	*Podocnemis expansa*	Guaporé River	Madeira	Costa Marques	Rondônia	WCS collection	Carapace scute – bony layer	$^{87}Sr/^{86}Sr$
84 to 86	wild	*Podocnemis unifilis*	Middle Solimões River	Solimões	Alvarães	Amazonas	Federal Police collection	Carapace scute – horny and bony layers	$\delta^{13}C$, $\delta^{15}N$ and $^{87}Sr/^{86}Sr$
87	wild	*Podocnemis unifilis*	Piraruacá Lake	Lower Amazon	Terra Santa	Pará	UFAM collection	Carapace scute – bony layer	$^{87}Sr/^{86}Sr$
88	wild	*Podocnemis erythrocephala*	Uneiuxi River	Negro	Santa Isabel do Rio Negro	Amazonas	IBAMA collection	Carapace scute – horny and bony layers	$\delta^{13}C$, $\delta^{15}N$ and $^{87}Sr/^{86}Sr$
89 to 91	wild	*Podocnemis erythrocephala*	Curicuriaí River	Negro	São Gabriel da Cachoeira	Amazonas	IBAMA collection	Carapace scute – bony layer	$^{87}Sr/^{86}Sr$
92, 93	wild	*Podocnemis erythrocephala*	Piraruacá Lake	Lower Amazon	Terra Santa	Pará	UFAM collection	Carapace scute – bony layer	$^{87}Sr/^{86}Sr$
94	wild	*Podocnemis* sp.	Andirá River	Lower Amazon	Barreirinha	Pará	UFAM collection	Carapace scute – bony layer	$^{87}Sr/^{86}Sr$
95	wild	*Caretta caretta*	Atlantic Ocean	--	Prado	Bahia	Federal Police collection	Carapace scute – bony layer	$^{87}Sr/^{86}Sr$

3.2.3 – Carbon and nitrogen isotopic analysis

For carbon and nitrogen isotopic analysis, we sampled the horny layer of marginal scutes of the turtles' carapaces. For $\delta^{13}C$ and $\delta^{15}N$ comparisons between wild and captive turtles, we used only samples from giant South American river turtles (*Podocnemis expansa*, family Podocnemididae) (Table 2 and Fig. 3), since there is evidence of differences in trophic niches and isotopic spaces between species of the Podocnemididae family that could interfere with this analysis (Lara *et al*., 2012). We selected this species due to its prominence as the most significant freshwater chelonian in terms of wildlife trafficking in the Brazilian Amazon (Chaves *et al*., 2019). Because of its large size, dietary preferences of local people, and the fact that this species nests collectively, it is heavily poached and trafficked. It is not uncommon for inspection operations to end up with several hundred animals or thousands of eggs seized at once (ICMBio, 2011, 2015a,b, 2016, 2019). The value of an adult giant South American river turtle on the illegal market can be as high as USD 50 in poaching areas and USD 450 in large urban centers such as Manaus (Schneider *et al*., 2011). The giant South American river turtle ranks among the six species most frequently seized by environmental law enforcement agencies throughout Brazil (Destro *et al*., 2012), and its unregulated large-scale poaching is a potential cause of population collapse (Antunes *et al*., 2016). Furthermore, it is the most commercially farmed river turtle species in Brazil (Andrade *et al*., 2008), which increases its potential for wildlife laundering. Other relevant species to the wildlife law enforcement scenario in the Brazilian Amazon are *Podocnemis unifilis*, *Podocnemis sextuberculata*, *Podocnemis erythrocephala* and *Peltocephalus dumerilianus*, all belonging to the Podocnemididae family (Kemenes & Pezzuti, 2007; Pantoja-Lima *et al*., 2014; Chaves *et al*., 2021).

Scute samples were cleaned with a 2:1 solution of chloroform and methanol, dried in an oven at 60ºC for 48 h, cut into small pieces, placed into tin capsules using tweezers, and weighed (approximately 0.5 – 0.6 mg per sample). Commercial feed samples were milled, encapsulated and weighed (mass from 0.6 to 0.7 mg per sample). The isotopic ratios of carbon and nitrogen were determined by combustion using an elemental analyzer (Carlo Erba, CHN-1100) coupled to an isotope ratio mass spectrometer (Thermo Finnigan Delta Plus) at the Isotope Ecology Laboratory of the Nuclear Energy Center in Agriculture, São Paulo University (CENA/USP), Piracicaba/SP, Brazil. Relative isotope abundance values were expressed in delta notation (δ) in parts per thousand (‰), using the following equation:

$$\delta^{h}E_{sample/standard} = [(R_{sample} - R_{standard})/R_{standard}] = [(R_{sample}/R_{standard}) - 1]$$

where R is the ratio of the heavier isotope to the lighter isotope of a given element (E) for samples and standards (Meier-Augenstein, 2019) (for example, as in the case of this study, $^{13}C/^{12}C$ or $^{15}N/^{14}N$). The outcome of this equation is typically a small decimal value, often reported to the second or third decimal place. To facilitate the interpretation of isotopic analysis data, it is internationally standardized to multiply the results of the equation by 1000. Consequently, the delta notation is expressed in parts per thousand (‰) and represents a relative value rather than an absolute measure.

$\delta^{13}C$ was reported according to the Vienna Pee Dee Belemnite standard (VPDB; $^{13}C/^{12}C$ ratio = 0.01118), and $\delta^{15}N$ was reported relative to atmospheric air (AIR; $^{15}N/^{14}N$ ratio = 0.0036765). Internal laboratory standard samples (sugarcane leaves) are routinely interspersed with target samples to correct the effects of mass and instrumental drift during and between runs (one standard sample for every ten target samples). The long-term analytical errors for internal standards are 0.2‰ for $\delta^{13}C$ and $\delta^{15}N$. The sugarcane internal standard is regularly calibrated against IAEA standards NBS18 and NBS22 for carbon and IAEA N1 and N2 for nitrogen. To ensure comparability of $\delta^{13}C$ and $\delta^{15}N$ values with the international reference scales, we applied a two-point (double-standard) normalization using multiple certified reference materials spanning a broad isotopic range. The reference materials used to derive the normalization equations were measured in a separate analytical session from the study samples because the sample analyses had been completed earlier. Although standards and samples were not analyzed in the same session, this correction remains valid because it addresses the instrument scale definition (linearity and intercept) used to express results on the VPDB (for $\delta^{13}C$) and AIR (for $\delta^{15}N$) scales, rather than short-term within-run drift. Carbon reference materials included NBS 19, NBS 22, and USGS 61, USGS 62, USGS 63, and USGS 89; nitrogen reference materials included IAEA-N1, IAEA-N2, and the same USGS materials. To strengthen the scale transfer, five carbon standards and five nitrogen standards were analyzed (more than is typical in routine practice). The resulting relationships were: $\delta^{13}C\_true = 1.01626 \times \delta^{13}C\_measured + 0.84085$ ($R^2 = 0.99$) and $\delta^{15}N\_true = 0.99278 \times \delta^{15}N\_measured - 0.72202$ ($R^2 = 0.99$). Reported $\delta^{13}C$ and $\delta^{15}N$ values were adjusted using these equations. The raw $\delta^{13}C$ and $\delta^{15}N$ analytical dataset used to generate all figures and tables is available as supplementary material (Mendeley Data, V1, doi: 10.17632/43x6h7sb22.1).

3.2.4 – Strontium isotopic analysis

We analyzed the strontium isotope ratio in the bony layer of turtle shell scutes. Given the absence of strontium isotopic fractionation among soil, water, plants, and animals (Flockhart *et al*., 2015), the lack of interference from specific dietary items in the absorption of bioavailable strontium by consumers and consequently in the $^{87}Sr/^{86}Sr$ ratio of their tissues (Bentley, 2006), as well as the relative diet similarity among Amazon river turtle species (Eisemberg *et al*., 2017), we sampled not only *Podocnemis expansa* but also multiple species within the Podocnemididae family for strontium isotopic analysis. This approach was intended to enhance the spatial representativeness of our sampling, considering the vast scale of the Amazon Basin.

Determinations of strontium isotopic ratios were carried out at the Laboratory of Geodynamic, Geochronological and Environmental Studies of the Institute of Geosciences, University of Brasília (LEGGA/UnB). We used an Analyte Excite ArF laser ablation system (LA) coupled to a Thermo Scientific™ Neptune XT multi-collector MC-ICP-MS. Analyses were performed using a square-shaped laser raster, with an aperture diameter of 80-150 μm, advancing with a speed of 10 μm/s, operating at 20 Hz and using a nominal energy of 7.55 J/cm^2. The ablated aerosol was flushed from the HelEx II two-volume laser cell using 0.7 L/min (0.35 + 0.35) of He. The Neptune XT is equipped with 9 Faraday detectors, which measured the masses 82 to 88 in static mode and using 10^{11} Ω amplifiers. A combination of a high efficiency dry mechanical pump and the "Jet" and "X" cones provided higher sensitivity during the analytical session. Background was measured before each raster for 20 s and the measured data were integrated for each 0.262 s.

For strontium isotope analyses by laser ablation, we prioritized carbonate matrices characterized by low rubidium concentrations, thereby minimizing the isobaric interference ^{87}Rb on ^{87}Sr. We used three reference materials and a sample-bracketing analytical strategy. As the primary reference material, we used marine fish otoliths composed predominantly of aragonite. Their isotopic composition had previously been established by solution analysis, yielding $^{87}Sr/^{86}Sr$ values of approximately 0.70922 ± 0.00002, similar to that of modern seawater (0.70918) (DePaolo & Ingram, 1985; El Meknassi *et al*., 2018). We also used the Walnut carbonate (Roberts *et al*., 2017; Rasbury *et al*., 2020) as secondary reference material as a secondary reference material for U–Pb dating of carbonates. In the present analyses, the Walnut returned results within accepted values. Processing of Sr isotope data included normalization and correction procedures. This

normalization refers to correction for instrumental mass fractionation, an inherent bias in mass spectrometric measurements (Woodhead *et al*., 2005). In the case of Sr isotopes, normalization is performed using the invariant ratio of two stable isotopes ($^{86}Sr/^{88}Sr$ = 0.1194) and applying the exponential law of mass fractionation. Since neither isotope is produced by radioactive decay and no natural mass-dependent fractionation between these isotopes has been detected in geological systems, their ratio is considered constant in nature. Mass Rb and Kr interferences were corrected using the exponential law and the natural ratios of $^{87}Rb/^{85}Rb$ = 0.38560, $^{84}Kr/^{83}Kr$ = 4.95565 and $^{86}Kr/^{83}Kr$ = 1.5026. Finally, residual bias was corrected by normalization to our *in-house* otolith, which was analyzed after every 10 unknown samples. The effectiveness of mass bias and isobaric interference corrections were monitored using the $^{84}Sr/^{86}Sr$ invariant ratio (0.0565). Uncertainties are reported at 2s. The raw $^{87}Sr/^{86}Sr$ analytical dataset used to generate all figures and tables is available as supplementary material (Mendeley Data, V1, doi: 10.17632/43x6h7sb22.1).

3.2.5 – Statistical analysis

We tested for differences in carbon and nitrogen isotope ratios between wild and captive turtles. Samples from captive animals were grouped by breeder and batch, whereas samples from wild animals were grouped by geographic location. Carbon and nitrogen isotope data were tested for normality using the Shapiro–Wilk test and for homogeneity of variances using the Fligner–Killeen test. Carbon data were normally distributed, whereas nitrogen data were not. However, both datasets met the assumption of homogeneity of variances. Consequently, carbon data were analyzed using ANOVA followed by Tukey's post hoc test for pairwise comparisons, whereas nitrogen data were analyzed using non-parametric tests, namely the Kruskal–Wallis test followed by Dunn's test. Differences were considered significant at $p < 0.05$. The statistical analyses were carried out in the R software version 4.4.2 with the RStudio interface version 2024.09.1+394.

3.3 – Results

3.3.1 – Carbon and nitrogen stable isotopes

Our results reveal a statistically significant difference in $\delta^{13}C$ values between wild and captive giant South American river turtles (*Podocnemis expansa*) (Table 2 and Fig. 3-A), which we attribute to differences in diet. C_3 plants typically exhibit $\delta^{13}C$ values ranging from approximately –24‰ to –32‰, whereas C_4 plants generally range from about –10‰ to –14‰ (Farquhar *et al*., 1989). With the exception of a single species of native aquatic grass, Amazonian vegetation is overwhelmingly dominated by C_3 plants (Ometto *et al*., 2006). Given the predominantly herbivorous diet of *P. expansa* (Eisemberg *et al*., 2017), it was therefore expected that wild individuals from different collection sites across the basin would show $\delta^{13}C$ values consistent with a C_3-based isotopic signature, as observed here (Table 2 and Fig. 3-A).

Conversely, captive turtles exhibited significantly higher $\delta^{13}C$ values than their wild counterparts, approaching the range typical of C_4 plants (Table 2; Fig. 3-A). This pattern is best explained by the use of commercial feed in the breeding farms where these individuals were raised. In Brazil, maize is a readily available and low-cost commodity that is widely used in both human and animal nutrition (Langner *et al*., 2019). Because maize is a major ingredient in commercial animal feeds, its use results in isotopic signatures strongly influenced by the C_4 signal (Galera *et al*., 2019).

Regarding $\delta^{15}N$, our results showed no clear distinction between captive and wild turtles (Table 2; Fig. 3-B). The fluctuations observed are likely attributable to variation in the nitrogen isotopic composition of food sources in both captive and wild settings. In captive animals, some of this variation may reflect differences in the $\delta^{15}N$ values of commercial fish feeds available in the Brazilian market. For example, the eight feed samples we analyzed spanned a $\delta^{15}N$ range of more than 2‰ (Fig. 5).

Table 2 – Mean, standard deviation, and confidence interval of carbon and nitrogen isotope ratios for the captive and wild reference samples of giant South American river turtles (*Podocnemis expansa*) listed in Table 1. Different letters indicate statistically significant differences ($p < 0.05$).

Sample type	Origin	n	δ^{13}C (‰)			δ^{15}N (‰)		
			Mean	sd	ci (95%)	Mean	sd	ci (95%)
Captive	Commercial breeder 1, batch 1	8	-13.8 [a*]	0.8	0.5	6.4 [e]	0.3	0.2
	Commercial breeder 1, batch 2	12	-17.8 [bc]	2.1	1.2	7.0 [e]	1.2	0.7
	Commercial breeder 1, batch 3	9	-16.0 [a*b]	1.2	0.8	6.1 [e]	0.6	0.4
	Commercial breeder 1, batch 4	6	-18.5 [c]	1.0	0.8	6.5 [e]	0.8	0.7
	Commercial breeder 2	16	-19.0 [c]	1.2	0.6	7.1 [e]	0.8	0.4
Wild	Guaporé River	5	-26.1 [d]	0.6	0.5	6.5 [e]	1.2	1.1
	Middle Juruá River	10	-26.0 [d]	1.7	1.0	7.1 [e]	0.8	0.5
	Piraruacá Lake	3	-25.4 [d]	0.7	0.8	6.2 [e]	0.3	0.4
	Low Purus River	1	-25.9 [d]	–	–	5.5 [e]	–	–

*Borderline result in the comparison of commercial breeder 1, batch 1 vs. commercial breeder 1, batch 3; $p = 0.0512$.

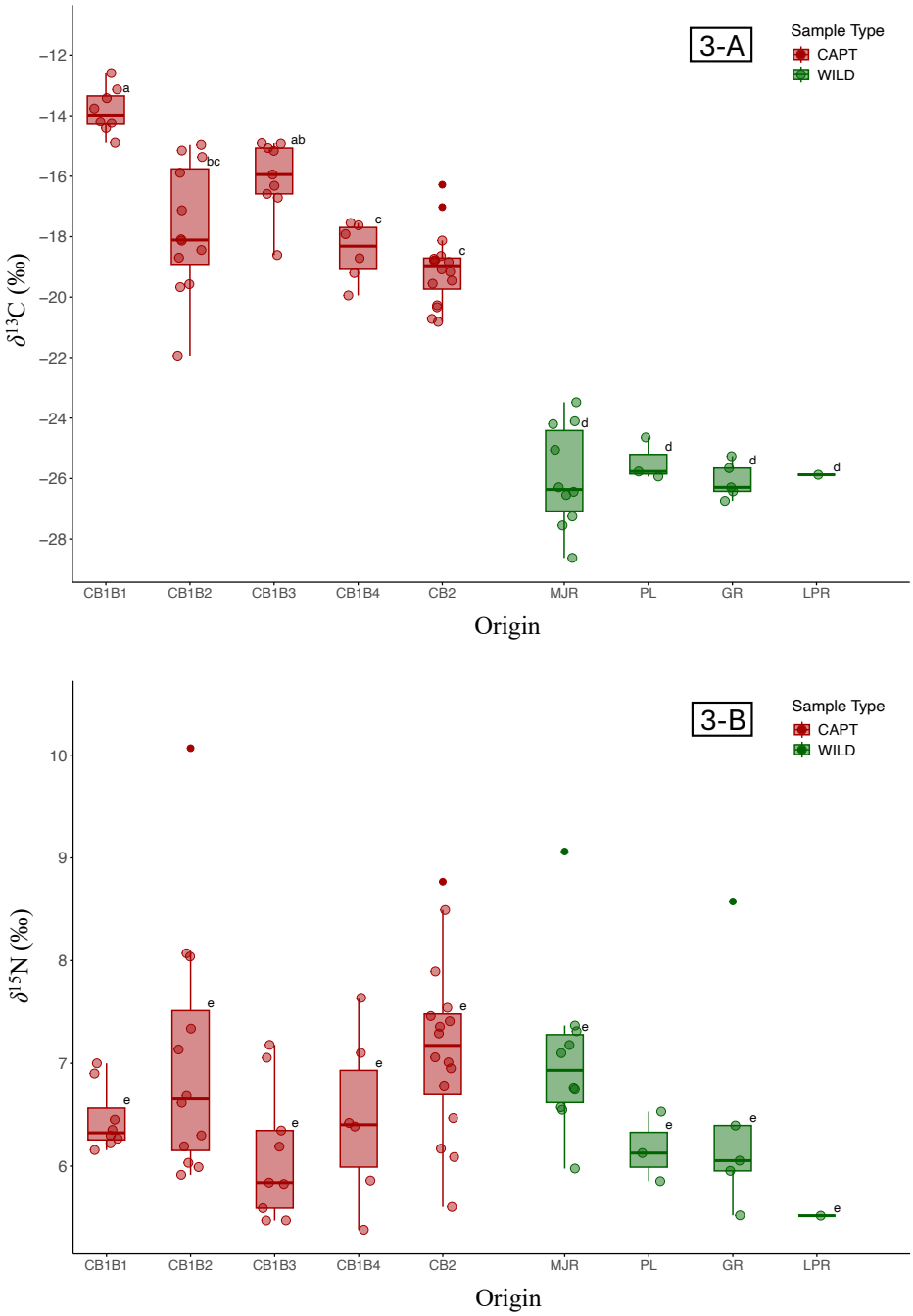

Figure 3 – Boxplot of carbon (Fig. 3-A) and nitrogen (Fig. 3-B) isotope ratios for captive and wild reference samples of giant South American river turtles (*Podocnemis expansa*) listed in Table 1. Captive groups (red boxes): CB1B1 = commercial breeder 1, batch 1; CB1B2 = commercial breeder 1, batch 2; CB1B3 = commercial breeder 1, batch 3; CB1B4 = commercial breeder 1, batch 4; CB2 = commercial breeder 2. Wild groups (green boxes): GR = Guaporé River; LPR = Lower Purus River; MJR = Middle Juruá River; PL = Piraruacá Lake. Distinct letters denote statistically significant differences ($p < 0.05$). The δ^{13}C comparison between CB1B1 and CB1B3 was borderline significant ($p = 0.0512$).

3.3.2 – Strontium isotopes

The $^{87}Sr/^{86}Sr$ data from rivers used for comparison with turtle samples represent dissolved strontium isotope ratios compiled from previous studies across the Amazon Basin (Palmer & Edmond, 1992; Gaillardet *et al*., 1997; Queiroz *et al*., 2009; Pouilly *et al*., 2014; Santos *et al*., 2015; Duponchelle *et al*., 2016; Barroco, 2019; Hauser *et al*., 2019; Mereles *et al*., 2025). Overall, our findings indicate that the bony matrix of the turtle shell records the strontium isotopic signature of the aquatic environments it inhabits. This pattern is supported by the reference samples from the Middle Juruá River, Middle Solimões River, Branco River, Guaporé River, and the Atlantic Ocean, whose $^{87}Sr/^{86}Sr$ ratios closely matched the dissolved strontium values reported for the corresponding water bodies (Figs. 4 and 6). Notably, these cases comprise all comparisons for which site-specific isotopic data were available for the aquatic environment. The agreement between the sea turtle sample and the Atlantic Ocean is particularly compelling, as it provides clear evidence that the strontium isotopic composition of the aquatic environment is incorporated into chelonian shell bone. This case is especially informative because seawater $^{87}Sr/^{86}Sr$ is globally homogeneous and restricted to a very narrow range around 0.7092 (Hodell, Mead & Mueller, 1990), and the value measured for our reference sea turtle (0.7094) fell squarely within this interval.

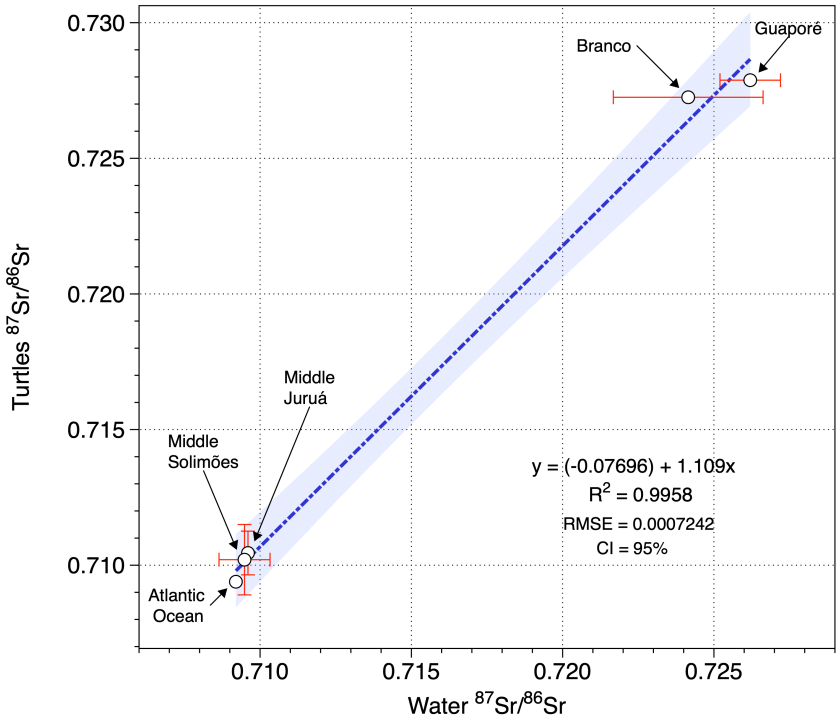

Figure 4 – $^{87}Sr/^{86}Sr$ ratio (mean ± SD) and linear regression between turtles (bony layer of carapace) and water from four Amazonian rivers and the Atlantic Ocean. The light blue band corresponds to the 95% confidence interval.

3.3.3 – Questioned samples

The $\delta^{13}C$ and $\delta^{15}N$ results for the questioned samples are shown in Fig. 5, alongside reference samples from wild and captive turtles and commercial feed collected from turtle farms in the Brazilian states of Amazonas and Pará. Some questioned samples overlapped with the $\delta^{13}C$ values of wild reference turtles, whereas others fell within the range of captive reference turtles. Fig. 6 shows the strontium isotope ratios of the questioned turtles relative to those of wild reference turtles and to $^{87}Sr/^{86}Sr$ baselines established for Amazonian rivers.

Seven of the questioned turtles (Q-1 to Q-7) were sampled from a licensed retailer in the city of Manaus. Regarding the remaining questioned samples, Q-8 consisted of a large carapace (straight carapace length > 60 cm) displayed as an ornament at a commercial breeding farm. Its size raised suspicion during an inspection by the Brazilian Federal Police, suggesting that it was unlikely to have originated from a captive-raised individual. The final two questioned turtles, Q-9 and Q-10, were collected during seizures conducted by the Brazilian Federal Police at the port of Manaus.

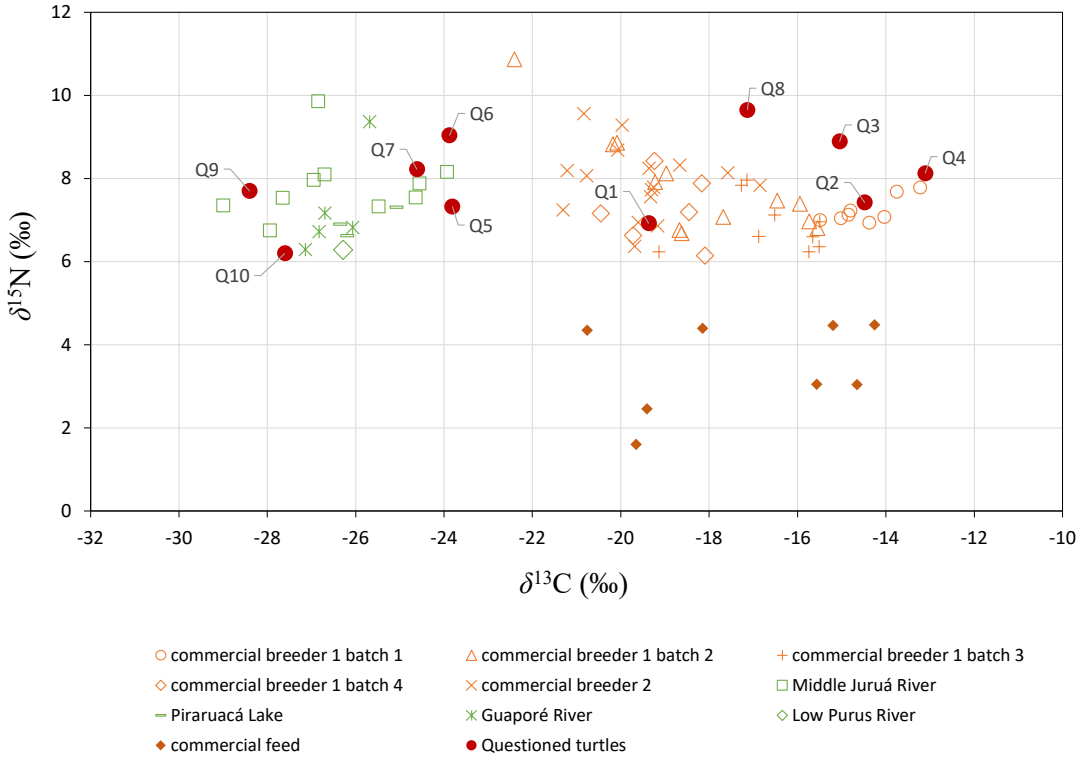

Figure 5 – Biplot $\delta^{13}C/\delta^{15}N$ of the wild, captive, and questioned giant South American river turtles (*Podocnemis expansa*) listed in Table 1, together with commercial feed samples collected on turtle farms in the states of Amazonas and Pará, Brazil.

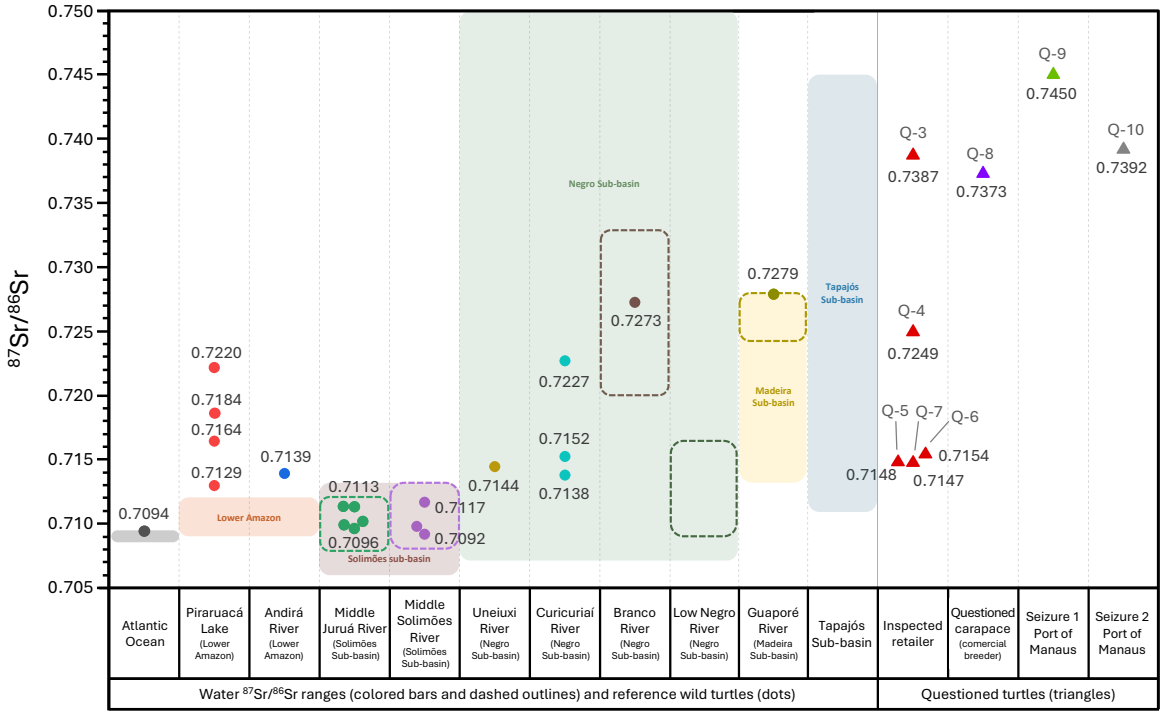

Figure 6 – Strontium isotopic ratios ($^{87}Sr/^{86}Sr$) of wild reference turtles, questioned turtles, and Amazonian water bodies. Each category on the horizontal axis indicates either a water body (left) or a locality where questioned turtles were collected (right). Dots indicate wild reference turtles, whereas triangles denote questioned turtles. Dashed boxes show the estimated $^{87}Sr/^{86}Sr$ ranges (mean ± 2 SD) for each river identified on the horizontal axis for which published data are available. Colored background bars represent the $^{87}Sr/^{86}Sr$ ranges (mean ± 2 SD) of the major Amazon sub-basins and the Atlantic Ocean. The reference ranges were derived from data compiled by Mereles *et al*. (2025) and Duponchelle *et al*. (2016), which in turn drew on multiple previous studies.

3.4 – Discussion

3.4.1 – Carbon and nitrogen stable isotopes

We found a statistically significant difference in carbon isotopic composition between captive and wild giant South American river turtles. Although some variation in $\delta^{13}C$ occurred within both groups, these within-group fluctuations were not sufficient to obscure the overall isotopic distinction between wild and captive individuals. Consequently, $\delta^{13}C$ emerges as a reliable marker for detecting wildlife laundering in Amazonian turtle farms. It is important to note that the captive animals analyzed in this study were raised on farms that predominantly used diets with a C_4 isotopic signature. This condition is central to generating isotopic contrast with the naturally C_3-based diet of wild turtles and, therefore, to enabling the detection of wildlife laundering based on $\delta^{13}C$ alone.

In Brazil, turtle farming relies predominantly on commercial extruded or pelleted fish feed. Up to 75% of legally traded turtles are estimated to be raised on this maize-rich diet, which carries a C_4 isotopic signature. In addition, some farms incorporate by-products from the filleting of captive fish or bovine offal into their feeding regimes (Andrade *et al*., 2021). Because farmed fish in Brazil are typically raised on C_4-based feeds and cattle are commonly raised on C_4 tropical grass pastures, these inputs may also confer a C_4 isotopic signature on an additional fraction of legally traded turtles. Therefore, in light of our findings and the characteristics of this production system, we infer that farmed turtles in the Brazilian Amazon will most commonly exhibit a $\delta^{13}C$ signature strongly influenced by C_4-derived inputs. This inference is further supported by the $\delta^{13}C$ values of the eight commercial fish feeds we analyzed, all of which showed a clear C_4 isotopic signature (Fig. 5). In this context, this $\delta^{13}C$-based forensic approach is likely to be broadly applicable across much of the formal turtle farming and trade sector in the region. This is particularly important when the scale of production for slaughter is taken into account, as larger and more technically intensive farms tend to rely more heavily on commercial feed than smaller producers.

Some groups of captive turtles exhibited significant differences in $\delta^{13}C$ values, most notably batch 1 from breeder 1. We attribute this variation to differences in the availability of naturally occurring C_3 resources within the rearing systems. Whereas batch 1 from breeder 1 consisted of juveniles maintained in a small pond surrounded by grasses, batches 2, 3, and 4 from the same breeder, representing the growth, finishing, and reproductive stages, respectively, as well as the batch from breeder 2, were maintained in extensive lagoons partially or fully bordered by tropical forest. The conditions in batch 1 likely increased dependence on commercial feed as the dominant dietary input, while in the other groups, larger body size, greater interaction with the surrounding environment, and access to natural C_3 food resources alongside commercial feed likely contributed to the slightly lower $\delta^{13}C$ values.

Like *P. expansa*, other Amazonian species in the family Podocnemididae are also predominantly herbivorous, with relatively small differences – particularly within the genus *Podocnemis* – in the relative contribution of animal matter and poorly digestible plant material to the diet (Eisemberg *et al*., 2017). Even when animal matter is considered, the diet of this group is still expected to be C_3-based, given the carbon isotopic composition of the Amazon forest and its food webs (Ometto *et al*., 2006). Therefore, we consider that $\delta^{13}C$ values of these species in the wild tend to resemble those of *Podocnemis expansa*, as

previously demonstrated in a comparison with *Podocnemis unifilis* (Lara *et al*., 2012). Our results for questioned turtles Q-9 and Q-10 (Fig. 5) corroborate this expectation. Both were *Podocnemis erythrocephala* and exhibited an isotopic signature consistent with a natural C_3-based diet, with $\delta^{13}C$ values similar to those of wild *Podocnemis expansa* specimens. Some interspecific variation in carbon isotopic composition may occur among wild turtle populations in the Amazon, particularly under specific ecological contexts, such as syntopic interactions that may affect the degree of trophic niche overlap (Cunha *et al*., 2020). Nevertheless, we consider that the statistically significant $\delta^{13}C$ contrast between wild and captive giant South American river turtles observed in this study is likely applicable to other river turtle species of the family Podocnemididae in the Brazilian Amazon.

In forensic investigations of specific criminal cases, captive turtles should be sampled alongside all food resources used on the farms under investigation from which the animals are purported to originate. This integrated approach provides a more complete understanding of farm feeding practices and their effects on tissue isotopic composition. It also makes it possible to evaluate whether dietary and tissue isotopic signatures are mutually consistent, thereby increasing the robustness of isotopic evidence for detecting wildlife laundering. Even so, given the predominant use of diets with a C_4 isotopic signature in the turtle farming sector of the Brazilian Amazon, the $\delta^{13}C$-based approach applied here is likely to be effective for detecting wildlife laundering across most farms, retailers, and restaurants legally authorized to keep or market captive-raised turtles.

In contrast to $\delta^{13}C$, $\delta^{15}N$ did not provide a consistent basis for distinguishing captive from wild turtles, indicating that its variation is better interpreted in terms of dietary and environmental heterogeneity than origin per se. Captive turtles may receive different dietary supplements depending on the breeder or batch, or may exploit other resources available in the rearing environment to varying degrees. Variation in the isotopic composition of commercial feeds may further contribute to these differences, as the feeds analyzed in this study differed by more than 2‰ in $\delta^{15}N$. In wild animals, comparable variation in food resources may likewise account for the observed differences in $\delta^{15}N$. Our results are consistent with those of the only other study on this species, conducted in a different Brazilian watershed (the Araguaia–Tocantins Basin), which reported a $\delta^{15}N$ range of approximately 3‰ for wild *Podocnemis expansa* (Lara *et al*., 2012). These findings suggest that substantial $\delta^{15}N$ variation may be an inherent feature of natural populations, reflecting spatial and ecological heterogeneity in nitrogen sources and trophic pathways.

Notably, wild giant South American river turtles from different locations across the Amazon Basin analyzed in this study exhibited higher δ15N values than those reported for the Araguaia–Tocantins Basin, by approximately 3‰ overall. This pattern suggests possible basin-scale differences in the nitrogen isotopic composition of *P. expansa* between these two major Brazilian watersheds, although this question was beyond the scope of the present study and deserves further investigation.

Although δ^{15}N did not discriminate wild from captive turtles in our study, it may still be useful for establishing farm-specific isotopic fingerprints in case-specific forensic investigations, especially when combined with other isotopic and elemental tracers (Brandis *et al*., 2018). For instance, some turtle farms in Brazil integrate fish production, processing fish on-site and using the resulting by-products as turtle feed, whereas others rely on bovine offal as a protein source. In such systems, captive turtles may show elevated δ^{15}N values relative to both wild individuals and turtles raised under different feeding regimes, reflecting ^{15}N enrichment associated with protein sources derived from higher trophic levels (Fry, 2006). Such differences may strengthen discrimination between wild and captive turtles, as well as among farming systems, thereby increasing the forensic power to detect wildlife laundering.

Our δ^{13}C results are consistent with previous studies comparing the isotopic composition of wild and captive freshwater turtles, which have generally reported more enriched values in captive individuals than in their wild conspecifics (Hill *et al*., 2020; Hopkins *et al*., 2022, 2023; Sung *et al*., 2025). Nevertheless, the isotopic ranges and the extent of differentiation between captive and wild groups vary across studies, likely reflecting interspecific differences as well as variation in diet composition and environmental conditions. For δ^{15}N, in contrast, those studies reported enrichment in captive turtles relative to wild individuals, a pattern not observed in our dataset. This discrepancy likely reflects differences in the isotopic composition of diets provided in breeding facilities, since captive animals in our study exhibited lower δ^{15}N values than those reported elsewhere and broadly overlapped the range observed in wild turtles. Together, these results indicate that isotopic contrasts between captive and wild turtles are not uniform across systems, but are shaped by the specific dietary and husbandry conditions under which captive animals are maintained, as well as by the isotopic baseline of wild food webs. These findings underscore the importance of accounting for context-dependent conditions when comparing the isotopic composition of captive and wild animals, as highlighted by Brasileiro *et al*. (2023).

3.4.2 – Strontium isotopes

As the largest watershed on the planet, the Amazon Basin comprises a vast and highly interconnected mosaic of rivers, streams, lakes, lagoons, wetlands, and floodplains. This hydrological network is shaped by annual flood-pulse dynamics, generating marked spatial and temporal heterogeneity in water flow and connectivity (Molinier *et al*., 1996). Such complexity makes the sampling and monitoring of biogeochemical processes across these aquatic systems particularly challenging.

The dissolved strontium isotope ratio data available in the literature for Amazonian rivers provide substantial temporal coverage but remain largely restricted to main river channels. Consequently, they do not capture potential heterogeneity among smaller water bodies, which may contribute to local-scale variation in strontium isotope ratios within major sub-basins (Pouilly *et al*., 2014). This limitation may partly account for the discrepancies observed in our comparison between the $^{87}Sr/^{86}Sr$ ratios of some rivers and turtles. Variations in turtles' $^{87}Sr/^{86}Sr$ ratios may also reflect differences in habitat use and movement patterns. Isotopic contrasts among adjacent environments at a sub-local scale can be recorded in animal tissues, potentially explaining mismatches with $^{87}Sr/^{86}Sr$ values measured in river mainstems (Pouilly *et al*., 2014). Studies on the migration of Amazonian river turtles (Carneiro, 2017), together with evidence from conservation management projects, indicate that these displacements are associated with both the flood pulse and the reproductive cycle (Ferrara *et al*., 2014). Movements may also occur among different water bodies through flooded forests during the high-water season, via nearby tributaries, or along the main river channels (Escalona *et al*., 2009).

Bone is a metabolically active tissue that undergoes continuous remodeling of both its organic and mineral phases. As a result, strontium measurements in bone reflect the isotopic composition of nutrients assimilated during the more recent years of an individual's life, rather than a single-time-point signal (Degryse *et al*., 2012). Bone may therefore retain the strontium isotopic imprint of past movements between contrasting aquatic environments, which could partly explain discrepancies in $^{87}Sr/^{86}Sr$ values when compared with river mainstems or with non-migratory individuals.

Catchment-scale $^{87}Sr/^{86}Sr$ values can be predicted from basin geology, allowing inferences about the strontium isotopic composition of unsampled rivers (Bataille & Bowen, 2012). This is particularly important for interpreting turtle samples from water bodies

lacking direct isotopic data, such as the Curicuriaí and Uneiuxi rivers (Fig. 1-A). Although both are tributaries of the Negro sub-basin, they drain the Amazon trough rather than the Guiana Shield, which likely explains why turtles collected there fall within the low-radiogenic portion of the strontium isotopic range of the Rio Negro basin, with $^{87}Sr/^{86}Sr$ values lower than those reported for the main stem of the river and for tributaries draining the Guiana Shield.

A comparable situation applies to Piraruacá Lake. Although the lake is adjacent to the Lower Amazon River and connected to its mainstem by a complex network of small channels, it also receives inflow from the Trombetas River, a Guiana Shield tributary with a dissolved $^{87}Sr/^{86}Sr$ ratio of 0.72546 ± 0.00428 (Mereles *et al*., 2025). Piraruacá Lake can thus be viewed as a mixing zone between two large lotic systems with contrasting strontium isotopic compositions. Similar mixing dynamics have been described for this sector of the Lower Amazon in relation to tributaries such as the Tapajós and Xingu rivers (Mereles *et al*., 2025). Under these conditions, turtles inhabiting the area would be expected to record this isotopic heterogeneity in bone, as observed in our data, which show $^{87}Sr/^{86}Sr$ values higher than those of the Lower Amazon. This interpretation is reinforced by the Amazon Basin surface-water strontium isoscape published by Mereles *et al*. (2025), whose predicted dissolved $^{87}Sr/^{86}Sr$ range for this floodplain segment encompasses the values measured in turtles from Piraruacá Lake and the Andirá River.

Although strontium is primarily present in the dissolved phase of aquatic systems, it also occurs in suspended sediments transported by rivers. Because its binding to particles may be relatively weak, strontium can remain mobile between sediment and water, as well as within sediment matrices, allowing suspended sediments to act over time as a reservoir that gradually releases strontium into the aqueous phase (Xu & Marcantonio, 2004; Chowdhury & Blust, 2011). In its soluble ionic form, strontium is highly bioavailable (Zanacic & McMartin, 2022), and even when complexed, it may retain considerable bioavailability, given that its predominant interactions in natural waters involve low-molecular-mass humic substances (Chowdhury & Blust, 2011).

This distinction may be relevant because $^{87}Sr/^{86}Sr$ ratios commonly differ between dissolved and particulate river loads, with higher values generally reported for the sediment-associated fraction (Andersson *et al*., 1994). The same pattern has been documented in Amazonian rivers. For example, Allègre *et al*. (1996) reported $^{87}Sr/^{86}Sr$ values of 0.7132 in suspended particulate matter and 0.7088 in the dissolved fraction of the

Solimões River, and 0.7564 and 0.7332, respectively, for the Tapajós River. Although the relative contribution of dissolved *versus* particulate strontium to uptake by Amazonian freshwater turtles remains unknown, this contrast raises the possibility that sediment-associated strontium may have contributed, at least in part, to the slight discrepancies we observed between $^{87}Sr/^{86}Sr$ ratios in turtle bone and in dissolved riverine strontium.

At the same time, evidence from other Amazonian aquatic organisms suggests that dissolved strontium is a strong predictor of isotopic composition in calcified tissues. Significant correlations have been reported between dissolved $^{87}Sr/^{86}Sr$ values in river water and the isotopic composition of fish scales and otoliths (Pouilly *et al*., 2014; Duponchelle *et al*., 2016; Hauser *et al*., 2019).

Taken together, these observations indicate that the extent to which suspended-sediment strontium influences the $^{87}Sr/^{86}Sr$ composition of turtle bone remains unresolved. Clarifying this issue will require targeted studies designed to partition the relative contributions of dissolved and particulate strontium sources in Amazonian freshwater turtles.

Based on our results, strontium isotope ratios are an efficient forensic tool for tracing the geographic origin of trafficked river turtles in the Brazilian Amazon, particularly when the suspected source regions include rivers for which dissolved $^{87}Sr/^{86}Sr$ values have already been characterized. Moreover, even when precise source assignment is constrained by limited baseline data, isotopic mismatch with seized animals can still be used to exclude broad candidate regions and thereby narrow the spatial focus of law enforcement efforts. These findings establish strontium isotopic analysis as an effective approach for investigating river turtle trafficking in the Amazon. This forensic application is especially relevant in the metropolitan region of Manaus, the largest urban center and the main hub of turtle consumption in the Amazon (Chaves *et al*., 2021). As a result, Manaus constitutes a major destination for trafficking routes originating from multiple surrounding areas (Kemenes & Pezzuti, 2007; Pezzuti *et al*., 2010; Pantoja-Lima *et al*., 2014; Polícia Federal, 2014), many of which are associated with contrasting strontium isotopic signatures.

3.4.3 – Questioned samples

Among the animals inspected at the suspected retailer (Q-1 to Q-7), the questioned turtles Q-1 to Q-4 exhibited $\delta^{13}C$ values consistent with a C_4-based diet, as expected for captive turtles fed commercial feed containing maize, whereas Q-5 to Q-7

displayed a C_3 isotopic signature (Fig. 5). In light of our isotopic results and the feeding practices reported for commercial turtle farming in Brazil, we infer that Q-5 to Q-7 were more likely wild-origin individuals than turtles raised on commercial farms using a C_4-signature diet. This interpretation is further supported by body size: Q-1 to Q-4 were smaller (straight carapace length < 30 cm), whereas Q-5 to Q-7 had straight carapace lengths of around 50 cm. Attaining this larger size class is generally more difficult, more costly, and less common under commercial farming conditions. A less likely alternative is that Q-5 to Q-7 originated from a farm that does not use commercial feed, bovine offal, or filleting by-products from captive fish raised on C4-based diets, but instead relies exclusively on C_3 food sources, such as vegetable leftovers or residues from the filleting of wild fish. In that case, additional isotopic and elemental analyses of both the questioned turtles and the farm's food resources would be necessary to refine the forensic investigation, as discussed below.

The questioned turtle Q-8, despite its large size, showed a carbon isotopic composition consistent with the C_4 signature typically associated with captive farming. By contrast, Q-9 and Q-10 exhibited $\delta^{13}C$ values indicative of a natural C_3-based diet, suggesting that they may have been poached and transported to the port of Manaus without passing through captive-breeding production chains.

Concerning strontium isotopic ratios, among the turtles sampled at the inspected retailer, Q-5, Q-6, and Q-7 exhibited a very narrow range of $^{87}Sr/^{86}Sr$ values, all close to 0.715 (Q-5 = 0.7148; Q-6 = 0.7154; Q-7 = 0.7147) (Fig. 6). These individuals also showed $\delta^{13}C$ values consistent with a natural C_3-based diet (Fig. 5). Assuming, from these $\delta^{13}C$ values, that they were wild-caught and subsequently introduced into the trade chain, the narrow strontium isotopic range, their similar body size, and the fact that they were housed together suggest that they may have been poached from the same region. Analyses based on wild reference turtles showed that their $^{87}Sr/^{86}Sr$ values overlap most closely with those of animals from the Amazon mainstem (Piraruacá Lake and the Andirá River) and from tributaries of the Negro River draining the Amazon sedimentary basin (the Uneiuxi and Curicuriaí rivers) (Fig. 6). These water bodies therefore emerge as plausible source areas for the inspected turtles. Beyond comparisons with wild reference animals, the $^{87}Sr/^{86}Sr$ values of these individuals can also be evaluated against dissolved strontium isotope signatures in Amazonian waters. From this perspective, based on currently available data (Mereles *et al*., 2025; Duponchelle *et al.*, 2016; and the studies compiled therein), the values observed in these three individuals are consistent with the lower-radiogenic portions of the isotopic-ratio

ranges reported for the Negro, Madeira, and Tapajós sub-basins. These regions may thus constitute additional potential areas of origin for these animals.

Despite these plausible source inferences, the absence of $^{87}Sr/^{86}Sr$ data for many water bodies, including lakes adjacent to major river channels, limits more precise source assignment. This limitation highlights the need to expand water sampling for strontium isotope analysis across Amazonian aquatic systems, particularly in areas most affected by river turtle poaching. Even so, the exclusion of potential source areas is highly informative for monitoring and disrupting trafficking networks. The $^{87}Sr/^{86}Sr$ values of these turtles differ markedly from the isotopic signatures reported for large parts of the Solimões, Negro, Madeira, and Tapajós basins (Fig. 1-B; Fig. 6). Notably, the excluded regions encompass two major rivers widely recognized as important source areas for turtles trafficked to Manaus: Branco River, in the Negro sub-basin, (Pezzuti *et al*., 2010; Polícia Federal, 2014) and the Purus River, in the Solimões sub-basin (Kemenes & Pezzuti, 2007; Pantoja-Lima *et al*., 2014).

The other two turtles analyzed for strontium at that retailer (Q-3 and Q-4), both of which showed $\delta^{13}C$ values consistent with captive origin, exhibited higher and clearly distinct $^{87}Sr/^{86}Sr$ ratios (Q-3 = 0.7387; Q-4 = 0.7249). Another turtle independently confirmed to be of captive origin (Q-8) also showed an elevated $^{87}Sr/^{86}Sr$ ratio (Q-8 = 0.7373). Because strontium is incorporated into animal tissues through ingested resources, including both diet and water (Burton & Katzenberg, 2018), these values reflect the isotopic composition of the inputs used at the farms where these turtles were raised. Although the limited sample size precludes definitive conclusions, these results raise the possibility that commercial turtle farms in the metropolitan region of Manaus may exhibit a distinct strontium isotopic signature characterized by elevated $^{87}Sr/^{86}Sr$ ratios. This pattern was not a primary focus of the present study and therefore warrants targeted investigation.

Strontium is incorporated into calcified tissues such as bone through both food intake and water consumption. However, the relative contribution of these sources may vary with water chemistry, diet composition, feeding behavior, and local environmental conditions, making broad generalizations difficult. As a result, the proportional contribution of food and water to tissue strontium remains incompletely resolved, and the available literature reports conflicting or inconclusive results (Buckel *et al*., 2004; Walther & Thorrold, 2006; Lahtinen *et al*., 2021). In natural environments, the geological composition of river waters integrates the effects of regional lithology and weathering, making dissolved $^{87}Sr/^{86}Sr$ a reliable proxy for the strontium available to aquatic food webs. Under such

conditions, the $^{87}Sr/^{86}Sr$ values of aquatic animals are expected to reflect local environmental signatures more strongly than the influence of particular dietary items (Bentley, 2006). In controlled production systems, by contrast, both the source of tank water and the inclusion of specific ingredients in high proportions, such as commercial feed, may substantially affect tissue $^{87}Sr/^{86}Sr$ ratios. Preliminary evidence for this effect has been reported for *Arapaima gigas*, a widely farmed Amazonian fish species in Brazil (Pereira *et al*., 2019).

Finally, the two turtles sampled from seizures at the port of Manaus (Q-9 and Q-10), both of which exhibited $\delta^{13}C$ values consistent with a natural C_3-based diet, showed notably elevated $^{87}Sr/^{86}Sr$ ratios (Q-9 = 0.7450; Q-10 = 0.7392). These values overlap with the range reported for the Negro and Tapajós sub-basins (Fig. 6), indicating that these regions are the likely areas of origin for these individuals.

3.4.4 – Future directions

Long-term datasets on dissolved strontium isotope ratios in major Amazonian catchments are already available in the scientific literature, enabling the discrimination of aquatic animal origins among major rivers and sub-basins (Palmer & Edmond, 1992; Gaillardet *et al*., 1997; Queiroz *et al*., 2009; Pouilly *et al*., 2014; Santos *et al*., 2015; Duponchelle *et al*., 2016; Barroco, 2019; Hauser *et al*., 2019; Pereira *et al*., 2019; Mereles *et al*., 2025). Nevertheless, further research is needed to expand spatial coverage and refine our understanding of variation in strontium isotope ratios across the complex hydrological network of the Amazon Basin. Broader sampling of wild turtles from multiple regions and aquatic environments throughout the basin will also be important to expand the empirical support for the relationship between $^{87}Sr/^{86}Sr$ in water bodies and turtle tissues identified in this study. Together, these advances will strengthen the predictive capacity of this forensic isotopic tool for geographic origin assignment in trafficked turtles.

Another important issue requiring further study is tissue isotopic turnover, as shown experimentally in Chapter 2. This process describes how rapidly the isotopic composition of a given tissue changes through time in response to diet assimilation and metabolic replacement. Because tissues differ in their protein metabolic activity and replacement dynamics, each is characterized by a distinct turnover rate. After an abrupt shift between isotopically contrasting diets, tissues incorporate the new isotopic signal over different timescales. Quantifying these dynamics is therefore essential for inferring the timing of dietary shifts (Vander Zanden *et al*., 2015; Carter *et al*., 2019). In a forensic context, if

wild turtles with a C_3 isotopic signature are trafficked, placed on a farm, and subsequently fed a C_4-based diet, knowledge of tissue-specific turnover rates becomes critical for establishing the time window during which isotopic analyses remain effective for detecting wildlife laundering (Sung *et al*., 2025).

3.5 – Conclusion

This study provides the first isotopic comparison of captive and wild Amazonian chelonians based on carbon and nitrogen, and the first application of strontium isotope ratios to geographic origin assignment in any chelonian species. The multi-isotopic approach proposed here proved effective for distinguishing wild from captive turtles and for supporting geographic origin inference. Carbon effectively discriminated wild from captive individuals, whereas nitrogen showed potential for detecting farm-specific isotopic signatures. In addition, wild turtles reflected the $^{87}Sr/^{86}Sr$ composition of the water bodies they inhabited, demonstrating the utility of strontium isotopes to infer geographic provenance.

By integrating these complementary tracers, we establish a robust forensic framework for detecting wildlife laundering and reconstructing trafficking routes associated with the poaching and illegal trade of Amazonian freshwater turtles, which is likely the most significant wildlife trafficking issue in the Brazilian Amazon. This approach offers practical value for environmental law enforcement by supporting the long-term monitoring of seizure patterns, the identification of trafficking hotspots and routes, and the evaluation of spatiotemporal shifts in illegal trade dynamics. It also has direct management relevance, as isotopic inference of origin can support more appropriate destination decisions for confiscated animals and help avoid mixing individuals from distinct geographic populations. Within legal production chains, routine isotopic screening of breeders, retailers, and restaurants could strengthen traceability, support the verification of captive origin, and increase deterrence against wildlife laundering. More broadly, our results highlight the wider forensic potential of this multi-isotopic approach for illegal wildlife trade investigations across the Amazon, including Brazil and other Amazonian countries, particularly for other freshwater taxa that record environmental strontium signatures and for terrestrial and aquatic species whose captive diets are isotopically distinct from natural food webs.

3.6 – References

Alexander J, Downs CT, Butler M, Woodborne S, Symes CT. 2019. Stable isotope analyses as a forensic tool to monitor illegally traded African grey parrots. *Animal Conservation* 22:134–143. DOI: 10.1111/acv.12445.

Allègre CJ, Dupré B, Négrel P, Gaillardet J. 1996. Sr-Nd-Pb isotope systematics in Amazon and Congo River systems: Constraints about erosion processes. *Chemical Geology* 131:93–112. DOI: 10.1016/0009-2541(96)00028-9.

Amazonas Atual. 2014. Empresária Charufe Nasser é presa em operação da Polícia Federal. *Available at https://amazonasatual.com.br/empresaria-charufe-nasser-e-presa-em-operacao-da-policia-federal-2/#:~:text=MANAUS%20–%20A%20Polícia%20Federal%20prendeu,zona%20centro%2Doeste%20de%20Manaus.* (accessed October 15, 2024).

Andersson PS, Wasserburg GJ, Ingri J, Stordal MC. 1994. Strontium, dissolved and particulate loads in fresh and brackish waters: The Baltic Sea and Mississippi Delta. *Earth and Planetary Science Letters* 124:195–210. DOI: 10.1016/0012-821X(94)00062-X.

Andrade PCM, Duarte JAM, Costa FS, Rodrigues W, Alves HRB, Brelaz AO. 2008. Instalações para a criação de quelônios. In: Andrade PCM ed. *Criação e Manejo de Quelônios no Amazonas*. Manaus: Ibama/Pró-Várzea, 222–258.

Andrade PCM, Garcez JR, Lima AC, Duarte JAM, Anízio TLF, Rodrigues WS, Oliveira AB, Alves HRB. 2021. Panorama da quelonicultura no Brasil – uma estratégia para conservação das espécies e geração de renda. *Aquaculture Brasil*:34–40.

Antunes AP, Fewster RM, Venticinque EM, Peres CA, Levi T, Rohe F, Shepard GH. 2016. Empty forest or empty rivers? A century of commercial hunting in Amazonia. *Science Advances* 2:e1600936. DOI: 10.1126/sciadv.1600936.

Barroco LSA. 2019. O efeito de barragens hidrelétricas sobre populações de peixes de rios de águas pretas na Amazônia: uma abordagem com o uso de marcadores biogeoquímicos e moleculares. Tese de Doutorado. Manaus: Universidade Federal do Amazonas.

Bataille CP, Bowen GJ. 2012. Mapping 87Sr/ 86Sr variations in bedrock and water for large scale provenance studies. *Chemical Geology* 304–305:39–52. DOI: 10.1016/j.chemgeo.2012.01.028.

Bataille CP, Crowley BE, Wooller MJ, Bowen GJ. 2020. Advances in global bioavailable strontium isoscapes. *Palaeogeography, Palaeoclimatology, Palaeoecology* 555. DOI: 10.1016/j.palaeo.2020.109849.

Bentley RA. 2006. Strontium isotopes from the earth to the archaeological skeleton: A review. *Journal of Archaeological Method and Theory* 13:135–187. DOI: 10.1007/s10816-006-9009-x.

Bowen GJ, Wassenaar LI, Hobson KA. 2005. Global application of stable hydrogen and oxygen isotopes to wildlife forensics. *Oecologia* 143:337–348. DOI: 10.1007/s00442-004-1813-y.

Brandis KJ, Meagher P, Schoppe S, Zawada K, Widmann I, Widmann P, Dolorosa RG, Francis R. 2023. Determining the Provenance of Traded Wildlife in the Philippines. *Animals* 13. DOI: 10.3390/ani13132165.

Brandis KJ, Meagher PJB, Tong LJ, Shaw M, Mazumder D, Gadd P, Ramp D. 2018. Novel detection of provenance in the illegal wildlife trade using elemental data. *Scientific Reports* 8. DOI: 10.1038/s41598-018-33786-0.

Brasileiro L, Mayrink RR, Pereira AC, Costa FJV, Nardoto GB. 2023. Differentiating wild from captive animals: an isotopic approach. *PeerJ* 11. DOI: 10.7717/peerj.16460.

Buckel JA, Sharack BL, Zdanowicz VS. 2004. Effect of diet on otolith composition in *Pomatomus saltatrix*, an estuarine piscivore. *Journal of Fish Biology*:1469–1484. DOI: 10.1111/j.1095-8649.2004.00393.x.

Burton J, Katzenberg MA. 2018. Strontium isotopes and the chemistry of bones and teeth. In: Katzenberg MA, Grauer AL eds. *Biological anthropology of the human skeleton*. John Wiley & Sons, Inc., 505–514. DOI: 10.1002/9781119151647.ch15.

Carneiro CC. 2017. Ecologia e Conservação de Podocnemis expansa (Testudines, Podocnemididae) no Baixo Rio Xingu, Pará, Brasil. Belém: Universidade Federal do Pará.
Carter WA, Bauchinger U, McWilliams SR. 2019. The Importance of Isotopic Turnover for Understanding Key Aspects of Animal Ecology and Nutrition. *Diversity* 11:84. DOI: 10.3390/d11050084.
Charity S, Ferreira JM. 2020. *Wildlife Trafficking in Brazil*. Cambridge: TRAFFIC International.
Chatfield MWH, Frederick CA, Yorks D, Pollock E, Hopkins JB. 2026. Combating the illegal turtle trade using chemical markers. *The Journal of Wildlife Management* 90. DOI: 10.1002/jwmg.70141.
Chaves WA, Monroe MC, Sieving KE. 2019. Wild Meat Trade and Consumption in the Central Amazon, Brazil. *Human Ecology* 47:733–746. DOI: 10.1007/s10745-019-00107-6.
Chaves WA, Valle D, Tavares AS, Morcatty TQ, Wilcove DS. 2021. Impacts of rural to urban migration, urbanization, and generational change on consumption of wild animals in the Amazon. *Conservation Biology* 35:1186–1197. DOI: 10.1111/cobi.13663.
Chesson LA, Barnette JE, Bowen GJ, Brooks JR, Casale JF, Cerling TE, Cook CS, Douthitt CB, Howa JD, Hurley JM, Kreuzer HW, Lott MJ, Martinelli LA, O'Grady SP, Podlesak DW, Tipple BJ, Valenzuela LO, West JB. 2018. Applying the principles of isotope analysis in plant and animal ecology to forensic science in the Americas. *Oecologia* 187:1077–1094. DOI: 10.1007/s00442-018-4188-1.
Chowdhury MJ, Blust R. 2011. Strontium. *Fish Physiology*:351–390. DOI: 10.1016/S1546-5098(11)31029-1.
Cunha FLR, Bernhard R, Vogt RC. 2020. Diet of an Assemblage of Four Species of Turtles (Podocnemis) in the Rio Uatumã, Amazonas, Brazil. *Copeia* 108:103–115. DOI: 10.1643/CE-18-117.
Degryse P, De Muynck D, Delporte S, Boyen S, Jadoul L, De Winne J, Ivaneanu T, Vanhaecke F. 2012. Strontium isotopic analysis as an experimental auxiliary technique in forensic identification of human remains. *Analytical Methods* 4:2674. DOI: 10.1039/c2ay25035g.
DePaolo DJ, Ingram BL. 1985. High-Resolution Stratigraphy with Strontium Isotopes. *Science* 227:938–941. DOI: 10.1126/science.227.4689.938.
Destro GFG, Lucena T, Monti R, Cabral R, Barreto R. 2012. Efforts to Combat Wild Animals Trafficking in Brazil. In: *Biodiversity Enrichment in a Diverse World*. InTech,. DOI: 10.5772/48351.
Dirzo R, Young HS, Galetti M, Ceballos G, Isaac NJB, Collen B. 2014. Defaunation in the Anthropocene. *Science* 345:401–406. DOI: 10.1126/SCIENCE.1251817.
Duponchelle F, Pouilly M, Pécheyran C, Hauser M, Renno JF, Panfili J, Darnaude AM, García-Vasquez A, Carvajal-Vallejos F, García-Dávila C, Doria C, Bérail S, Donard A, Sondag F, Santos R V., Nuñez J, Point D, Labonne M, Baras E. 2016. Trans-Amazonian natal homing in giant catfish. *Journal of Applied Ecology* 53:1511–1520. DOI: 10.1111/1365-2664.12665.
Eisemberg CC, Reynolds SJ, Christian KA, Vogt RC. 2017. Diet of Amazon river turtles (Podocnemididae): a review of the effects of body size, phylogeny, season and habitat. *Zoology* 120:92–100. DOI: 10.1016/j.zool.2016.07.003.
El Meknassi S, Dera G, Cardone T, De Rafélis M, Brahmi C, Chavagnac V. 2018. Sr isotope ratios of modern carbonate shells: Good and bad news for chemostratigraphy. *Geology* 46:1003–1006. DOI: 10.1130/G45380.1.
Escalona T, Engstrom TN, Hernandez OE, Bock BC, Vogt RC, Valenzuela N. 2009. Population genetics of the endangered South American freshwater turtle, Podocnemis unifilis, inferred from microsatellite DNA data. *Conservation Genetics* 10:1683–1696. DOI: 10.1007/s10592-008-9746-3.
Farquhar GD, Ehleringer JR, Hubick KT. 1989. Carbon Isotope Discrimination and Photosynthesis. *Annual Review of Plant Physiology and Plant Molecular Biology* 40:503–537. DOI: 10.1146/annurev.pp.40.060189.002443.

Ferrara CR, Vogt RC, Sousa-Lima RS, Tardio BMR, Bernardes VCD. 2014. Sound Communication and Social Behavior in an Amazonian River Turtle (*Podocnemis expansa*). *Herpetologica* 70:149–156. DOI: 10.1655/HERPETOLOGICA-D-13-00050R2.

Flockhart DTT, Kyser TK, Chipley D, Miller NG, Norris DR. 2015. Experimental evidence shows no fractionation of strontium isotopes (87Sr/86Sr) among soil, plants, and herbivores: implications for tracking wildlife and forensic science. *Isotopes in Environmental and Health Studies* 51:372–381. DOI: 10.1080/10256016.2015.1021345.

Forero-Medina G, Ferrara CR, Vogt RC, Fagundes CK, Balestra RAM, Andrade PCM, Lacava R, Bernhard R, Lipman AJ, Lenz AJ, Ferrer A, Calle A, Aponte AF, Calle-Rendón BR, Santos Camilo C, Perrone E, Miraña E, Cunha FAG, Loja E, Del Rio J, Vera Fernandez JL, Hermández OE, Del Aguila R, Pino R, Cueva R, Martinez S, Diniz Bernardes VC, Sainz L, Horne BD. 2019. On the future of the giant South American river turtle Podocnemis expansa. *ORYX* 55:73–80. DOI: 10.1017/S0030605318001370.

Fry B. 2006. *Stable Isotope Ecology*. New York, NY: Springer New York. DOI: 10.1007/0-387-33745-8.

Gaillardet J, Dupré B, Allègre CJ, Négrel P. 1997. Chemical and physical denudation in the Amazon River Basin. *Chemical Geology* 142:141–173. DOI: 10.1016/S0009-2541(97)00074-0.

Galera L de A, Filho ALA, Reis LS, De Souza JL, Hernandez YA, Martinelli LA. 2019. Carbon and nitrogen isotopic composition of commercial dog food in Brazil. *PeerJ* 7:e5828. DOI: 10.7717/peerj.5828.

Gilmore RM. 1986. Fauna e etnozoologia da América do Sul tropical. In: Ribeiro D ed. *Suma Etnológica Brasileira*. Petrópolis: Vozes, Finep, 187–234.

Guynup S, Shepherd CR, Shepherd L. 2020. The True Costs of Wildlife Trafficking. *Georgetown Journal of International Affairs* 21:28–37. DOI: 10.1353/gia.2020.0023.

Haines AM, Webb SL, Wallace JR. 2021. Conservation Forensics: The Intersection of Wildlife Crime, Forensics, and Conservation. In: *Wildlife Biodiversity Conservation*. Cham: Springer International Publishing, 125–146. DOI: 10.1007/978-3-030-64682-0_6.

Hauser M, Doria CRC, Santos R V., García-Vasquez A, Pouilly M, Pécheyran C, Ponzevera E, Torrente-Vilara G, Bérail S, Panfili J, Darnaude A, Renno JF, García-Dávila C, Nuñez J, Ferraton F, Vargas G, Duponchelle F. 2019. Shedding light on the migratory patterns of the Amazonian goliath catfish, Brachyplatystoma platynemum, using otolith 87 Sr/ 86 Sr analyses. *Aquatic Conservation: Marine and Freshwater Ecosystems* 29:397–408. DOI: 10.1002/aqc.3046.

Hill KGW, Nielson KE, Tyler JJ, Mcinerney FA, Doubleday ZA, Frankham GJ, Johnson RN, Gillanders BM, Delean S, Cassey P. 2020. Pet or pest? Stable isotope methods for determining the provenance of an invasive alien species. *NeoBiota* 59:21–37. DOI: 10.3897/NEOBIOTA.59.53671.

Hodell DA, Mead GA, Mueller PA. 1990. Variation in the strontium isotopic composition of seawater (8 Ma to present): Implications for chemical weathering rates and dissolved fluxes to the oceans. *Chemical Geology: Isotope Geoscience Section* 80(4):291-307. DOI: 10.1016/0168-9622(90)90011-Z.

Hopkins JB, Frederick CA, Yorks D, Pollock E, Chatfield MWH. 2022. Forensic Application of Stable Isotopes to Distinguish between Wild and Captive Turtles. *Biology* 11. DOI: 10.3390/biology11121728.

Hopkins JB, Frederick CA, Yorks D, Pollock E, Chatfield MWH. 2023. Advancing Forensic Chemical Analysis to Classify Wild and Captive Turtles. *Diversity* 15. DOI: 10.3390/d15101056.

ICMBio. 2011. ICMBio e Ibama apreendem mais de 300 tartarugas em Roraima. *Available at https://www.gov.br/icmbio/pt-br/assuntos/noticias/ultimas-noticias/icmbio-e-ibama-apreendem-mais-de-300-tartarugas-em-rondonia* (accessed October 16, 2024).

ICMBio. 2015a. Maior apreensão dos últimos anos resgata 383 tartarugas da Amazônia. *Available at https://www.gov.br/icmbio/pt-br/assuntos/noticias/ultimas-noticias/maior-*

apreensao-dos-ultimos-anos-resgata-383-tartarugas-da-amazonia (accessed October 16, 2024).
ICMBio. 2015b. Nova operação recupera 268 tartarugas-da-Amazônia. *Available at https://uc.socioambiental.org/pt-br/noticia/157319* (accessed October 16, 2024).
ICMBio. 2016. Operação devolve à natureza 800 tartarugas-da-Amazônia. *Available at https://www.gov.br/icmbio/pt-br/assuntos/noticias/ultimas-noticias/operacao-devolve-a-natureza-800-tartarugas-da-amazonia* (accessed October 16, 2024)
ICMBio. 2019. Mais de 2,3 mil ovos de quelônios são apreendidos dentro das embarcações no Parque Nacional do Jaú. *Available at https://www.gov.br/icmbio/pt-br/assuntos/noticias/ultimas-noticias/mais-de-2-3-mil-ovos-de-quelonios-sao-apreendidos* (accessed October 16, 2024)
Jiguet F, Kardynal KJ, Hobson KA. 2019. Stable isotopes reveal captive vs wild origin of illegally captured songbirds in France. *Forensic Science International* 302. DOI: 10.1016/j.forsciint.2019.109884.
Kafino CV, de Sousa IMC, Barbieri CB, de Amorim AM, Santos RV. 2024. A proof-of-concept study: Determining the geographical origin of Brazilwood, (Paubrasilia echinata) with the use of strontium isotopic fingerprinting. *Science and Justice* 64:159–165. DOI: 10.1016/j.scijus.2023.12.006.
Kemenes A, Pezzuti JCB. 2007. Estimate of Trade Traffic of Podocnemis (Testudines, Pedocnemididae) from the Middle Purus River, Amazonas, Brazil. *Chelonian Conservation and Biology* 6:259–262. DOI: 10.2744/1071-8443(2007)6[259:EOTTOP]2.0.CO;2.
Lahtinen M, Arppe L, Nowell G. 2021. Source of strontium in archaeological mobility studies-marine diet contribution to the isotopic composition. *Archaeological and Anthropological Sciences* 13. DOI: 10.1007/s12520-020-01240-w.
Langner JA, Zanon AJ, Streck NA, Reiniger LRS, Kaufmann MP, Alves AF. 2019. Maize: Key agricultural crop in food security and sovereignty in a future with water scarcity. *Revista Brasileira de Engenharia Agricola e Ambiental* 23:648–654. DOI: 10.1590/1807-1929/agriambi.v23n9p648-654.
Lara NRF, Marques TS, Montelo KM, de Ataídes AG, Verdade LM, Malvásio A, de Camargo PB. 2012. A trophic study of the sympatric amazonian freshwater turtles *Podocnemis unifilis* and *Podocnemis expansa* (testudines, podocnemidae) using carbon and nitrogen stable isotope analyses. *Canadian Journal of Zoology* 90:1394–1401. DOI: 10.1139/cjz-2012-0143.
Lovich JE, Ennen JR, Agha M, Whitfield Gibbons J. 2018. Where have all the turtles gone, and why does it matter? *BioScience* 68:771–781. DOI: 10.1093/biosci/biy095.
Malhi Y, Roberts JT, Betts RA, Killeen TJ, Li W, Nobre CA. 2008. Climate Change, Deforestation, and the Fate of the Amazon. *Science* 319:169–72. DOI: 10.1126/science.1146961.
Marques D. 2021. In fight against wildlife trafficking, Brazil police turn to nuclear science. *Available at https://news.mongabay.com/2021/06/in-fight-against-wildlife-trafficking-brazil-police-turn-to-nuclear-science/* (accessed October 15, 2024).
Meier-Augenstein W. 2019. From stable isotope ecology to forensic isotope ecology — Isotopes' tales. *Forensic Science International* 300:89–98. DOI: 10.1016/j.forsciint.2019.04.023.
Mereles M de A, Sousa RGC, Pouilly M, Pereira DV, Mc Comb GL, Filizola N, Santos RV, Freitas CE de C. 2025. Distribution of strontium isotopes (87Sr/86Sr) in surface waters of the Amazon Basin: A basis for studies on provenance. *Science of the Total Environment* 965. DOI: 10.1016/j.scitotenv.2025.178630.
Molinier M, Guyot JL, Oliveira E, Guimarães V. 1996. Les régimes hydrologiques de l'Amazone et de ses affluents. In: *L'hydrologie tropicale: géoscience et outil pour le développement*. Paris: IAHS publication, 209–222.
Mozer A, Prost S. 2023. An introduction to illegal wildlife trade and its effects on biodiversity and society. *Forensic Science International: Animals and Environments* 3. DOI: 10.1016/j.fsiae.2023.100064.

Ometto JPHB, Ehleringer JR, Domingues TF, Berry JA, Ishida FY, Mazzi E, Higuchi N, Flanagan LB, Nardoto GB, Martinelli LA. 2006. The stable carbon and nitrogen isotopic composition of vegetation in tropical forests of the Amazon Basin, Brazil. *Biogeochemistry* 79:251–274. DOI: 10.1007/s10533-006-9008-8.

Palmer MR, Edmond JM. 1992. Controls over the strontium isotope composition of river water. *Geochimica et Cosmochimica Acta* 56:2099–2111. DOI: 10.1016/0016-7037(92)90332-D.

Pantoja-Lima J, Aride PHR, de Oliveira AT, Félix-Silva D, Pezzuti JCB, Rebêlo GH. 2014. Chain of commercialization of Podocnemis spp. turtles (Testudines: Podocnemididae) in the Purus River, Amazon Basin, Brazil: Current status and perspectives. *Journal of Ethnobiology and Ethnomedicine* 10. DOI: 10.1186/1746-4269-10-8.

Pauli JN, Rodriguez Curras M. 2024. Strange brew: Genetic and isotopic analyses to identify the provenance for wildlife forensics and food safety. *Forensic Science International: Animals and Environments* 5. DOI: 10.1016/j.fsiae.2024.100081.

Pereira LA, Santos R V., Hauser M, Duponchelle F, Carvajal F, Pecheyran C, Bérail S, Pouilly M. 2019. Commercial traceability of Arapaima spp. fisheries in the Amazon Basin: Can biogeochemical tags be useful. *Biogeosciences* 16:1781–1797. DOI: 10.5194/bg-16-1781-2019.

Pezzuti JCB, Lima JP, Da Silva DF, Begossi A. 2010. Uses and taboos of turtles and tortoises along Rio Negro, Amazon Basin. *Journal of Ethnobiology* 30:153–168. DOI: 10.2993/0278-0771-30.1.153.

Pimm SL, Jenkins CN, Abell R, Brooks TM, Gittleman JL, Joppa LN, Raven PH, Roberts CM, Sexton JO. 2014. The biodiversity of species and their rates of extinction, distribution, and protection. *Science* 344:1246752. DOI: https://doi.org/10.1126/science.1246752.

Polícia Federal. 2014. Operação Podocnemis combate a prática de crime ambiental em dois estados. *Available at https://www.pf.gov.br/agencia/noticias/2014/08/operacao-podocnemis-combate-a-pratica-de-crime-ambiental-em-dois-estados* (accessed July 29, 2020).

Pouilly M, Point D, Sondag F, Henry M, Santos R V. 2014. Geographical origin of Amazonian freshwater fishes fingerprinted by 87Sr/86Sr ratios on fish otoliths and scales. *Environmental Science and Technology* 48:8980–8987. DOI: 10.1021/es500071w.

Prigge T, Andersson AA, Hatten CER, Leung EYM, Baker DM, Bonebrake TC, Dingle C. 2024. Wildlife trade investigations benefit from multivariate stable isotope analyses. Biological Reviews. DOI: 10.1111/brv.13175.

Queiroz MMA, Horbe AMC, Seyler P, Moura CA V. 2009. Hidroquímica do rio Solimões na região entre Manacapuru e Alvarães-Amazonas-Brasil. *Acta Amazonica* 39:943–952. DOI: 10.1590/S0044-59672009000400022.

Rasbury ET, Present TM, Northrup P, Tappero R V., Lanzirotti A, Cole JM, Wooton K, Hatton K. 2020. A Sample Characterization Toolkit for Carbonate U-Pb Geochronology. DOI: 10.5194/gchron-2020-20.

Reis NR, Teixeira W, D'Agrella-Filho MS, Bispo-Santos F. 2010. The Avanavero Large Igneous Province: A Paleoproterozoic LIP In The Guiana Shield, Amazonian Craton. *Available at http://www.largeigneousprovinces.org/10jul* (accessed November 28, 2024).

Rhodin AGJ, Iverson JB, Bour R, Fritz U, Georges A, Shaffer HB, van Dijk PP. 2017. Turtles of the world: Annotated Checklist and Atlas of Taxonomy, Synonymy, Distribution and Conservation Status. In: Rhodin AGJ, Iverson JB, van Dijk PP, Saumure RA, Buhlmann KA, Pritchard PCH, Mittermeier RA eds. *Conservation Biology of Freshwater Turtles and Tortoises: A Compilation Project of the IUCN/SSC Tortoise and Freshwater Turtle Specialist Group. Chelonian Research Monographs*. 1–292. DOI: 10.3854/cmr.7.checklist.atlas.v8.2017.

Richardson K, Steffen W, Lucht W, Bendtsen J, Cornell SE, Donges JF, Drüke M, Fetzer I, Bala G, von Bloh W, Feulner G, Fiedler S, Gerten D, Gleeson T, Hofmann M, Huiskamp W, Kummu M, Mohan C, Nogués-Bravo D, Petri S, Porkka M, Rahmstorf S, Schaphoff S, Thonicke K, Tobian A, Virkki V, Wang-Erlandsson L, Weber L, Rockström J. 2023. Earth

beyond six of nine planetary boundaries. *Science Advances* 9. DOI: 10.1126/sciadv.adh2458.
Roberts NMW, Rasbury ET, Parrish RR, Smith CJ, Horstwood MSA, Condon DJ. 2017. A calcite reference material for LA-ICP-MS U-Pb geochronology. *Geochemistry, Geophysics, Geosystems* 18:2807–2814. DOI: 10.1002/2016GC006784.
Salera Jr. G, Balestra RAM, Luz VLF. 2016. Breve histórico da conservação dos quelônios amazônicos no Brasil. In: Balestra RAM ed. *Manejo Conservacionista e Monitoramento Populacional de Quelônios Amazônicos*. Brasília, 11–14.
Santos R V., Sondag F, Cochonneau G, Lagane C, Brunet P, Hattingh K, Chaves JGS. 2015. Source area and seasonal 87Sr/86Sr variations in rivers of the Amazon Basin. *Hydrological Processes* 29:187–197. DOI: 10.1002/hyp.10131.
Schneider L, Ferrara CR, Vogt RC, Burger J. 2011. History of Turtle Exploitation and Management Techniques to Conserve Turtles in the Rio Negro Basin of the Brazilian Amazon. *Chelonian Conservation and Biology* 10:149–157. DOI: 10.2744/CCB-0848.1.
Semenishchev VS, Voronina AV. 2020. Isotopes of Strontium: Properties and Applications. In: Pathak P, Gupta DK eds. *Strontium Contamination in the Environment*. Springer International Publishing, 25–42. DOI: 10.1007/978-3-030-15314-4_2.
Sung Y-H, Liew JH, Chan WS, Fok AWL, Leung J, Wong HF, Baker DM, Bonebrake TC, Dingle C, Dudgeon D, Karraker NE, Lau A, Colon VA, Magouras I, Ades G, Crow P, Rose-Jeffreys L, Spencer R, Fong JJ. 2025. Stable isotope analysis successfully identifies wild-caught individuals of threatened Asian freshwater turtles in illegal trade. *Global Ecology and Conservation* 64:e03947. DOI: 10.1016/j.gecco.2025.e03947.
United Nations. 2015. UN General Assembly Resolution A/RES/69/314 - Tackling illicit trafficking in wildlife. *Available at https://docs.un.org/en/A/res/69/314* (accessed October 17, 2024).
United Nations. 2025. UN General Assembly Resolution A/RES/79/313 - Tackling illicit trafficking in wildlife. *Available at https://documents.un.org/doc/undoc/gen/n25/177/66/pdf/n2517766.pdf* (accessed August 5, 2025).
UNODC. 2024. World Wildlife Crime Report 2024: Trafficking in Protected Species. *Available at https://www.unodc.org/documents/data-and-analysis/wildlife/2024/Wildlife2024_Final.pdf* (accessed October 18, 2024).
Vander Zanden MJ, Clayton MK, Moody EK, Solomon CT, Weidel BC. 2015. Stable Isotope Turnover and Half-Life in Animal Tissues: A Literature Synthesis. *PLOS ONE* 10:e0116182. DOI: 10.1371/journal.pone.0116182.
Walther BD, Thorrold SR. 2006. Water, not food, contributes the majority of strontium and barium deposited in the otoliths of a marine fish. *Marine Ecology Progress Series*:125–130. DOI: 10.3354/meps311125.
Woodhead J, Swearer S, Hergt J, Maas R. 2005. In situ Sr-isotope analysis of carbonates by LA-MC-ICP-MS: interference corrections, high spatial resolution and an example from otolith studies. *Journal of Analytical Atomic Spectrometry* 20:22. DOI: 10.1039/b412730g.
Xu Y, Marcantonio F. 2004. Speciation of strontium in particulates and sediments from the Mississippi River mixing zone. *Geochimica et Cosmochimica Acta* 68:2649–2657. DOI: 10.1016/j.gca.2003.12.016.
Zanacic E, McMartin DW. 2022. Calibration and Validation of Calcium Carbonate Precipitation Potential (CCPP) Model for Strontium Quantification in Cold Climate Aquatic Environments. *Environments - MDPI* 9. DOI: 10.3390/environments9060074.

FINAL CONSIDERATIONS

This thesis addressed both fundational and applied questions in the use of stable and radiogenic isotopes for the conservation of Amazonian chelonians. In parallel, it developed a critical, conceptually grounded analysis of Brazilian legislation and core issues in environmental criminology, culminating in a concrete legislative proposal to strengthen Brazil's legal framework for the effective prosecution of wildlife trafficking cases involving wildlife laundering.

The results presented here provide Brazilian environmental inspection and law-enforcement agencies with forensic tools to help curb trafficking in Amazonian freshwater turtles, particularly the large-scale illegal trade concentrated in major urban centers such as Manaus, which may be partly enabled by wildlife-laundering schemes involving authorized breeding facilities. The isotopic approaches developed for discriminating between wild and captive freshwater turtles and for assigning the geographic origin of seized animals are sufficiently developed to be integrated into inspection and criminal investigation workflows. When adopted routinely in breeding farms and retail establishments, these techniques can serve as a practical compliance tool for the freshwater turtle production sector and as a deterrent against wildlife laundering.

Permanent monitoring of seizures can generate intelligence on trafficking hotspots, recurrent routes, and temporal fluctuations in illegal trade dynamics, thereby improving the targeting and efficiency of enforcement actions. Moreover, information on the likely origin of seized animals can support better-informed reintroduction strategies, increasing the probability that confiscated individuals are returned to ecologically appropriate regions.

Future research should expand field sampling for both stable and radiogenic isotopes (carbon, nitrogen, and strontium) to improve geographic inference. It should also broaden the taxonomic scope of isotopic turnover experiments to include other relevant Amazonian chelonian species (e.g., *Podocnemis unifilis, P. sextuberculata, P. erythrocephala, P. lewyana*, and *Peltocephalus dumerilianus*). Additional priorities include examining turnover under the reverse isotopic transition, with animals first equilibrated to the natural C_3-based diet of the Amazon forest and then transferred to commercial feed; establishing trophic discrimination factors for free-ranging animals relative to the Amazon forest C_3 diet; and extending isotopic applications to additional elements, such as oxygen, hydrogen, and sulfur.

Given the ecological importance of these species in the Amazon, advancing knowledge of their trophic ecology is essential to inform long-term conservation strategies. At the same time, the forensic application of this knowledge is equally important for protecting these taxa from illegal trade and wildlife laundering, as well as for enhancing the effectiveness of enforcement responses.